Politecnico di Torino

Master Degree in Automotive Engineering

A.y. 2020/2021

Degree session October 2021

# Design and Standardization Methodology for Automotive Manufacturing

## Application to the field of heavy duty vehicles

**Supervisor:**
Prof. Carlo Rosso

**Candidate:**
Alessio Santini

**Company tutor:**
OMAR S.R.L.
Ing. Pierpaolo Castellani

II

# Dedication

*I would like to thank my mom and grandmother who have always been by my side on this journey, allowed me to face the difficulties and pushed me to improve every day.*

*A special dedication goes to my grandfather Luciano who has always been with me and who has boosted me to this moment even if today he cannot be by my side.*

# Abstract

The work carried out within the company OMAR S.R.L. is part of a large project that provides for the growth of the company's production level.

The project develops starting from the will of the company to standardize some components used in most of the works carried out in order to increase the production level. This desire clashes with the company's request to maintain its value of customization, one of the key elements that makes the company unique and highlights the characteristics of craftsmanship at European and world level of the company.

As a first point of the project, the company's volumes will be analyzed in order to understand which is the vastness of the products made, the common elements and the differencies between vehicles aiming to understand in detail the level of customization of the products made.

It will go then to study in analytical way and subsequently also through the numerical method the actual model of the present vehicles in company. The study will be concentrated more on the chassis realized by the firm.

The purpose of this thesis will allow the collection of frames produced today and the implementation of modules applicable to more vehicles.
Within the modules there are components that will remain standard, and therefore applicable to most of the vehicles produced while some parts will remain variable in order to ensure the customization required.

At the end of the project there will be an attempt to realize the studied module close to production for prototyping.

# Acknowledgements

An important thanks goes to the company OMAR S.R.L. for the trust given in the realization of the project.
Special thanks goes to the Ing.CASTELLANI and Mr.TONUCCI for the availability granted during the period of tutoring.

# Contents

# List of Figures

# List of Tables

# Introduction

OMAR S.R.L. is a company that since 1963 has been producing vehicles and bodies in the automotive field and more specifically it is dedicated to the realization of trailers, semi-trailers and bodies for heavy-duty vehicles.

The firm currently provides a very high level of customization and does not plan to make vehicles with a standard base, to this end it is useful to report on the process by which the product is made.

The starting point is the customer's request, collected by the sales department where the product is defined in every single component, the order is collected and inserted into a company configurator which responding to a series of detailed and meticulous questions defines the technical characteristics (about 200 queries).

Here comes into play the technical department, through the Creo software and the management database collects the requests of the product and goes to develop it obtaining the 3D body and the corresponding 2D tables.
The projects made are based on previous works, once identified a similar model is proceed to the modification of the project in order to obtain the new product. As can be imagined, this process can take hours as well as whole days of work depending on the customization changes that need to be made.

The company here inserts its request to standardize some components and go to design at a modular level that is subdividing the project into various subprojects in order to allow the office to use existing modules on new works.

# Chapter 1

# State of Art

The firm, with its decades of experience, realizes heavy duty vehicles such as trailers and semi-trailers in every aspect under the customer's request and is also able to equip vehicles such as trucks that constitute the road train.

The aspect that has made the company grow and has given it visibility both in Europe and worldwide is the customization applicable to each vehicle made. In order to achieve this, the company has a production approach that starts from the customer's request, this demand is accepted by the commercial department; consequently the project is realized starting from the order received and is respected in every detail. The realization of the vehicles in this way is very meticulous and highlights the craftsmanship and manufacturing skills of the Italian company.

The company target is to increase production volumes while trying to reduce the complexity of design and aiming to standardize a number of components in order to increase production and at the same time limit the variability of parts.

The purpose of the project is to streamline the main parts, the one that produces the largest number of volumes, in order to speed up the design and production time but at the same time maintain the quality and customization of the product.

The design bases of the firm derives from years of experience, for this reason each new project takes shape starting from a similar one already realized and modified to fit the new customer's request.

The design method described provides for the completion of the project and redaction of the bill of material before production start-up. The standardization of vehicle parts allows to have a stock of components ready for assembly and at the same time a standard part decreases the number of codes allowing to accelerate the assembly line due to the fact that it is known how to mount the component on the vehicle.

# Chapter 2

# Corporate products introduction

## 2.1 Category division

This chapter goes into detail about the company's heavy vehicle production. The firm more specifically manufactures trailers, semi-trailers, both in terms of chassis and body, and makes bodies for towing truck units supplied by other manufacturers.

A description of the company's products is now provided.

### 2.1.1 Auto-trailer


Figure 2.1: Auto-trailer vehicle

An auto-trailer (see **Figure 2.1**) is defined as a convoy consisting of a traction unit and one or more towed units without an engine.

The two semi-units are joined by a special mechanism consisting of a drawbar located at the front of the trailer and a hook located at the rear of the towing truck. The drawbar generally ends with an eye in which a steel pin is inserted that also passes through the hook located on the towing vehicle, known as a bell; on the most advanced vehicles, instead of the more classic eye, a "ball" coupling system is used which, by allowing a better distribution of stresses, guarantees a longer duration of the coupling system, reducing the maintenance costs of the vehicle.

In this way the towed unit maintains a fixed distance from the towing unit and is able to follow the curves of the road thanks to the possibility of movement of the drawbar in the hook. The drawbar and the hitch must be kept under observation because they must be perfectly straight.

Technological progress has increasingly improved hitching methods, reducing the required safety distance between units, achieving a greater volume of cargo without increasing the length of the convoy.

In turn, the truck world has two types of towed or trailer units:


Figure 2.2: Biga VS Trailer

- The biga-trailer, usually composed of 1 or 2 adjacent axles, with a lower drawbar than the fifth wheel trailer. (Left side of **Figure 2.2**)
- The trailer (or trailer with fifth wheel) is usually composed of two or three axles, one of which is always placed in front, linked to the mechanical system defined "fifth wheel", that is a rotating mechanism that allows the trailer to rotate not only around the coupling pin with the trailer but also around the axis of the fifth wheel, allowing the towed unit to better follow the towing vehicle. Another feature that makes the trailer different from the biga is the aspect related to the stability of the vehicle, here the front axle makes the unit more stable to pitching reducing the load discharged on the drawbar pin. (Right side of **Figure 2.2**)

### 2.1.2 Articulated vehicle


Figure 2.3: 18-wheeler (articulated vehicle)

The articulated vehicle or 18-wheeler (see **Figure 2.3**), is one of the most common types of road convoy; similar to the truck-trailer, it differs mainly for the fact that the articulated vehicle is composed of a road tractor, i.e. a vehicle equipped with a cabin but no load compartment; the latter is replaced by a fifth wheel on which rests (and is fixed) a part of the semi-trailer.

In this context, OMAR S.R.L. is involved in the production of semi-trailers that can range from 1 axle to the common 3 axles (reported in the left side of **Figure 2.4**), and also considering the size of the vehicles.

Figure 2.4: 3-axles semitrailer VS 1-axle city-trailer

One of the company's technologies that has been very successful in recent years is the Tridec technology adopted on semi-trailers for city use (Right side of **Figure 2.4**). Through a mechanical system that develops between the axle and the fifth wheel-pivot junction of the vehicle, a steering axle is created with a radius that depends on the rotation between the pivot and the fifth wheel.

This technology is fundamental in city driving where there are tight curves, and tire consumption is also reduced as there is less scraping during manoeuvres.

## 2.2 Sub-assemblies

The company provides all types of bodywork also for special applications.[1]
Bodyworks:

- Flat-bed
- Box-type
- Curtain-sided
- Plywood
- Aluminum van

Special applications:

- Lowered towing hooks
- Swap body clamping systems
- Retractable, rebated and racing type tail lifts
- Hydraulic lifting hooks for unloadable equipment
- Systems for tipping bodies
- Hydraulic cranes of all capacities

Each vehicle, as already mentioned, can be customized according to the requests, see the internal height of the vehicle, the length, the type of axle and the number of axles, the adoption of a rib compared to another of the customer always remaining within the legislative regulations.

After this brief introduction it is already possible to understand the wide range of products manufactured by the company and therefore the complexity and abundance of codes that are formed considering the customer's requests and the regulations imposed by the Highway Code.

As it will be seen in the next chapters, the focus will be carried out in the part related to the chassis of the vehicles made.

[1] for a broader view of the vehicles produced please visit the company website.[12]

An overview of the three most commonly produced vehicles at the company level is now given in order to highlight the similarities and differences between them.

For the purposes of this subject, it is defined as:

- Fixed bodywork: a bodywork, which may be a body or a van or a tanker, structurally integral with the vehicle, i.e., an integral part of the vehicle itself.

- Interchangeable bodywork: a bodywork which is not permanently attached to the vehicle, but which can be replaced with other interchangeable bodies having the same type of connections to the vehicle chassis. Said connections will normally be of the "rapid" type.

### 2.2.1 Curtain-sided

The curtain-sided vehicle (**Figure 2.5**) is a useful system for covering, protecting and concealing the amount of cargo transported and at the same time a very flexible system.

The vehicle is in fact easy to open on all three sides for loading and unloading of goods with mechanical means (such as forklifts), thanks to the use of a cage in removable pieces consisting of a metal frame with removable horizontal bars in metal or wood, covered with sheets (often equipped with mechanisms to make them sliding), thick and strong made of plastic material.

Figure 2.5: Curtain-sided biga

The rear part of the vehicle may present, as an alternative to the classic rib, full-height doors. Many curtain-sided vehicles also have a roof that can be opened thanks to a sliding mechanism, which makes them suitable for loads from above through cranes and overhead travelling cranes.

### 2.2.2 Roll-off

Figure 2.6: Roll-off biga

As previously mentioned, roll-off vehicles can change their bodywork, the vehicle produced has hooks commonly referred to as twists that allow for the attachment of boxes that are made through the swap bodies (**Figure 2.6**).

### 2.2.3 Bare chassis

The last product described is the bare-frame vehicle, it is produced only at the frame level without any boxe or hooks for boxes; this is commonly done for companies that do not produce frames but only boxes or for customers who have special needs not included in the company production (**Figure 2.7**).

### 2.2.4 Differences and similarities

On closer inspection, **Figures 2.5, 2.6, 2.7** already give an introduction to the analysis that will be carried out.

As can be seen, the vehicles are composed of two main side members and two axles (one of which can be liftable) and various cross members that connect the two longitudinal side members.

The differences that are noted are the coachability of these vehicles, all three of which are very different in their functionality and top-end. In the

Figure 2.7: Bare chassis biga

next chapters the vehicles are analyzed in order to find out how to make them as similar as possible in some aspects and different in the features that make them so.

# Chapter 3

# Analitycal study of the firm volumes

The purpose of this chapter is to analyze, through the available data referred to the last years of company production, the most manufactured products.

The data that will be described derive from a firm configurator; this configurator allows to convert the customer's requests into useful information for the technical office.

The configurator is based on a series of questions whose answers lead to a technical draft of the components that will be used for the production of the vehicle.
This step is very important in order to make a first draft of the bill of materials useful to order the components from the suppliers. Within this database there is a lot of information but in a raw way, for this reason a pivot table has been created through Excel in order to purify the data and bring to light the similarities between the various vehicles.

Here below are reported the informations obtained, useful for a first grouping of manufactured goods.

## 3.1 Company production volumes

The company's request to optimize current production is based mainly on the analysis of company volumes and sales.

As brought back from the company revenues, that for privacy reasons will not be reported, approximately 60% of the business invoiced is given from vehicles which bigas, trailers and semitrailers. The idea now arises to ask if it is possible to optimize the production in order to have modules common to these different types of vehicles, making the production more modular for some parts, going to speed up the production system with a future robotized implementation.

The data that will be analyzed have been retrieved from a company database with three-year history referred to the time frame beginning 2018 end 2020. In the graph of **Figure 3.1** are reported the data relative to the

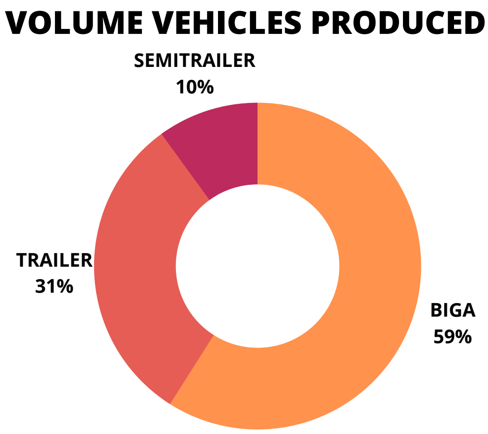


Figure 3.1: Pie-chart company production volumes

production in terms of volumes of the last three years; the vehicles most frequently produced, such as biga, semi-trailer and trailer, can be seen immediately.

A first analysis will be carried out on the biga vehicle to see if it is possible to obtain some grouping given the great difference in volumes that the biga element brings at company level. To this end, it is emphasized that today the realization of each vehicle takes place only after the customer's request through the company's commercial department.

The main features to obtain a first draft of the vehicle are the internal height required by the customer, the choice of the number and brand of axles that will be mounted on the vehicle.

## 3.2 Customer choices and technical requests

The section that will now be introduced deals with the main characteristics of the vehicle, these define the basis for the realization of the final product.

### 3.2.1 Internal height

The choice of the height is a fundamental aspect depending on the type of work that is carried out, some transports require a certain volume of transport that must be guaranteed by the adopted equipment but to make some vehicles "MEGA" a lowered chassis is adopted in order to have the maximum internal span and respect the 4 meters height imposed by the Highway Code. The **Figure 3.2** reports in a schematic and simplified way

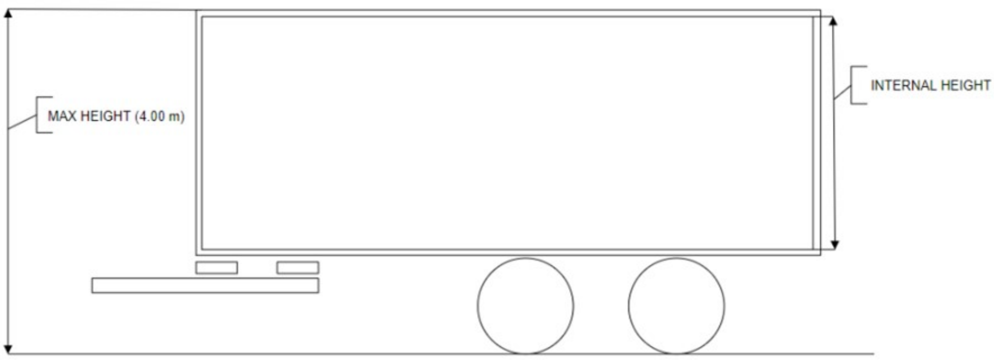


Figure 3.2: Vehicle side view and reference heights

the heights described above. Usually the interior height is also called the loading height or interior clearance.

### 3.2.2 Axles

The number of axles is usually included between one and three in towed vehicles, for trailers two twin-axles are commonly adopted while for semi-trailers three axles with non-twin tires are most commonly used.

This aspect is also fundamental in the realization of the chassis since the part linked to the axles is the most stressed and must be correctly sized.

The realization of the product within the company is mainly done using internal machinery and only a few components that are part of the project are purchased and not produced by the company itself.

In this description are included the axles, there are several brands of them (ROR, BPW, SAF are the ones most applied) that are present on the market and are proposed to the customer, the choice will affect not only the final cost of the vehicle but especially the realization at the chassis level, this is because each supplier of axles engineers its own in different ways making the attack on the frame different in various cases, even between the same brand by varying the tire can vary the wheelbase and then the assembly of the suspension.

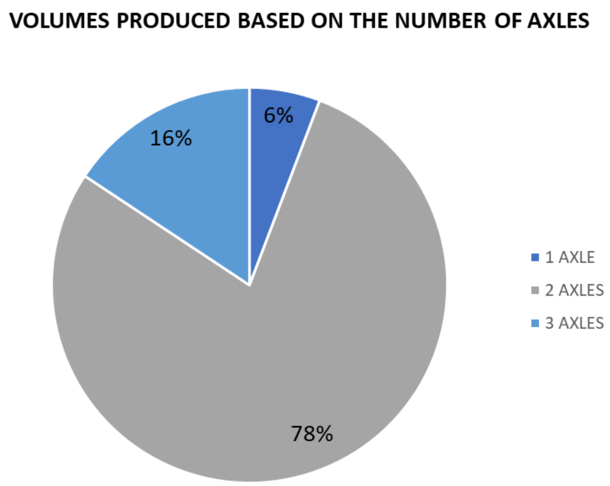


Figure 3.3: Volumes produced based on number of axles

As can be seen from the analysis shown in **Figure 3.3**, about 78% of the company's volumes are made with two axles. The implementation of a 2-axis module can be the solution for the project modulation, another useful implementation can be the single-axis module combined with the double axis in such a way as to collect more than 84% of the total production.

The graph of **Figure 3.4** shows, referring to the percentage value, the number of axles for each type of vehicle produced; the production of 2-axle vehicles is the majority in all three cases analyzed. The graph indicates a particular characteristic of the biga-trailer, which is usually produced with two axles, while the semi-trailer is almost equal between 2 and 3 axles.
The case of the trailer does not have 1 axle, as can be easily deduced from the configuration of the vehicle, and is mainly produced with two axles (one front and one rear).

The data shown in the graph in **Figure 3.4** consider the weight of each vehicle on the total company volumes in the three years considered.

The graph reported in **Figure 3.5** shows the choice of axles by type of

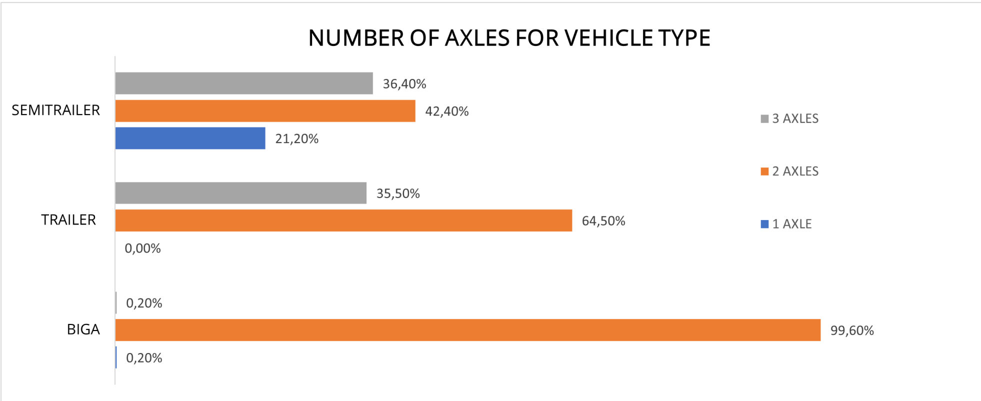


Figure 3.4: Number of axles for vehicle type

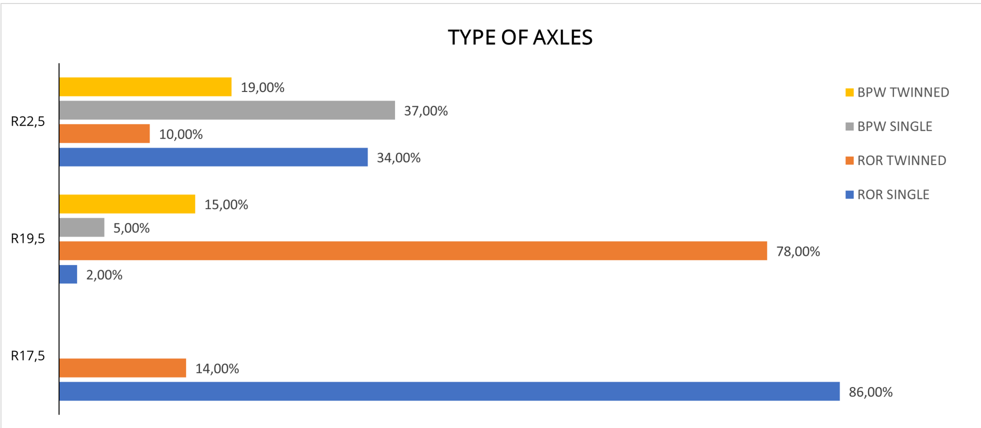


Figure 3.5: Type of axles

rim radius, moreover thanks to the scale chosen there is an excellent view of the ratio of volumes produced. The initials ROR and BPW represent the brand of axles chosen while the indication twinned or single stands for the number of wheels per axle, in the case of twinned-wheels there are 4 tires per axle while in the case of single there are only 2. The majority of vehicles produced are manufactured by mounting R19.5 axles and mainly with the ROR brand. In the field of R22.5 radii, it can be seen that the axle most often mounted is the single-wheel one, this is also due to the fact that they are mainly installed on semi-trailers that have this configuration for history.

### 3.2.3 Vehicle tires

Another important aspect for the definition of the chassis and, more specifically, a component that defines the wheelbase of the chassis beams is the vehicle's tires, both in terms of the number of tires per axle, which can be 2 or 4 (single or twin wheels), and in terms of tire size.

Table 3.1: Wheels on axle for manufactured vehicles

| | **BIGA** | **TRAILER** | **SEMITRAILER** |
|---|---|---|---|
| SINGLE | 31.3% | 14.0% | 56.4% |
| TWINNED | 68.7% | 86.0% | 43.6% |
| WEIGHT | 58.7% | 10.3% | 31.0% |

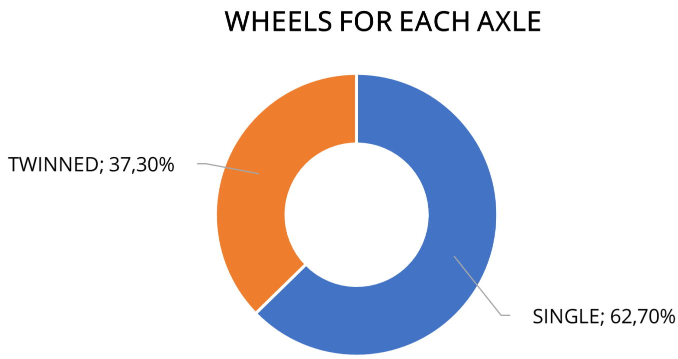


Figure 3.6: Wheels for each axle (Global volumes)

In the **Table 3.1** are reported the volumes of vehicles produced using twin tires in the first row and single tires in the second row. As can be seen, the weights of each vehicle are also reported in relation to total volumes and, as already mentioned, around 60% is represented by the biga product. It can be noted, therefore, that over 60% of vehicles are realized with twin tire. (**Figure 3.6** )

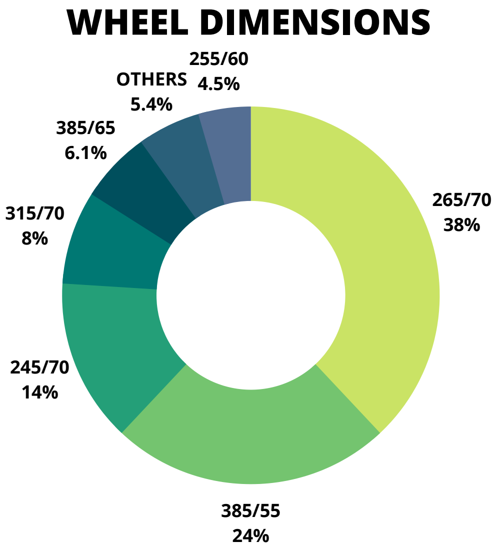


Figure 3.7: Wheel dimensions

**Figure 3.7** shows another analysis regarding the size of the tires adopted and the diameter of the rim.

The majority of vehicles, adopt 19.5 and 22.5 rims. The 19.5 rims are more frequently used for biga and trailers, while 22.5 rims are used for semi-trailers (70%). This fact is due both to the different configuration of the vehicles, the biga in particular is hooked to the towing at a height of about 30/35 cm from the ground while the semi-trailer is hooked to the fifth wheel at a height of one meter.

The most common type of tire is a 265/70R19.5 (mounted in twinned) while the second is a 385/55R22.5 (usually mounted individually). **Figure 3.8** shows in a schematic way the distinction between single and twinned wheels, from the scheme it is easy to understand the definition of twinned wheels.

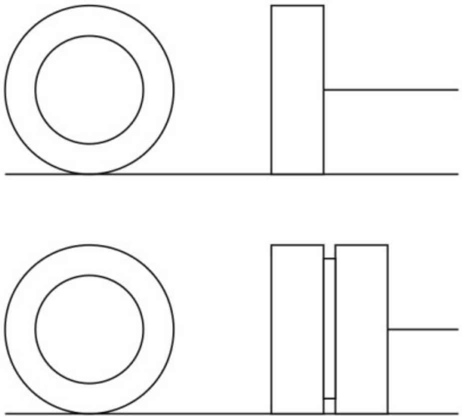

Figure 3.8: Single on top, twinned on bottom

## 3.3 Pneumatic suspension

Another important aspect related to the axles and tires is the adoption of suspensions. Nowadays all heavy duty vehicles in production adopt pneumatic suspensions.

The starting point of the suspension is the leaf spring configuration of the vehicle on which the self-adjusting suspension system is then mounted. Thanks to the pressurized air inside the chamber (diapress or air bellows), the damping effect of the suspension takes place.

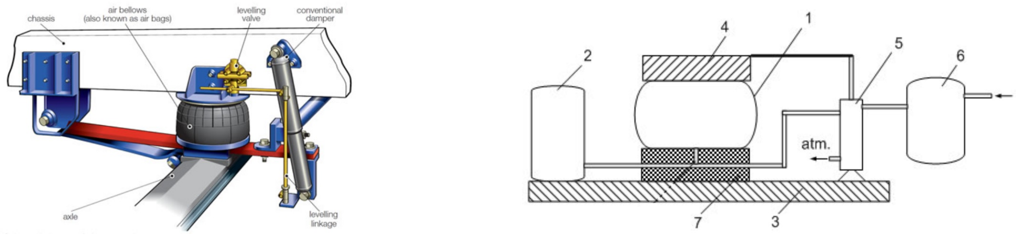


Figure 3.9: Overview of pneumatic suspension for heavy-duty application

The pneumatic suspension consists of an air spring 1 (rubber airbag) located between the bogie 3 and the car body 4, connected to an auxiliary reservoir 2.

The central pneumatic suspension includes usually a rubber spring 7 arranged in series with the air spring, in order to provide extra flexibility and to act as a safety device in the case of air spring deflation.

One of the main features of the pneumatic suspension is the ability to

Table 3.2: Main suspension components of **Figure 3.9**

| | |
|---|---|
| RUBBER AIRBAG | 1 |
| AUXILIARY RESERVOIR | 2 |
| BOGIE | 3 |
| CAR BODY | 4 |
| LEVELLING VALVE | 5 |
| MAIN RESERVOIR | 6 |
| RUBBER SPRING | 7 |

maintain a constant height of the car body, regardless of vehicle static load. This is achieved through the levelling valve 5, which controls the air flow between the air spring 1, the main reservoir 6 and the atmosphere. Thus, it can either increase the air spring internal pressure by connecting it to the main reservoir (if the static load increases) or to decrease the air spring internal pressure by connecting it to the atmosphere (if the static load decreases). In this way it is obtained a stiffness progressive with the static load.

Adjusting the stiffness with the load allows also maintaining comfortable vibration frequencies for the entire range of static load.

## 3.4 Mainly adopted material

The material used in recent years by the company represents a compromise between the cost itself and the goodness of the material. Over the years different materials have been experimented with and to date S355J0 has been the choice. The chemical and mechanical characteristics of the material are reported. (**Table 3.3**) (**Table 3.4**)

Table 3.3: Chemical composition of S355J0

| CHEMICAL COMPOSITION | | | | | | |
|---|---|---|---|---|---|---|
| C (%) | Mn (%) | P (%) | S (%) | Si (%) | N (%) | Cu (%) |
| 0.20 | 1.60 | 0.030 | 0.030 | 0.55 | 0.012 | 0.55 |

S355J0 is a medium tensile, low carbon manganese steel which is readily weldable and possess good impact resistance. This material is commonly supplied in the untreated or normalized condition. Machinability of this material is similar to that of mild steel.

The structural steel S355J0 has low carbon content. Therefore it is easily welded and high tensile strength. The plate is also known for its high corro-

Table 3.4: Main mechanical properties of S355J0

| MECHANICAL PROPERTIES | |
|---|---|
| Re (MPa) | Rm (MPa) |
| 355 | 510 |

sion resistance property, good mechanical strength, ductility, yield strength. The plates offer good thermal property and conductivity at elevated temperatures, high resistance to oxidation, crevice and pitting.

The material S355J0 is used in various industries because of its excellent features like easy to use, workability, durability, easy to fabricate, formability, reliability, dimensional accuracy, good surface structure, and many other features.

The good workability of this material allows it to be processed through a laser machinery and furthermore most of the frames are made through the welding.

The welding process requires special attention not only to the material chosen but also to the preparation of the surface to be welded, and requires an experienced welder.
The application of welding within the company is very present since the frames are made entirely through welding.

# Chapter 4

# Fundamental chassis components

In this chapter a broad description of the structural components of the frame is given, this will be useful for the understanding of the following chapters.

In **Figure 4.1** there are two 3D views of a common chassis of the biga-trailer vehicle. The various parts will now be analyzed and the functionalities of each one will be described.

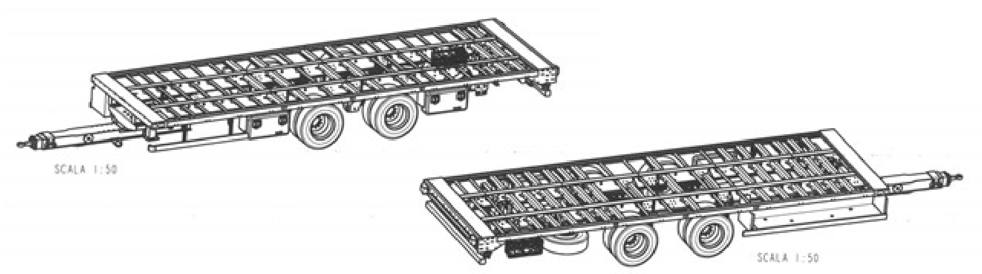


Figure 4.1: Biga-trailer chassis

The **Figure 4.2** shows an exploded view of the biga-trailer chassis, one of the most common, which mounts tires 265/70 R19.5. More in details in **Figure 4.3** is reported a lateral view of the chassis. It is a two-axle chassis visible from the configuration of the pneumatic suspensions connected to the central beams of the frame. Moreover, in the front part there is the nose (yellow box) which is joined to the chassis through two supports. As already mentioned, the suspensions (red box in **Figure 4.3** ) are of the pneumatic type and through the air pressure they carry out the task of supporting the load and dampening the oscillations due to the disconnections of the road surface.

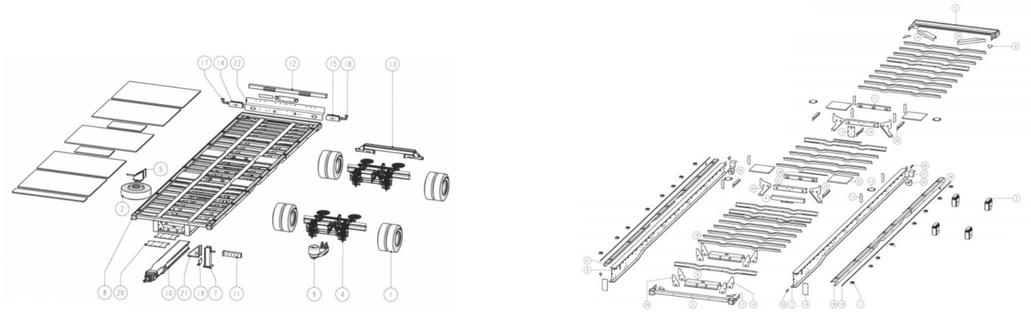

Figure 4.2: Exploded views of chassis

An overview related to the suspension zone is reported in **Figure 4.6**. As the image shows, this area is very crowded due to the fact that in this zone of the chassis it is necessary to connect the axles (and therefore the wheels) with the chassis itself and at the same time it is the area in which there is the connection between the vehicle and the ground, therefore there will also be forces in play of important module.

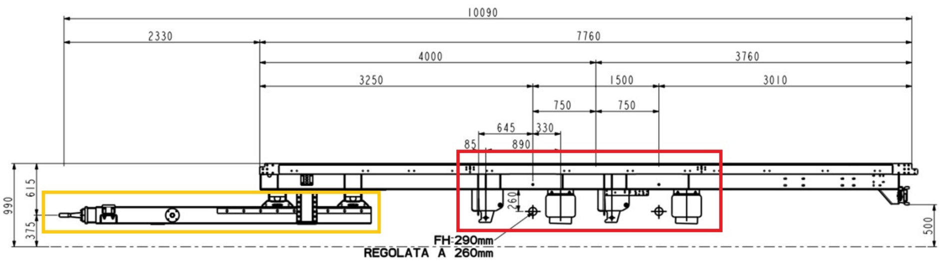


Figure 4.3: Biga-trailer chassis - lateral view

In the top view (**Figure 4.4**) it is possible to appreciate the frame with the longitudinal beams (blue color) and the supporting crossbeams for the axles (green color).

The **Figure 4.5** reports the main longitudinal beam that forms the central body of the chassis. As mentioned above, the double-T section beam is made by welding 3 different components.
It can be seen how the central part is complex in the number of holes and slots present, these will later be used for the insertion of the sleepers that will support the floor while other holes will be used for the installation of auxiliary objects such as boxes, bike guards and others for the insertion of supports for mechanical components such as suspension parts and control units.

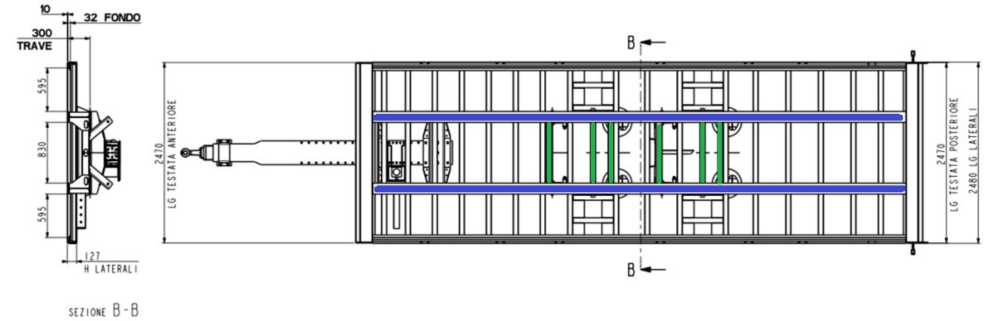


Figure 4.4: Biga-trailer chassis - top view

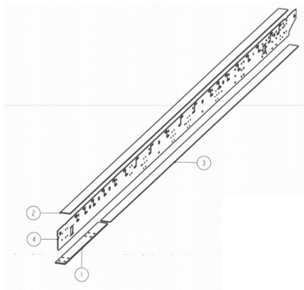

Figure 4.5: Longitudinal trailer beam

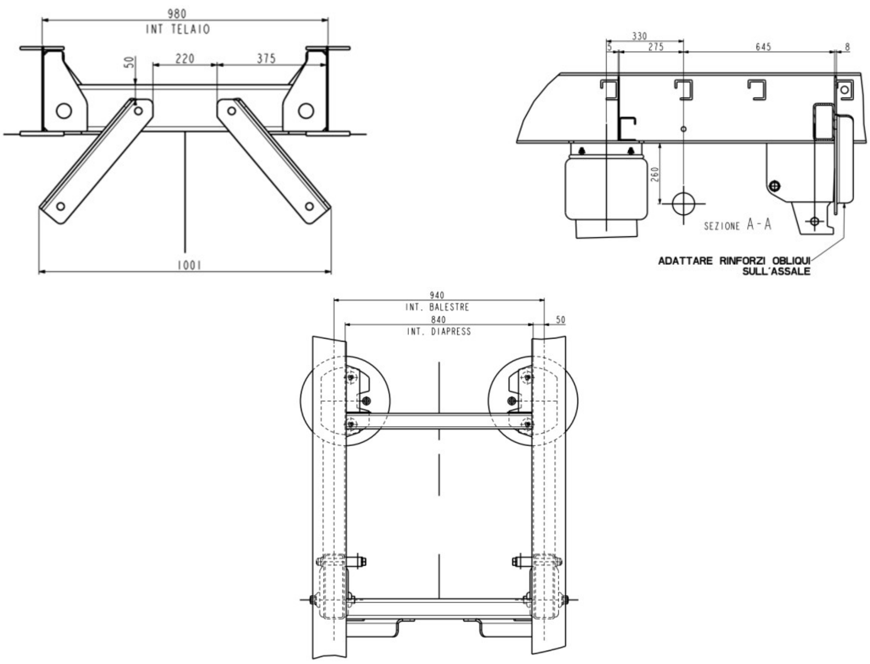


Figure 4.6: Detailed view of the suspension area

## 4.1 Structural components

The purpose of this section is to identify the main structural components of the chassis of the vehicle studied in order to model each component and the couplings between them in order to create a simplified model for the study of stresses and strains.

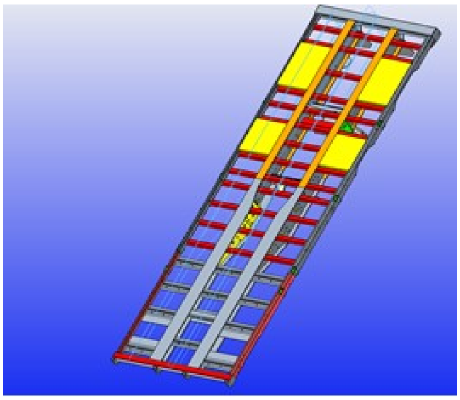

Figure 4.7: Chassis of the trailer taken as an example

### 4.1.1 Longitudinal beam

The first component is the longitudinal beam, the section of the beam is an I-section or double T-section and will be analyzed as a "beam" model within the finite element calculation software. The choice of this approximation is granted by considering the size of the section relative to its overall length.

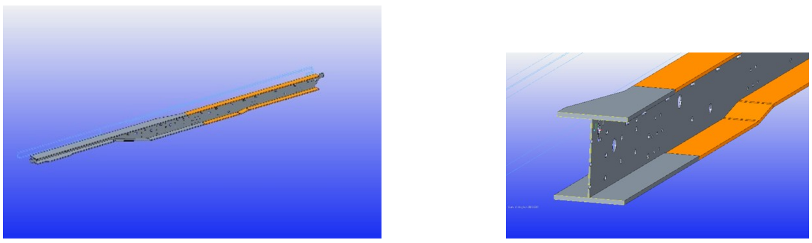

Figure 4.8: Longitudinal beam of the biga-trailer

The production of this element comes from three different components, the central core and the two plates (upper and lower) that are welded together through the submerged arc welding method, the welding is not done on both sides but only on one side.

The **Figure 4.8** shows the actual configuration used in the case of the biga-trailer structure.

The holes that are drilled on the core of the beam are also worth of notice; these holes allow the insertion of the lateral crossbeams on which the floor will then be placed. The cut made on the core can be Z-shaped or C-shaped in the most used configurations. Other holes in the core allow the lightening of the structure and the insertion of electrical wiring, pneumatic system and brackets of various accessories.

### 4.1.2 Crossbeam

The crossbeams, as mentioned above, can have two different configurations, a z section **Figure 4.9** and an open section similar to a c section **Figure 4.10**.

Figure 4.9: Z Crossbeam section

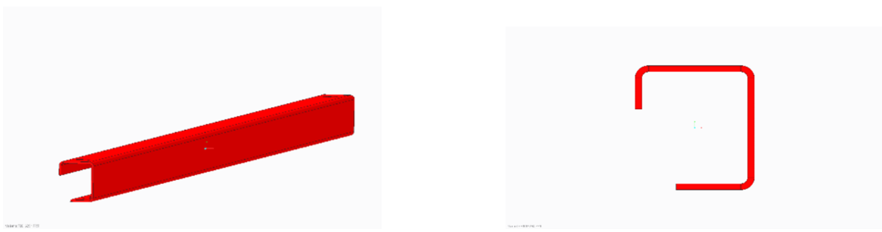

Figure 4.10: C-closed Crossbeam section

Also in this case the 1D approximation is applicable in the finite element calculation software since the dimensions of the section are much smaller than the length of the beam itself.

The cross beams are inserted into the notches that are made on the core of the longitudinal beam and then welded to both the longitudinal beams and the side members.

### 4.1.3 Side member

Another structural element of the chassis is constituted by the side members as represented in the **Figure 4.11**, these also contribute to increase the vehicle stiffness since they are linked to the cross members. They also have section dimensions that are possible to study such as 1D element for the purpose of a finite element analysis.

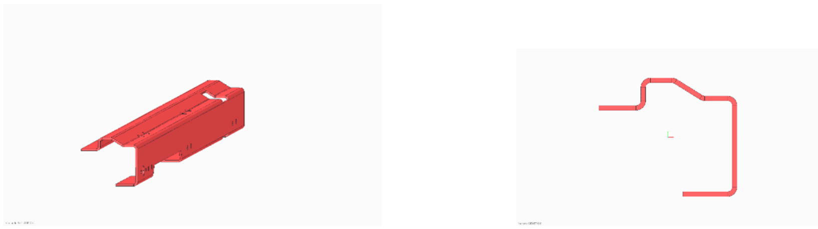

Figure 4.11: Mainly adopted side member section

### 4.1.4 Joints

The connections between the parts shown above are made by submerged-arc welding. The **Figure 4.12** shown, in a simple way, the welding spots that are performed on the frame to join the different components.

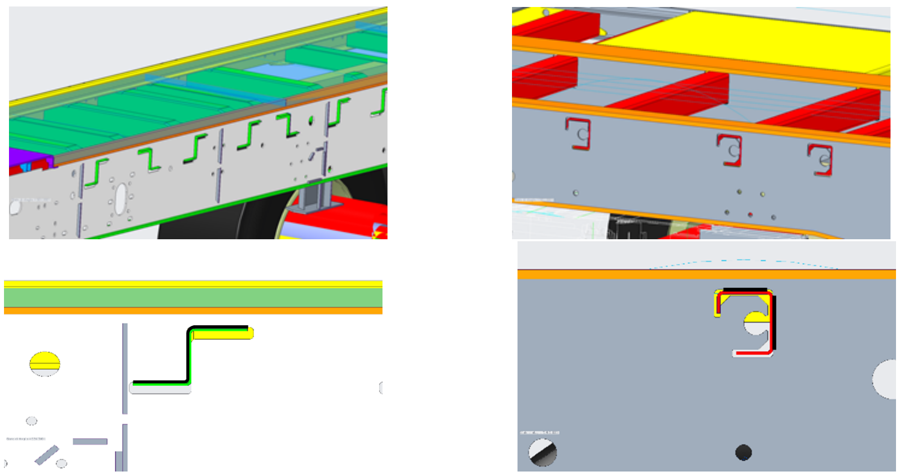

Figure 4.12: Different views of weld spots

# Chapter 5

# Analytical study of the main models

The steps that are going to be carried out provide first an analysis at analytical level the idealization and the study through the finite element software of the various components and of the overall frame that is going to be schematized.

## 5.1 Strengths at play

The design of the chassis structure of towed vehicles takes shape thanks to the company's many years of experience. The configurations of the analyzed structures base their calculations on the conventions given by the Ministerial Decree of Transport (Prot. N. 1722/DC - MOT B074 Subject: Calculation of the resistant structures of road vehicles).

The directive presents the fundamental regulations for the production of vehicles and at the same time defines the characteristics that the vehicle must respect in order to be tested and therefore made circulable according to the law.

### 5.1.1 Forces and torques for the design

In order to analyze the frame structure present in the produced vehicles, it is now necessary to define the forces and moments involved.

The forces which will be introduced have the purpose to dimension the longitudinal beam element (main element of the chassis), the other components of the vehicle such as crossbars and various reinforcements have been inserted through company considerations based on company experience and observation of vehicle behavior.

### Distributed load

This loading represents the heaviest stress acting on vehicles.
The load capacity of the vehicle is taken and distributed over the entire length of the beam considered. The **Table 5.1** shows the characteristic loads for each vehicle.

The gross weight is imposed by legislation, the unladen weight is derived from the various vehicles produced and the net weight (difference between gross and tare) represents how much the vehicle is able to load. It is therefore normal that a lighter structure (with a lower tare) will be able to carry a greater load and this will cause an increase in the distributed load acting on the structure.

Table 5.1: Table of loadings according to european vehicle regulations

| | SEMITRAILER | TRAILER | BIGA-TRAILER |
|---|---|---|---|
| GROSS WEIGHT | 38 ton | 26 ton | 22 ton |
| UNLADEN WEIGHT | 7.5 ton | 7 ton | 6 ton |
| NET WEIGHT | 30.5 ton | 19 ton | 16 ton |

### Driving force

At the connection point with the towing vehicle, a driving force is applied in a horizontal direction that can generate tension or compression depending on the operation performed (braking or acceleration).

The analytical study that will be carried out as a first approximation considers the longitudinal beam as the main element of study, this is because it represents the starting point of the realization and every main component is related to it.

## 5.2 Trailer

As a first schematization of the longitudinal beam, the trailer vehicle is considered (**Figure 5.1**).
It is schematized as a straight beam, constrained through two carriages and a support.

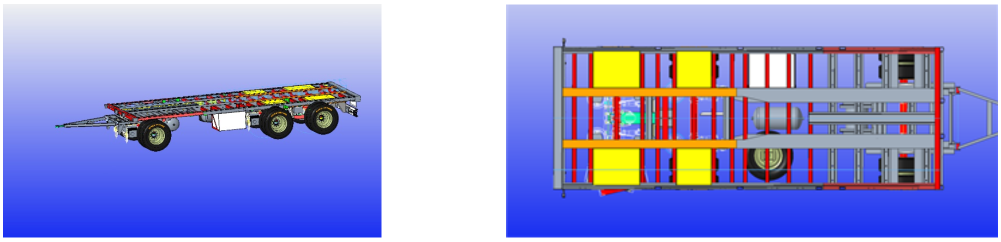

Figure 5.1: Views of the trailer vehicle

The front carriage schematizes the front axle to which the towing hook is connected, the rear carriage and the support simulate the two axles of the vehicle. It was chosen to adopt the support in the rear axle so as to consider the towing stresses and also simulate the case of the first rear axle lifted.

The **Figure 5.2** shows the representation adopted for the study of the structure and the main lengths. The **Figure 5.3** shows the reaction forces that are applied by the corresponding constraints.

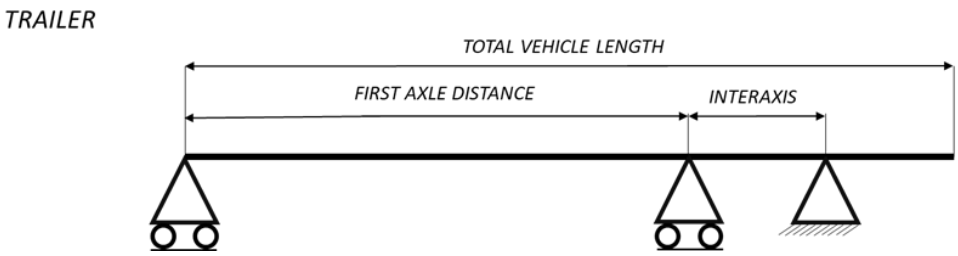


Figure 5.2: Scheme of the analytical beam model trailer

The **Figure 5.4** shows the loads on the structure. The distributed load represents the total mass of the vehicle distributed over the entire structure, the front and rear forces have been inserted as loads due to the weight of the rib that is to be unloaded on the beams and the horizontal force indicates the towing force exerted by the towing vehicle.

The **Figure 5.5** shows how the driving force that is applied between the self-driving and self-driven vehicle is evaluated.

$$D_{value} = g * \frac{T * R}{T + R}$$

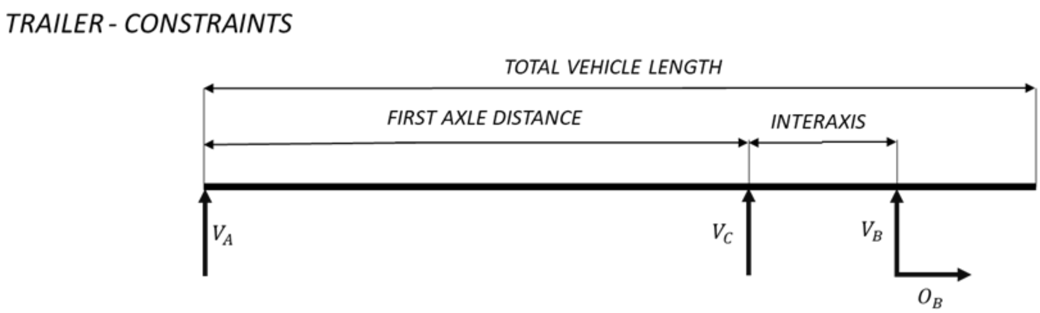


Figure 5.3: Scheme of reaction forces trailer

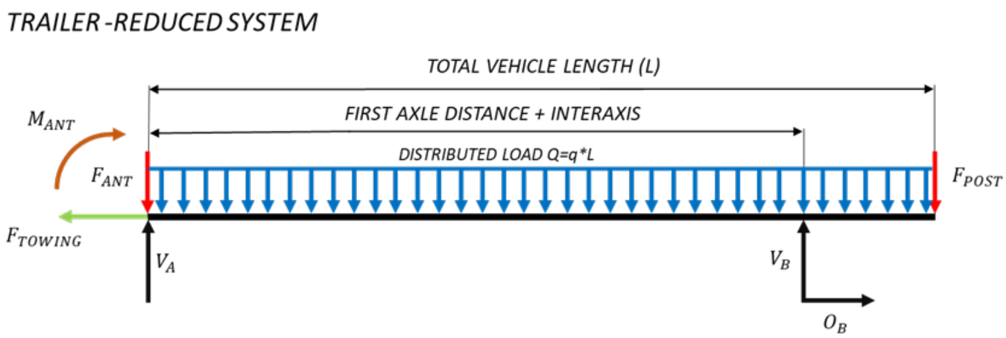


Figure 5.4: Analytical beam model trailer with loads

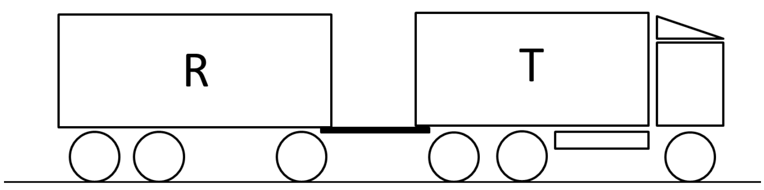


Figure 5.5: Driving force calculation trailer

Where:

- g is the gravity acceleration [9.81 m/$s^2$]
- T is the technically permissible mass, in tonnes, of the towing vehicle
- R is the technically permissible mass, in tonnes, of the trailer
- $D_{value}$ is defined as the theoretical reference load for determining the theoretical horizontal dynamic force exchanged between towing vehicle and trailer

The analytical resolution of the structure is presented as a 1-time overconstrained structure and was solved by considering the reduced system and then moving on to solve the additional system.

The bending moment, shear, and tension force trends were then summed between the two systems. The resolution of these systems was carried out both manually and then through the use of Matlab software so as to obtain the trends of the structure in its length. The **Table 5.2** shows the parameters that are inserted inside the MatLab program, the external stresses and the dimensions of the vehicle useful for the calculation.

Table 5.2: Parameters applied to the analytical model (TRAILER)

| PARAMETERS | | | | |
|---|---|---|---|---|
| DISTANCES | | | | |
| | L [m] | First axle [m] | Axles distance [m] | |
| | 8 | 4.7 | 1.5 | |
| LOADS | | | | |
| Q [kN] | Fant [kN] | Mant [kNm] | Ftowing [kN] | Fpost [kN] |
| 140 | 1.5 | 7.8 | 52 | 2.5 |

The **Figure 5.6** shows the reference system adopted for the study of the sections, the loads considered in the calculations and relative indications of the bending moment, shear and axial force.

The study of sections by analytical method reports the following trends:

In the above graphs of **Figure 5.7, 5.8, 5.9**, the loads trends along the longitudinal beam studied can be seen, the position of the two axles and the trailer hitch are also shown.

The graphs present the isostatic solution referred to the reduced system solution and the trends of the overconstrained solution relative to the entire

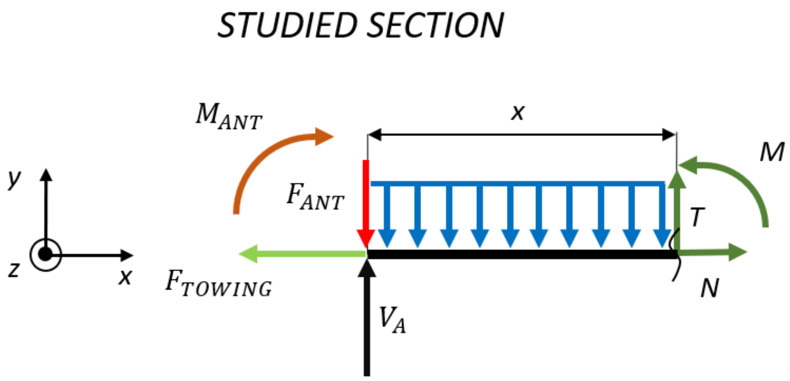


Figure 5.6: Section and reference system for analytical study

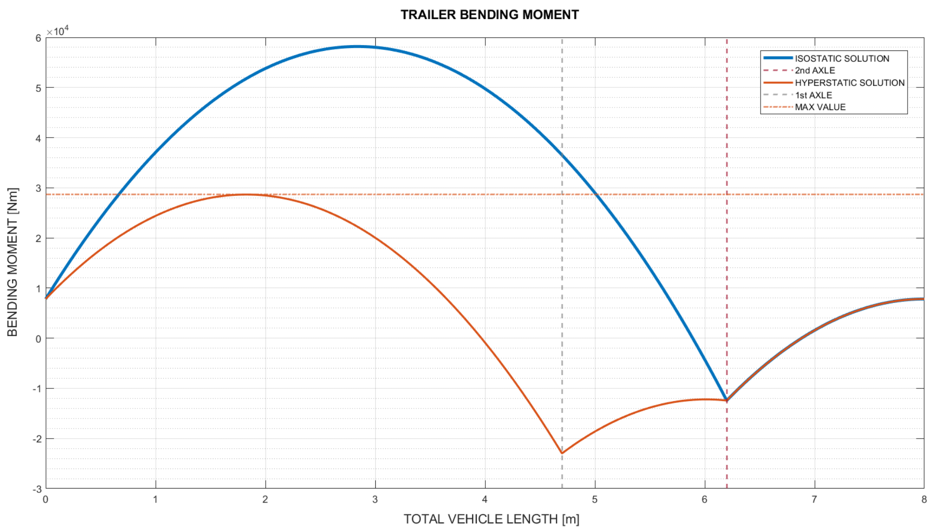


Figure 5.7: Trailer bending moment

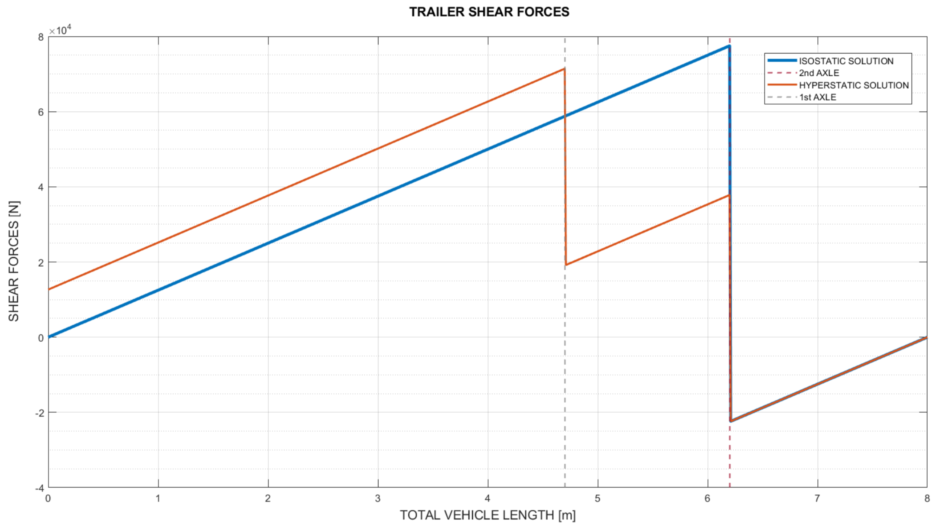


Figure 5.8: Trailer shear forces

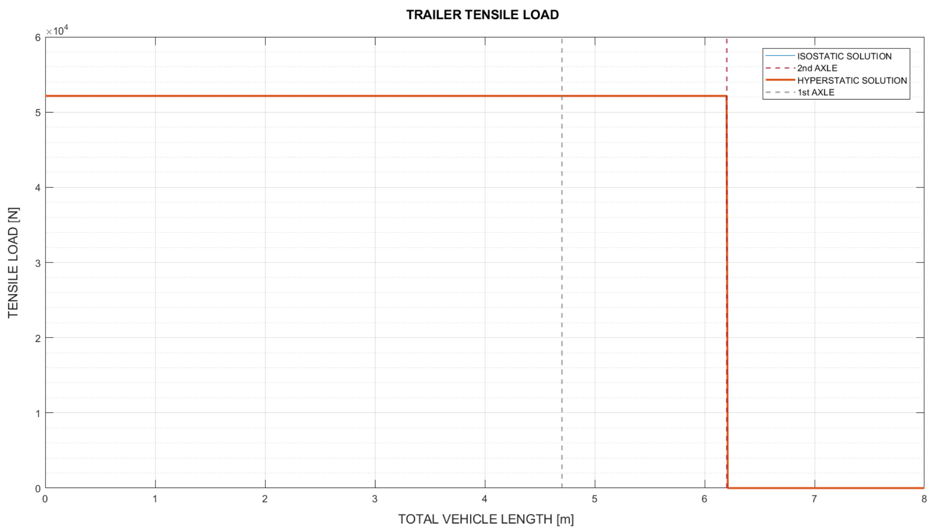


Figure 5.9: Trailer tensile load

system. It can be seen that the isostatic solution can also be considered as a solution adaptable to the case of the first liftable rear axle.

Considering the uniform section on the entire beam, it can be seen that the greatest stresses occur around the area of the two axes and, more precisely, it can be seen that the area of the first axis is the most stressed.

This first model, even if raw has allowed to understand which is the course of the stresses in the length of the beam, it has been possible therefore to understand which are the sections more stressed.

## 5.3 Semitrailer

The second product analyzed is the semitrailer (**Figure 5.10**). A two-axle semitrailer is considered as a case study, one of the most common, as seen in the previous chapter on the analysis of company volumes.

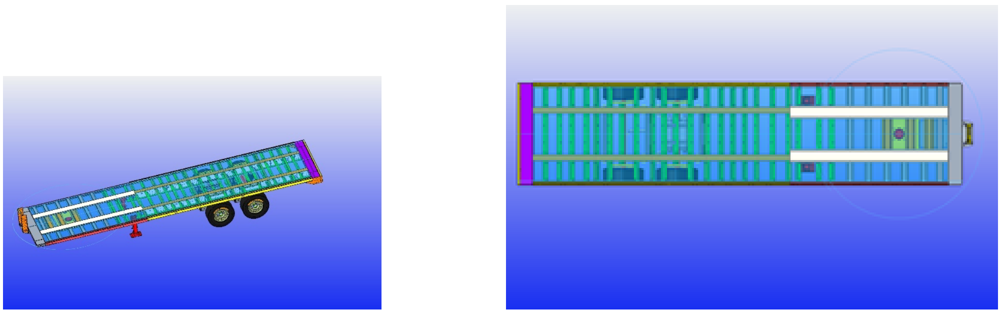

Figure 5.10: Views of the semitrailer vehicle

In the following **Figure 5.11** is reported the simple scheme of the semitrailer beam and **Figure 5.12** for the constraints are reported. The scheme used for the study of the structure, also in this case the main element studied is the longitudinal beam, however remain valid the regulations and the considerations on the applied forces carried out previously in the case of the trailer.

In the case of the semitrailer, the longitudinal beam will have a greater length than the previous one of the trailer. In this case, as can be clearly seen from the images (in particular **Figure 5.13**), an overhang has been inserted between the front part and the pin on which the semitrailer rests to be towed.

It can be seen that also in this case the system is overconstained, the constraints inserted are two carriages and a support (placed on the last axle of the vehicle).

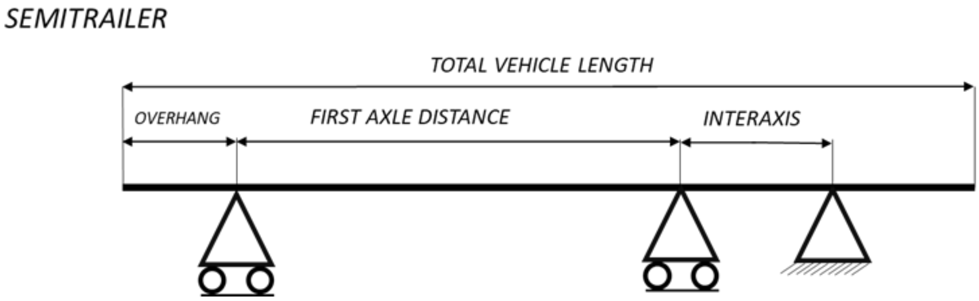


Figure 5.11: Scheme of the analytical beam model semitrailer

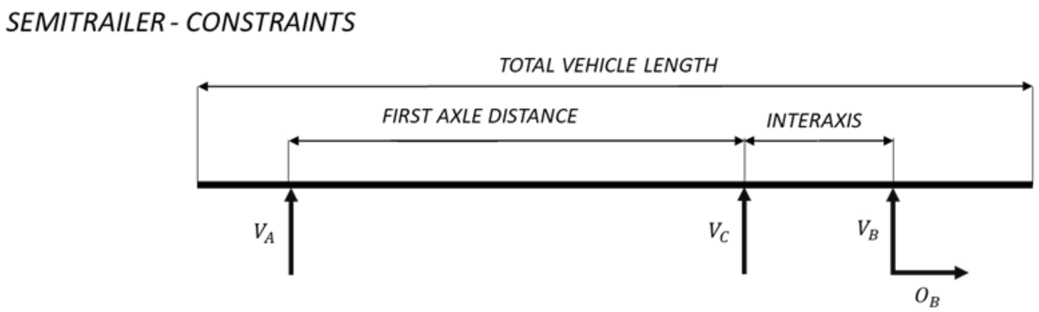


Figure 5.12: Scheme of reaction forces semitrailer

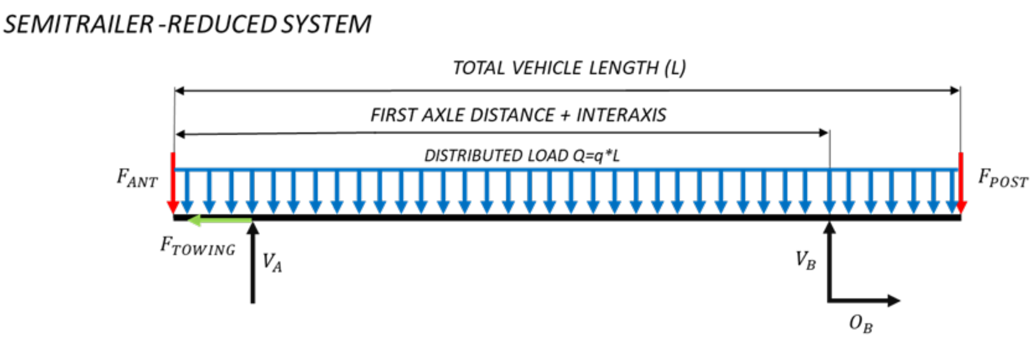


Figure 5.13: Analytical beam model semitrailer with loads

The figure **Figure 5.13** shows the complete reduced system of forces that will be studied for the evaluation of the stresses present on the studied beam.

Here is the formula for calculating the driving force exchanged between the vehicles:

$$D_{value} = g * \frac{0.6 * T * R}{T + R - U}$$

Where:

- g is the gravity acceleration [9.81 m/$s^2$]
- T is the mass of the tractor including the vertical load transmitted on the fifth wheel.
- R is the semitrailer mass
- U is the part of the mass of the semitrailer that weights directly on the fifth wheel.
- $D_{value}$ is defined as the theoretical reference load for determining the theoretical horizontal dynamic force exchanged between towing vehicle and trailer

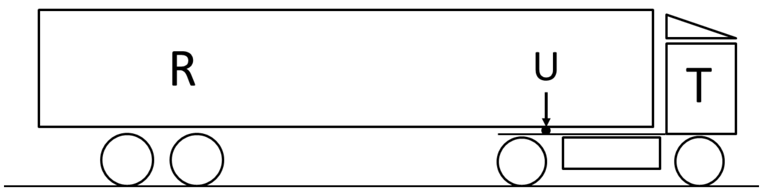


Figure 5.14: Driving force calculation semitrailer

The **Table 5.3** shows the forces and dimensions used for the structural calculation carried out of which will now be reported the results of the trends. As in the previous case of the trailer, section and reference system have been considered in the same way.

The graphs of bending moment, shear and axial tension are shown, in the graph it is also possible to observe the presence of the position of the two axles and of the kingpin.

Table 5.3: Parameters applied to the analytical model (SEMITRAILER)

| PARAMETERS | | | |
|---|---|---|---|
| DISTANCES | | | |
| Overhang [m] | L [m] | First axle [m] | Axles distance [m] |
| 0.9 | 13.6 | 7.3 | 1.5 |
| LOADS | | | |
| Q [kN] | Fant [kN] | Ftowing [kN] | Fpost [kN] |
| 190 | 2.0 | 61.8 | 3.0 |

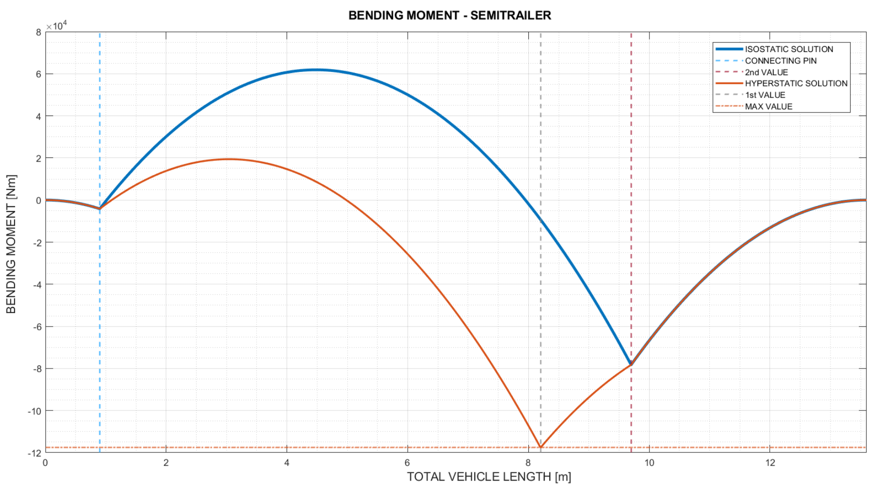


Figure 5.15: Semitrailer bending moment

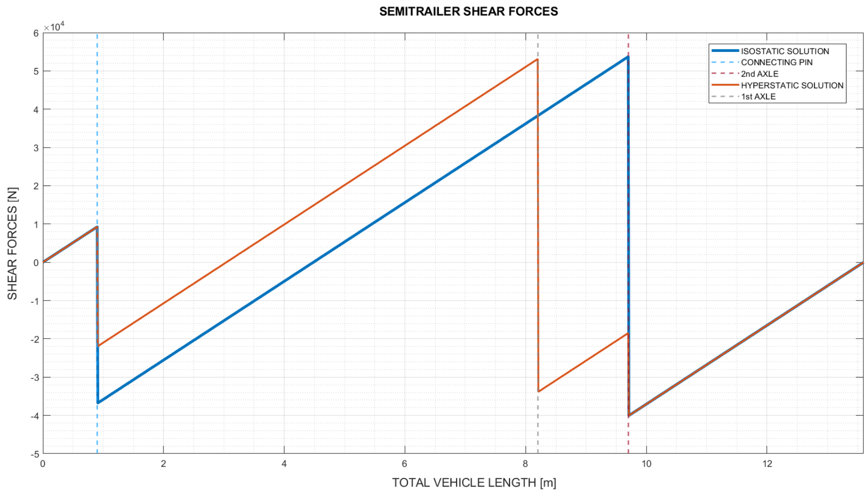


Figure 5.16: Semitrailer shear forces

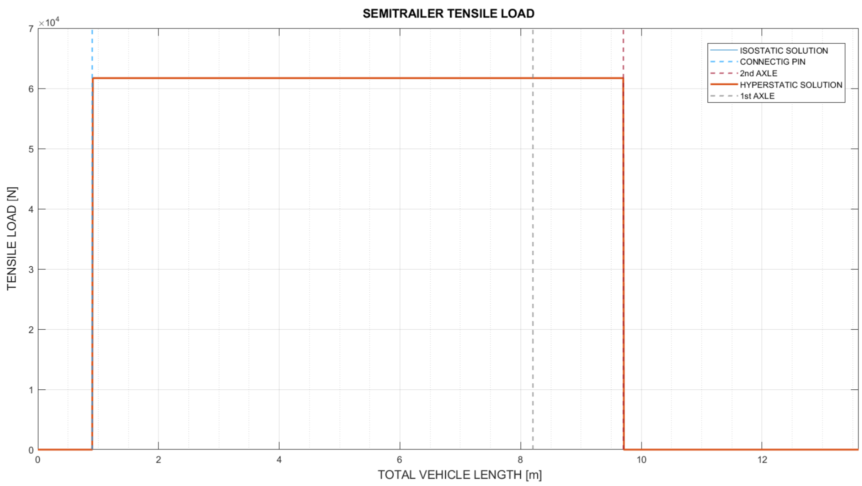


Figure 5.17: Semitrailer tensile load

## 5.4 Biga-trailer

Now the description of the biga-trailer is presented. In this case the schematization of the element has been a bit more complicated due to the fact that it presents an offset from the loading surface of the vehicle.

The overhang represents the part of the vehicle that connects with the towing vehicle and to which it is not possible to apply the distributed load.

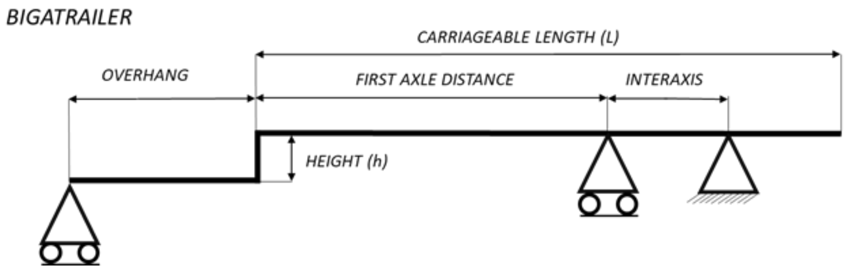


Figure 5.18: Scheme of the analytical beam model biga-trailer

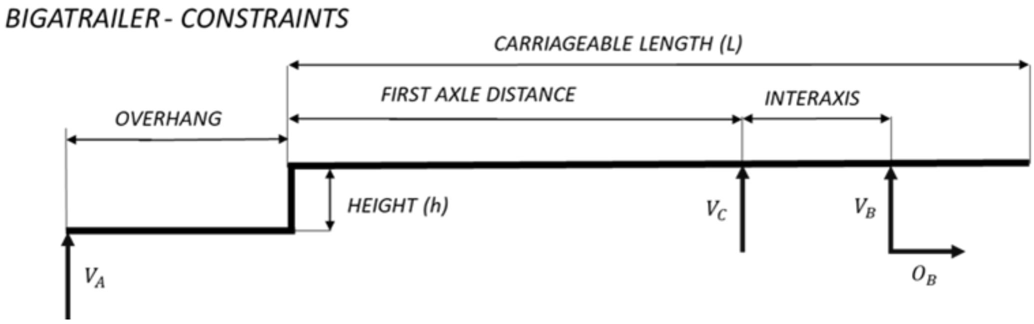


Figure 5.19: Scheme of reaction forces biga-trailer

The offset is schematized through the height (h) and overhang in the **Figure 5.18**. The constraints reported in **Figure 5.18** are two carriage (one mounted on the biga-driver coupling) and the other on the first axle, the support instead was placed in the second axle of the vehicle.

The solution of this model is presented as a overconstrained system and solving the reduced system (isostatic) it is possible to obtain the solution adaptable to the case with the first liftable axis.

The driving force calculation is reported also in this third case, as seen in the previous cases, however in this last example not only the weight of the vehicles is involved in the calculation but also the lengths of the vehicles themselves.

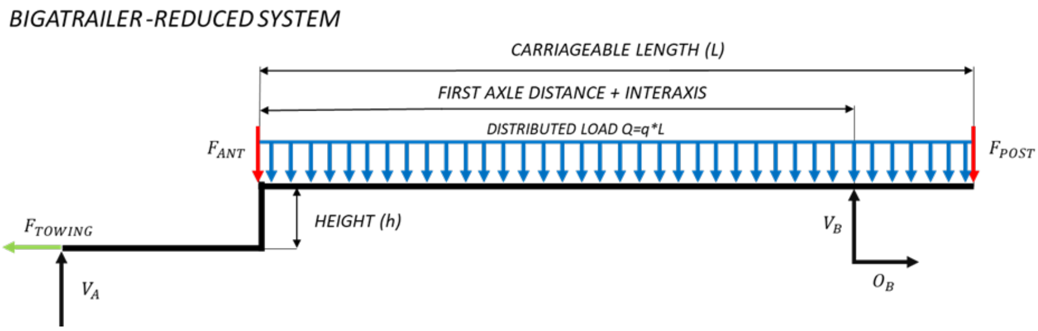


Figure 5.20: Analytical beam model biga-trailer with loads

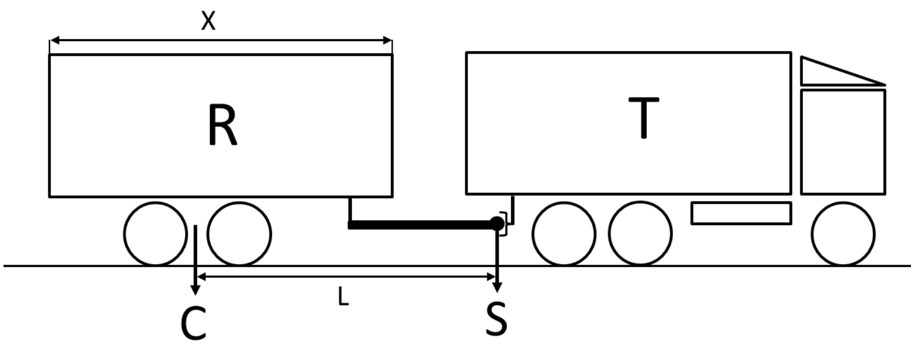


Figure 5.21: Driving force calculation biga-trailer

Table 5.4: Parameters applied to the analytical model (BIGA-TRAILER)

| PARAMETERS | | | | |
|---|---|---|---|---|
| DISTANCES | | | | |
| Height [m] | Overhang [m] | Carr. length [m] | First axle [m] | Axles dist. [m] |
| 0.3 | 2.4 | 8.0 | 3.25 | 1.5 |
| LOADS | | | | |
| Q [kN] | Fant [kN] | Ftowing [kN] | Fpost [kN] | |
| 75 | 1.5 | 57.5 | 2.5 | |

$$D_{value} = g * \frac{T*C}{T+C}$$

Where:

- g is the gravity acceleration [9.81 m/$s^2$]
- T represents the maximum technically permissible mass, expressed in tons of the towing vehicle including the static vertical load transmitted to the hook by the eye;.
- C represents the sum, expressed in tons, of the maximum axial loads that the trailer transmits to the ground.
- $D_{value}$ is defined as the theoretical reference load for determining the theoretical horizontal dynamic force exchanged between towing vehicle and trailer

As seen for the previous cases, the trends of bending moment, shear and axial force are reported; the indications of the positions of the axes and the end of the nose are also reported with lines parallel to the y-axis.

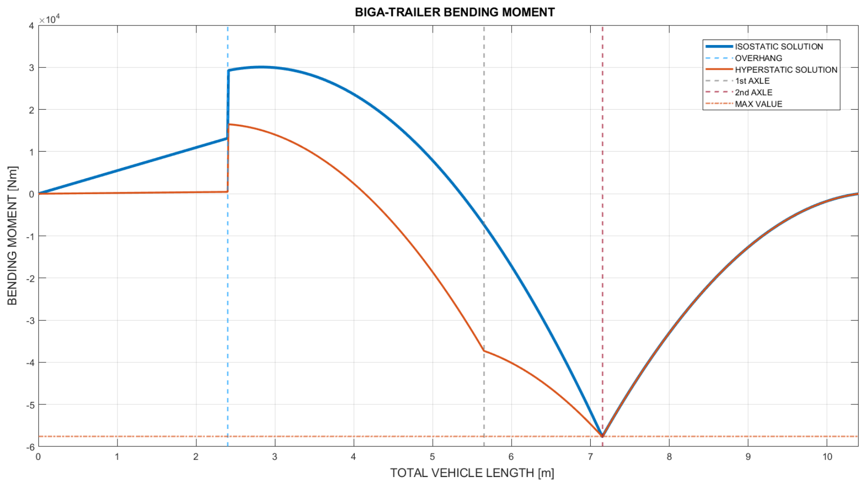


Figure 5.22: Biga-trailer bending moment

Considering the **Figure 5.22** it can be seen that the bending moment is maximum on the second axis of the vehicle. The area around the second axis will represent the area most stressed by bending.

This chapter has allowed to face the calculation of the structures in an analytical way in order to have a first idea of the stress trends in the company vehicles.

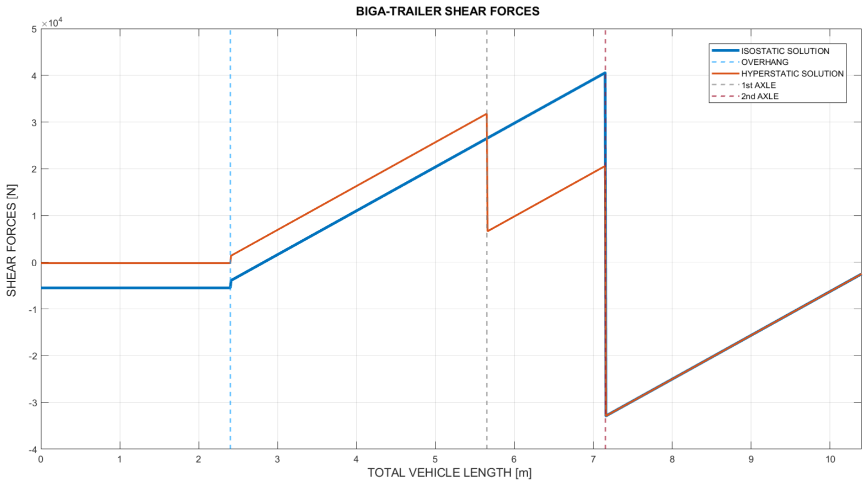


Figure 5.23: Biga-trailer shear forces

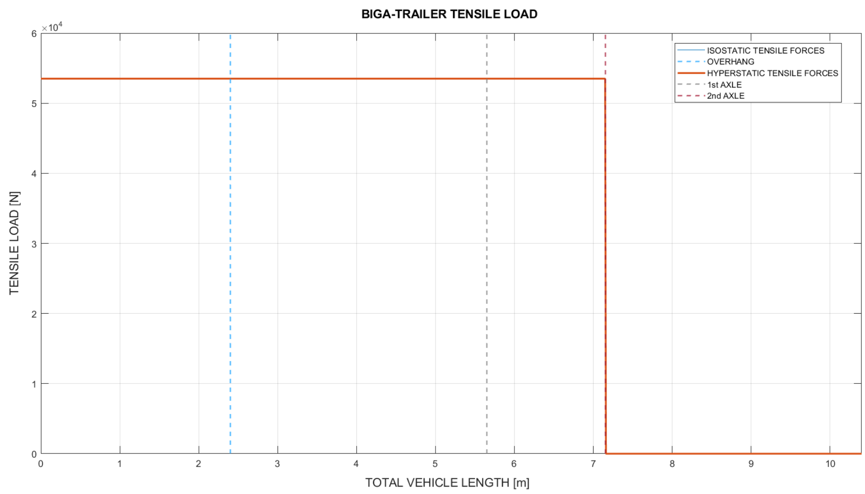


Figure 5.24: Biga-trailer tensile load

# Chapter 6

# Finite Element Analysis

Following the analytical analysis carried out with the aid of Matlab software, it is now possible to move on to finite element analysis. Altair Hypermesh was chosen as software for FEM analysis.

The finite element study was carried out step by step, starting from the longitudinal beam element and then adding components to get a description of the entire frame. As for the analytical analysis, the three vehicles were studied: trailer, semi-trailer and biga-trailer.

The description of the applied model for the finite element analysis is now discussed.

## 6.1 Model definition

### 6.1.1 Section definition

As it will be had occasion to see in the next sections, it has been started from the simplest element of the structural frame that is the beam in order then to pass to a simplified model of the various vehicles.

As a first approximation the longitudinal beam is considered as a 1D element since it has the dimensions of the section much smaller than its entire length.

### 6.1.2 Material

As an element within the software, the characteristics of the structural material S355J0 have been inserted.

### 6.1.3 Loads and constraints

Then resuming the sections of **Chapter 5** where the loads for the analyzed structures have been defined, they are now applied to the FEM model.

More in detail it has been applied concentrated loads on the rear part and on the front part in order to simulate the weight due to the parts installed on the chassis and then is added the maximum loadable weight for each vehicle as distributed load.

### 6.1.4 Elements study

Given the complexity of the entire vehicle and chassis, it is chosen to analyze the vehicles by subdividing them into components and studying each of them to arrive at the entire vehicle chassis assembly.

The study was conducted on the three vehicles already seen in the analytical case in order to verify the correctness of the analytical method and the deviation between the analytical and the finite element analysis.

In this case the structure has been realized with PTC CREO Parametric 5.0 software and then imported into Altair Hyperworks as geometry and a 1D mesh has been executed on it.

### 6.1.5 Beam element

As a first study it is considered the longitudinal beam of the vehicle as studied in the analytical section, in this case Altair Hypermesh 1D model is used and the studied section is created by 'HyperBeam' function. In the analyzed case, the beam with double T section is taken (the dimensions of it are reported in the **Figure 6.32** and the dimensions come from the analytical model. The length of the beam was considered of the same dimensions as in the analytical case.

The stress trend has been obtained thanks to the activation of the 'CHARACTERSTIC 2' command inside the 'PROPERTY' section.

## 6.2 Trailer

### 6.2.1 Longitudinal beam trailer

The structure of the beam and the constraints are visible in the **Figure 6.1**, the force due to the distributed load has been divided for the different nodes on the structure and are reported in **Figure 6.2**.

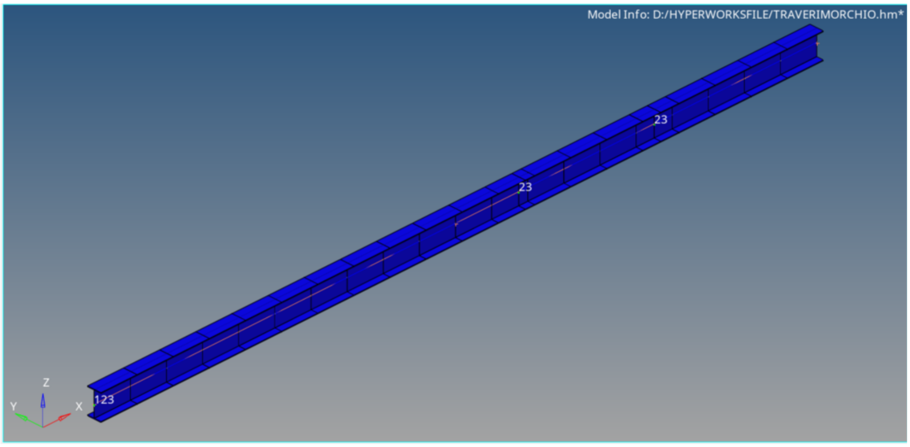


Figure 6.1: Trailer beam on Hypermesh

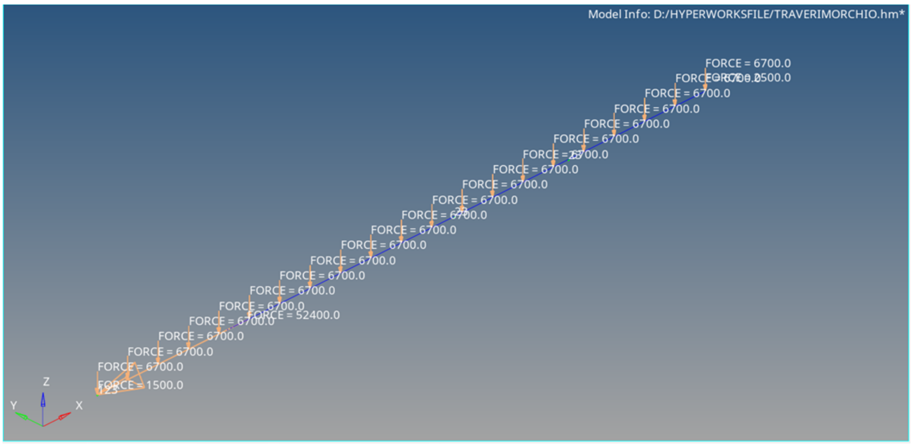


Figure 6.2: Load and constraints focus on trailer beam

Since the model is constituted from nodes, the simulation carried out sees the application of the distributed load divided between the various nodes that compose the structure. In the creation of the model of the beam it has been tried to choose a compromise of the number of the nodes, it has been limited an excessive number in order not to weight too much the calculator and at the same time an adequate number in order to make that the model had a good quality of simulation.

### Results

The figure **Figure 6.3** shows the deformation of the beam in the XZ plane, as shown in the figure the greatest deformation caused by the load is in the final part of the vehicle; another part that presents a deformation to be noted is the part that is between the front axle and the first rear axle. The deformation scale shown in the figure is expressed in mm. The results obtained are reliable since experience has shown that the deformation of the vehicle is about 10 mm at full load. The obtained results can be considered acceptable.

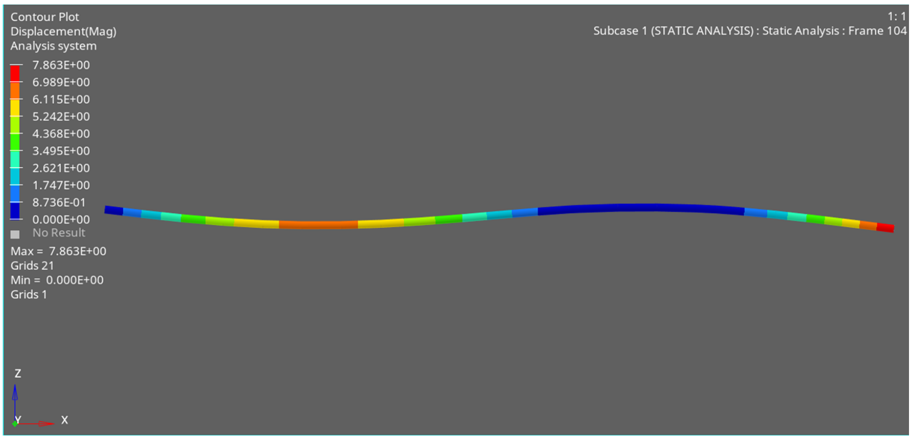


Figure 6.3: Deformation of trailer beam

The figure **Figure 6.4** shows the distribution of stresses on the trailer beam, the scale shows values in MPa. As shown in the figure, the maximum stress distribution is in the area corresponding to the axles, while the rest of the structure is more unloaded.

The load applied to the vehicle, represents the structure loaded with the maximum distributed load.

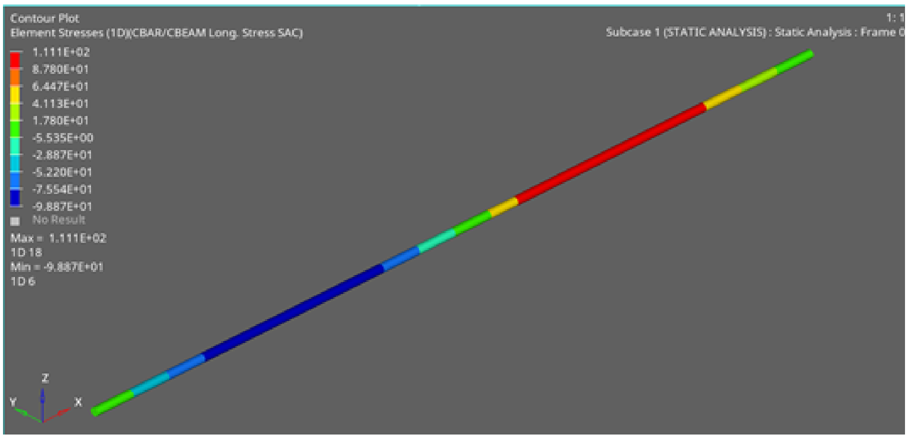


Figure 6.4: Equivalent stress on trailer beam

### 6.2.2 Simple frame trailer

The second step carried out in the finite element study was to introduce the central crossbeams that represent the axles and the external profile of the vehicle with side members and front and rear heads.

The front and rear headers and the side members were also considered as 1D elements, but this time with a C section (visible in **Figure 6.32**). The crossbars that indicate the axles instead have been considered as 1D elements with closed circular section. (**Figure 6.5** )

The constraints in this case have been applied to the intersection between the longitudinal beams and the crossbeams that indicate the axles, while the front supports have been positioned on the longitudinal beams at a distance equal to the front overhang.

Regarding the applied forces, the distributed load was placed on the two longitudinal beams and two additional loads simulating the forces of the rear doors and the front beam were applied at the front and rear of the frame.

The results shown in the **Figure 6.6** and **Figure 6.7** show as expected a smaller deformation than in the case of the simple longitudinal beam.

### 6.2.3 Complete frame trailer

As the last step of the finite element analysis, the lateral crossbeams have been inserted, which are going to perform the task of joining the longitudinal beams with the lateral stringers and will also be the support on which the flooring will be mounted.

The application of the constraints and loads remained unchanged from the simple frame case seen above.

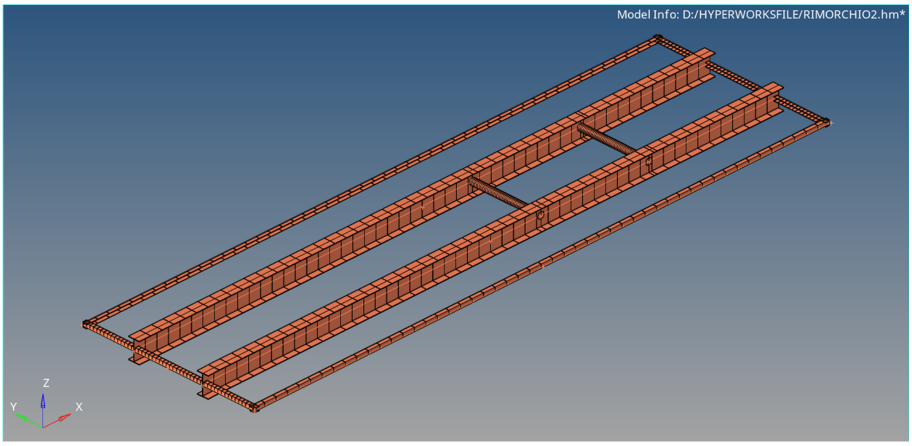


Figure 6.5: Simple structural trailer chassis

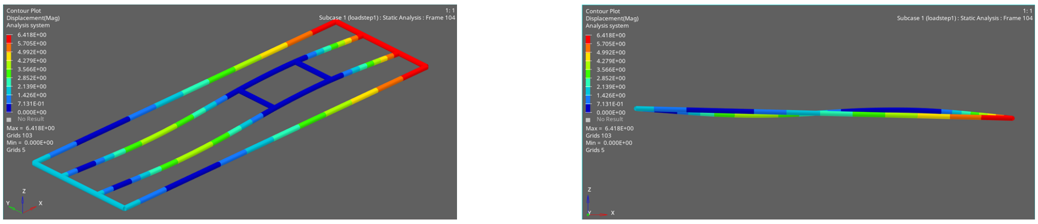

Figure 6.6: Deformation of simple trailer chassis

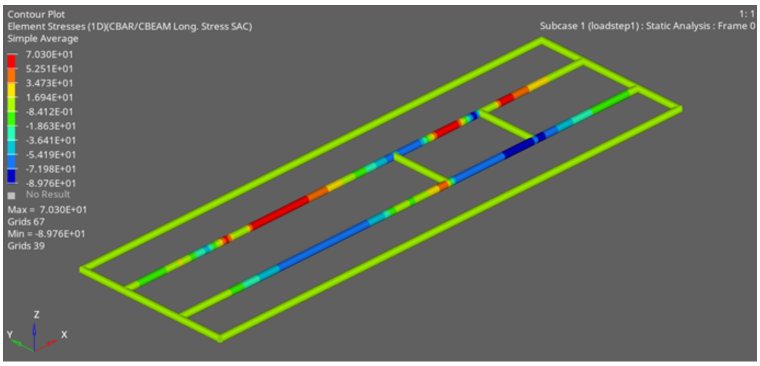


Figure 6.7: Equivalent stress of simple trailer chassis

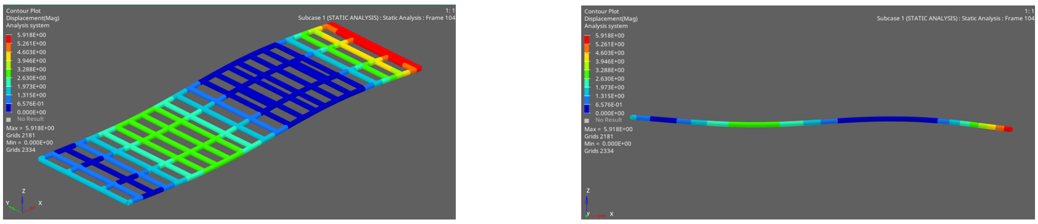

Figure 6.8: Deformation of complete trailer chassis

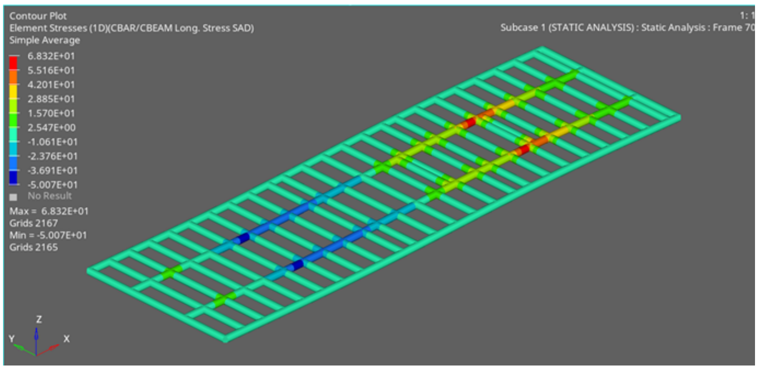


Figure 6.9: Equivalent stress of complete trailer chassis

The results of (**Figure 6.8**), show that the deformation of the structure and the most deformed parts are as seen above, there is however a decrease in the maximum deformation due to increased stiffness of the frame as a whole.

With regard to stresses (**Figure 6.9**), in the image can be seen the distribution of them in the entire structure, it is partially loaded throughout the frame, it is also noted the points with higher value of stress that, as expected are in the part of the axles.

## 6.3 Semitrailer

### 6.3.1 Longitudinal beam semitrailer

The study of the semi-trailer is now carried on, also in this case the constraints and the distributed load have been included as in the analytical study.

As first part is studied the longitudinal beam with the known double T section and dimensions reported in **Figure 6.32**. The **Figures 6.10,6.11**, report the application of constraints and the loads applied to the semitrailer longitudinal beam.

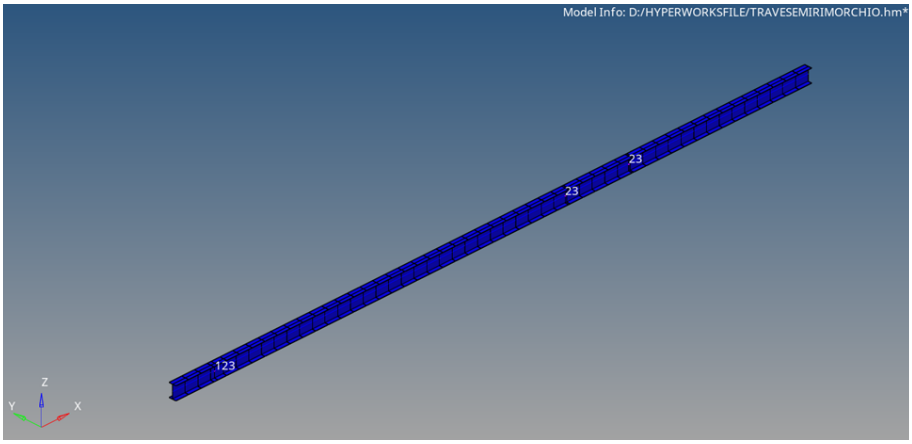


Figure 6.10: Semitrailer beam on Hypermesh

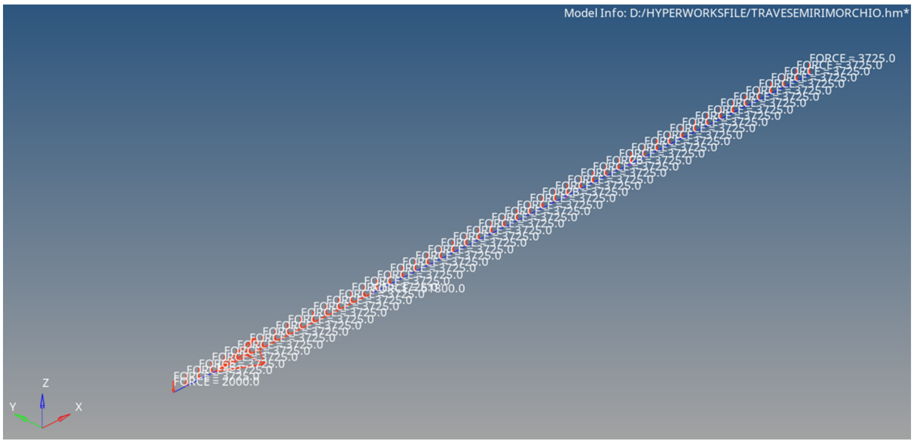


Figure 6.11: Load and constraints focus on semitrailer beam

The **Figure 6.12** shows the overall deformation of the semi-trailer vehicle, in this case the greatest vertical deformation (arrow) occurs at the rear end of the beam and is about 98 mm, this value is similar of what is known from the experience.

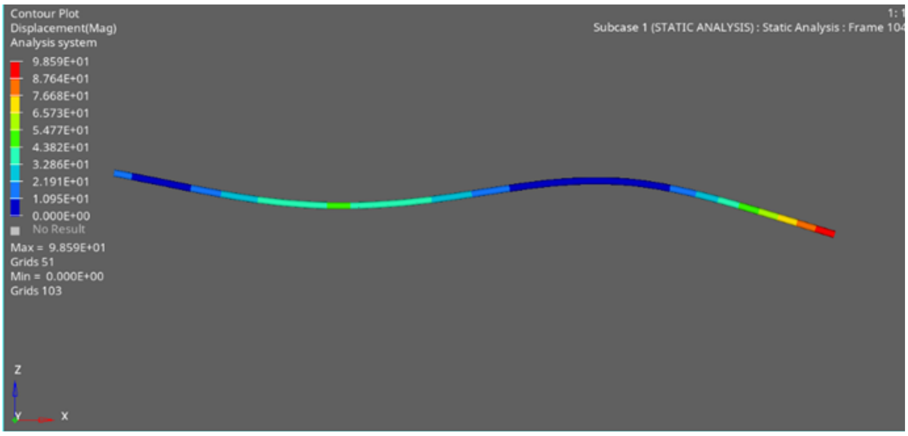


Figure 6.12: Deformation of semitrailer beam

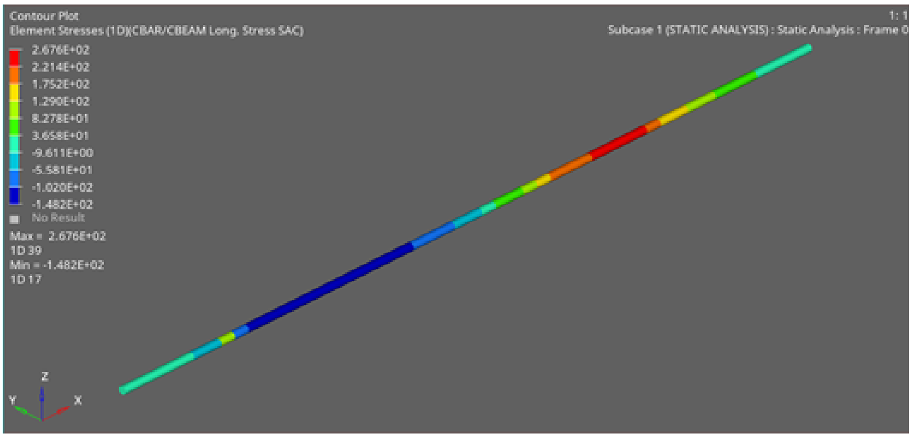


Figure 6.13: Equivalent stress of semitrailer beam

The **Figure 6.13** shows the stress in the semitrailer beam, as already known from the case of the trailer the most stressed section is located around the axles.

### 6.3.2 Simple frame semitrailer

As in the case of the trailer seen previously, having studied the longitudinal beam, now the study focus on the insertion of some additional components such as the side members, the two crossbars of the axles and in this case a crossbar representing the position of the tow hook has been inserted in the front part.

Lateral side members, front and rear header have been considered as C sections of similar dimensions to those realized by the company while the crossbars have been maintained as in the previous case with a closed ring section. The sections are visibile in (**Figure 6.32**) and the simple frame semitrailer is reported on **Figure 6.14**.

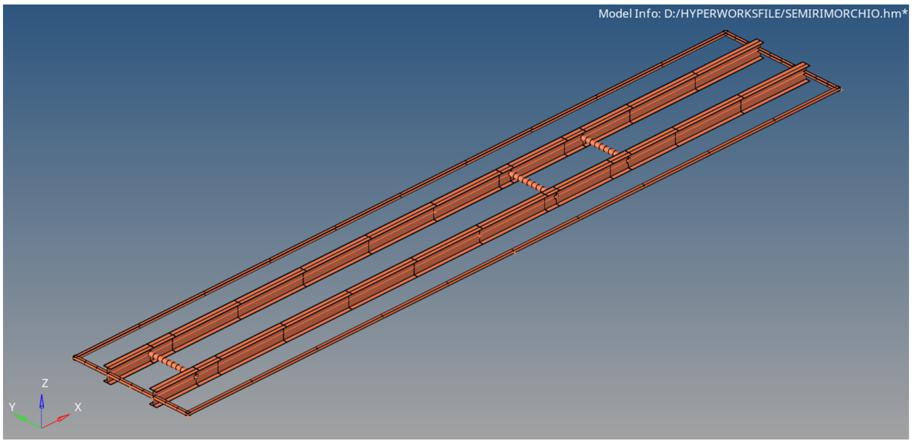


Figure 6.14: Simple semitrailer chassis

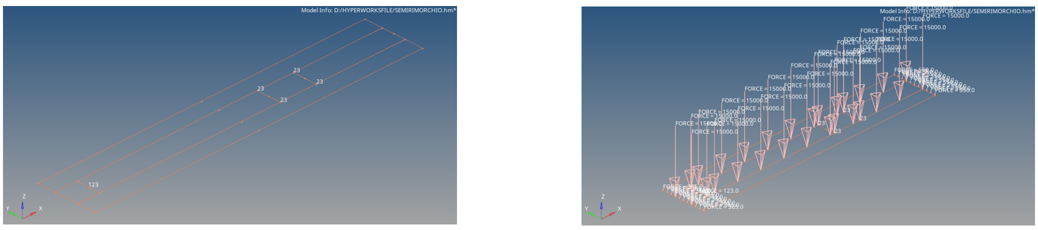

Figure 6.15: Loads and constraints on simple semitrailer chassis

The two images of **Figure 6.15** represent the applied constraints and loads, as it is possible to see the constraints that are applied on the axles and on the towing hook.

The applied forces are taken from the analytical case and are therefore forces on the front and rear heads and distributed load applied to the longitudinal beams.

In the **Figure 6.16** is shown the overall deformation of the structure studied, it can be seen that the part of the frame where the arrow is greater is the rear as already seen above.

It has been chosen to study the longitudinal beam of the semi-trailer with the same section as the trailer because in the case of the semi-trailer it results to be the smaller section applied in the projects of such frame and moreover it is possible to compare the two results obtained in order to draw the right considerations for the next part of the project.

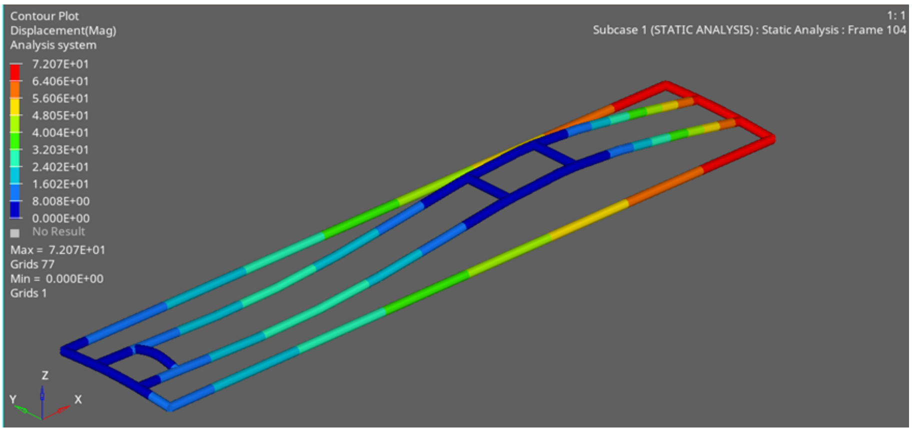


Figure 6.16: Deformation of simple semitrailer chassis

The **Figure 6.17** shows the stresses in MPa that are obtained in the structure studied, also in this case the part of the vehicle most stressed turns out to be the part related to the axles and in particular the rear part of the second axle, there is also a total stress that is distributed over the entire structure.

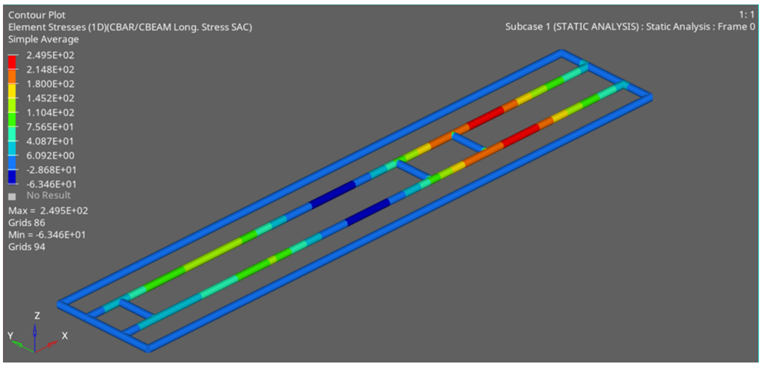


Figure 6.17: Equivalent stress of simple semitrailer chassis

## 6.4 Biga-trailer

### 6.4.1 Longitudinal beam biga-trailer

As seen for the trailer and semi-trailer cases the biga-trailer is now studied. It starts from the simplest case of the longitudinal beam.

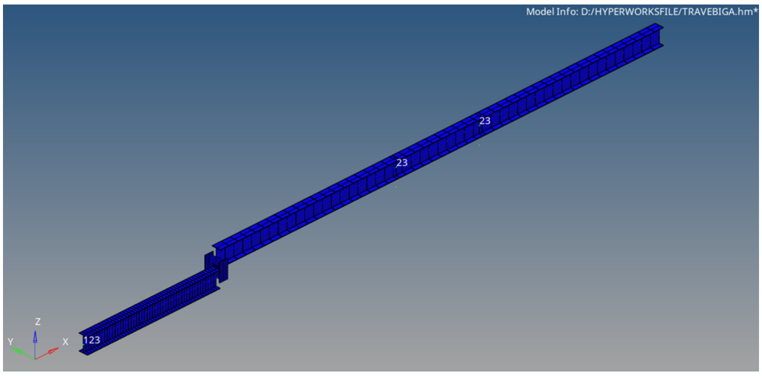


Figure 6.18: Constraints applied to the biga long. beam

The **Figure 6.18** and **Figure 6.19** are representative of the constraints inserted and of the loads applied to the structure, as seen in the analytical case there are two constraints (carriage in the first axle and support in the second one) in the presence of the two axles while the third is placed in the towing hook (another carriage) of the vehicle.

It has been chosen to constrain in the two translational degrees of freedom the axles and the trailer hook as established by law, the hook also has the first translational degree bound that go to simulate the towing of the vehicle.

The forces applied on the beam are the distributed load of the vehicle, in the front and rear part of the loaded part have been inserted the front and

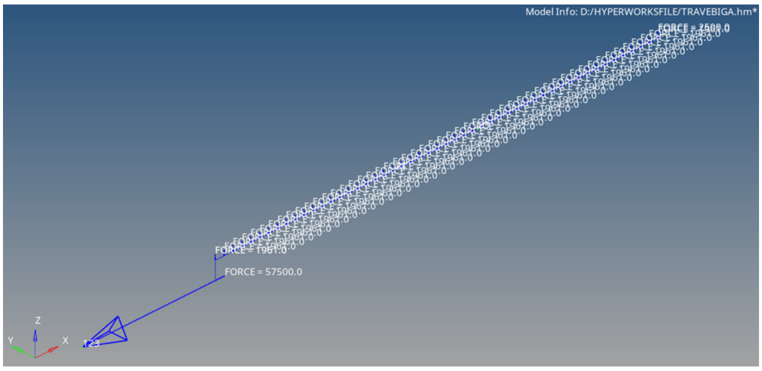


Figure 6.19: Loads applied to the biga long. beam

rear forces related to the weight force unloaded by the rib and in the hook has been reported the horizontal towing force.

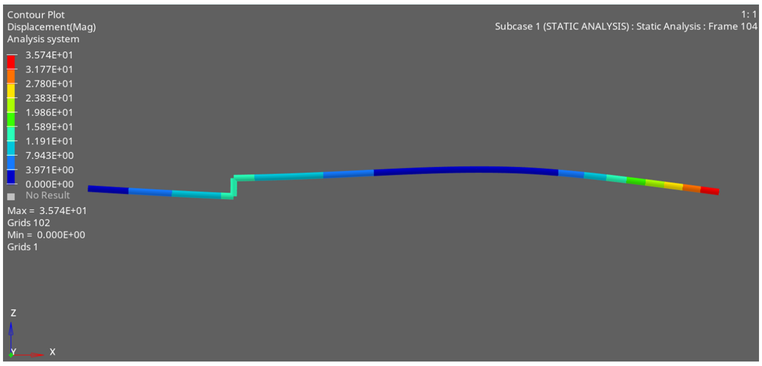


Figure 6.20: Deformation of biga long. beam

The **Figure 6.20** shows the deformation of the biga beam considered, the maximum deformation is in the rear part of the vehicle, note to be considered is also the front deformation that occurs in this case due to the presence of the tow hook positioned differently than in the two previous cases.

In **Figure 6.21** it is reported the stress related to the studied beam, also in this case the beam section is a double T with the same dimensions of the previous cases, (always reported in **Figure 6.32**).

The most stressed part results to be the central part of the vehicle body where also this time there are the axles of the vehicle. The front carriageable part presents negative stresses, while the rear part and the overhang part are also stressed with positive stress.

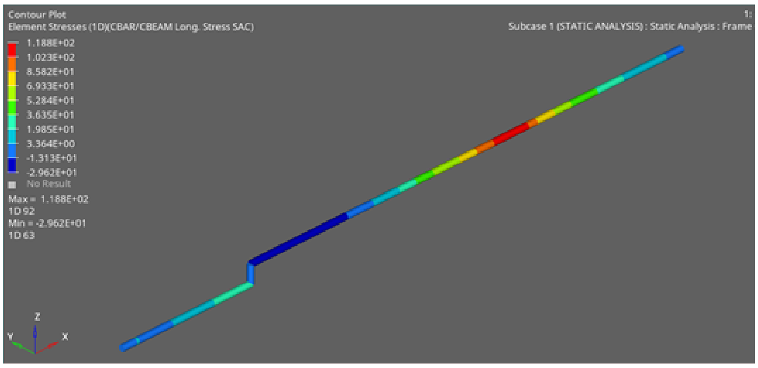


Figure 6.21: Equivalent stress of biga long. beam

### 6.4.2 Simple frame biga-trailer

In the case of the simple biga frame it is chosen to study two different cases, the difference between these studies is related to the front configuration with which the drawbar is assembled with the vehicle body frame. In the first case there is only one triangular system of crossbars (**Figure 6.22** left) while in the second there are two anchorage points of the drawbar (**Figure 6.22** right).

The second configuration represents the case currently in production while the first represents a more simplified case that is no longer in production.

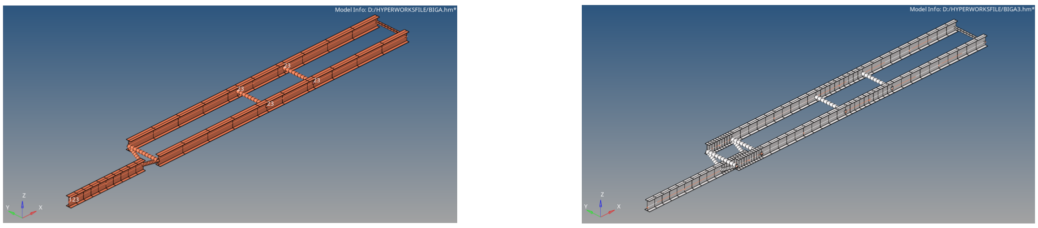


Figure 6.22: Simple biga-trailer chassis in the two configurations

In both cases the constraints were applied in the same way. As in the analytical case studied the second axis was also constrained in translational motion along its axis.

The loads applied also in this case are the load distributed on the longitudinal beams, the towing force applied to the hook and the forces due to the weight of the rib applied on the front and rear rails (**Figure 6.23**).

The **Figure 6.24** and **Figure 6.25** show the deformations (arrow) of both frames studied. As it can be well seen from the scale, the second configuration allows to obtain values of deformation much smaller than the

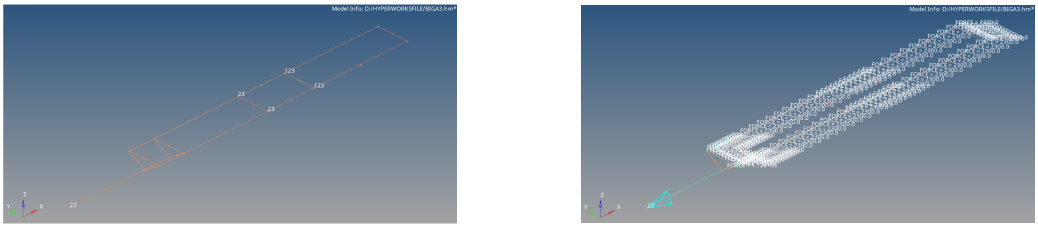

Figure 6.23: Simple biga-trailer chassis with constraints and loads

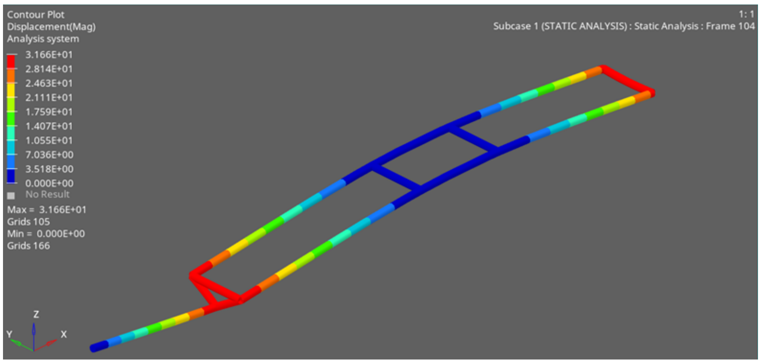


Figure 6.24: Total deformation of simple biga chassis 1st config.

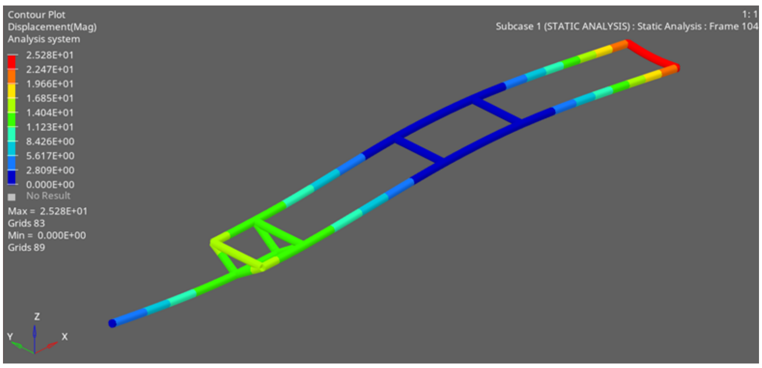


Figure 6.25: Total deformation of simple biga chassis 2nd config.

first case and above all such difference is noticed in the front part where before the displacement was very evident and now it results very reduced, another consideration that can be drawn is that in this second case the deformation goes to distribute itself much more uniformly in comparison to the first case. The part with greater deformation results however always to be the rear part of the vehicle.

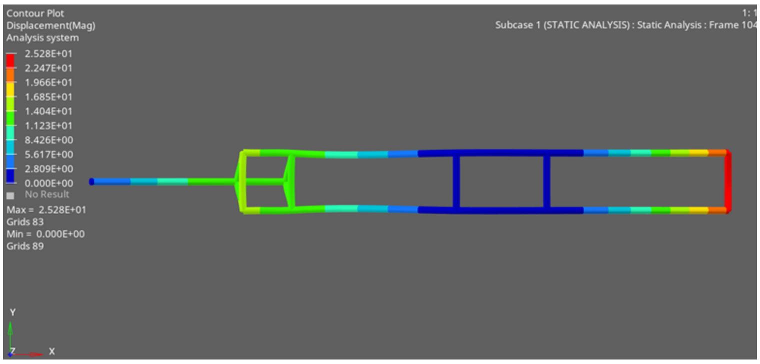


Figure 6.26: Top view of biga simple chassis deformation

The **Figure 6.26** shows a top view of the frame, this sight allows to highlight that in both cases the driving force goes to create an effect that tends to approach the two longitudinal beams between the second support of the overhang and the first axis of the vehicle.

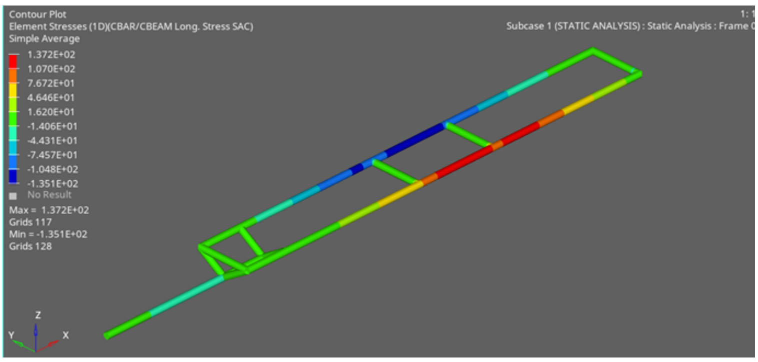


Figure 6.27: Equivalent stress of biga simple chassis

The stresses are shown in the **Figure 6.27**, as can be seen, the load prompts more the sections close to the axles, in this case there are stresses with the same module but opposite direction in the two longitudinal beams.

### 6.4.3 Complete frame biga-trailer

As seen in previous cases, this final analysis of the biga frame includes the side members, the cross members joining the longitudinal beams to the side members, and the front and rear portions. Constraints (**Figure 6.28**) are applied in the same manner as in the previous cases, the front and rear loads distributed across the front and rear shoulders (**Figure 6.29**).

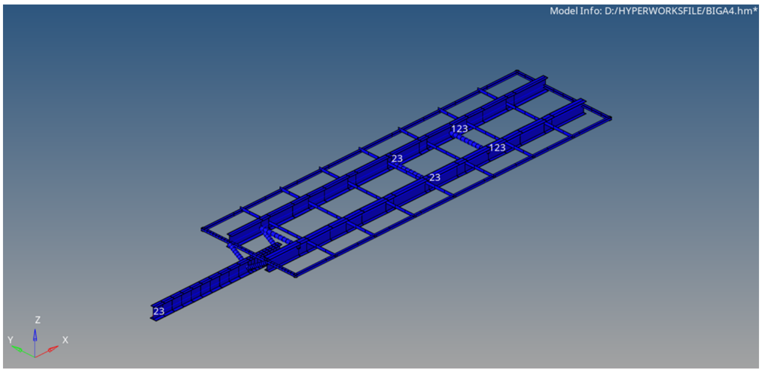


Figure 6.28: Complete structural frame of the biga-trailer

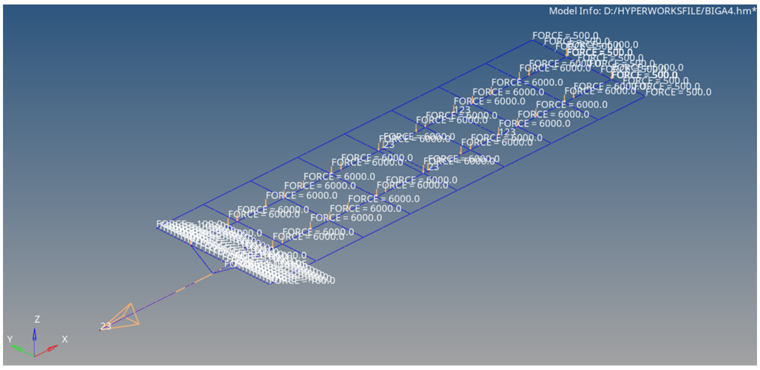


Figure 6.29: Complete frame biga (loads and constraints)

The deformation of the complete frame is shown in **Figure 6.30**, the largest deformation can be seen in the front and rear corners of the frame where the distance from the constraint is greatest.

From the finite element analysis it is possible to obtain the trend of stresses (**Figure 6.31**) acting on the structure of the complete frame, as expected the most stressed part is located between the two axles of the vehicle.

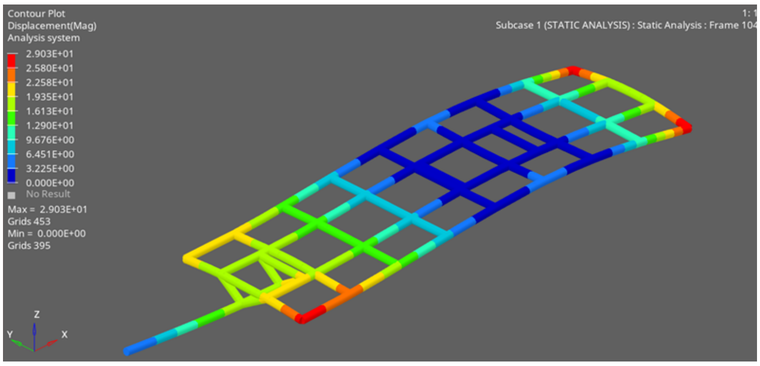


Figure 6.30: Defromation of complete structural frame of the biga

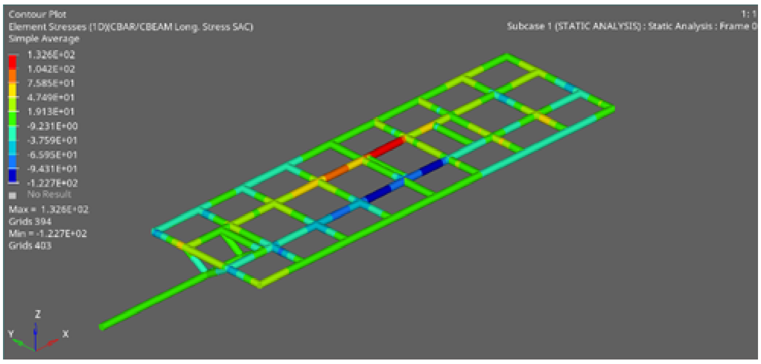


Figure 6.31: Equivalent stress of complete structural frame of the biga

The maximum stress is lower than in the case of the single beam, this is due to the fact that the entire structure goes to download the weight in a more uniform way.

### 6.4.4 Sections used in the various 1D numerical studies

The dimensions and type of sections used in the HyperMesh software for the evaluation of the studied stresses and deformations are shown below.

- Section used for longitudinal beams: double T section
- Section for suspension beams: ring
- Section for longitudinal beams-beams connection: L-shaped section
- Section for front and rear header and side members: C section

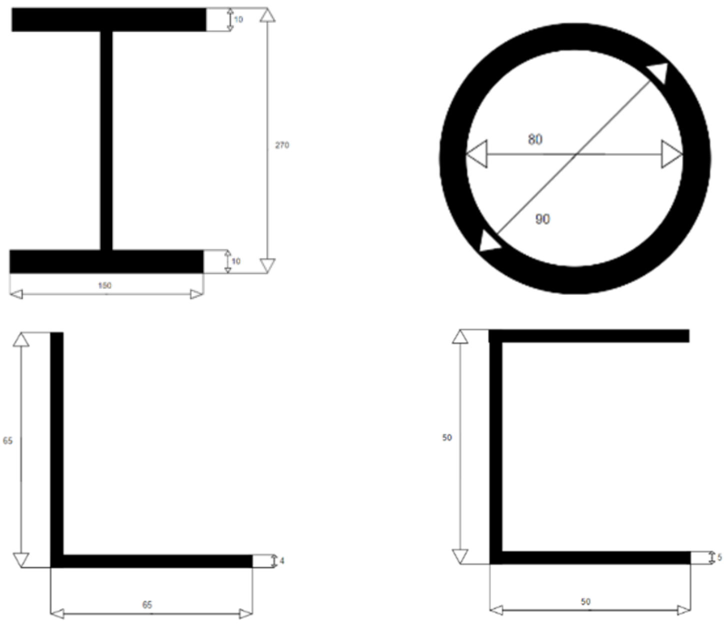


Figure 6.32: Sections used for the models

# Chapter 7

# Analytical against numerical results

This chapter discuss the comparison between analytical and numerical results.

The analytical results are obtained using the formula reported in **Chapter 5** and the numerical results are obtained by the simulation done using the software Altair Hypermesh and shown in **Chapter 6**.

It will now be reported the results obtained for the three vehicles examined. The stresses reported concern the greatest load on the structure, that is the load due to bending.

In the analytical case, obtained the value of the bending moment as seen in the graphs shown in the figure, the stress is then calculated according to the formula:

$$\sigma_{bending} = \frac{M_{bending}}{W_z}$$

Where:

- $\sigma_{bending}$= stress due to bending.
- $M_{bending}$= bending moment.
- $W_z$= modulus of resistance to bending with respect to the z axis.

$$W_z = \frac{B*H^3-b*h^3}{6*H}$$

The parameters for the calculations are reported in **Figure 7.1**

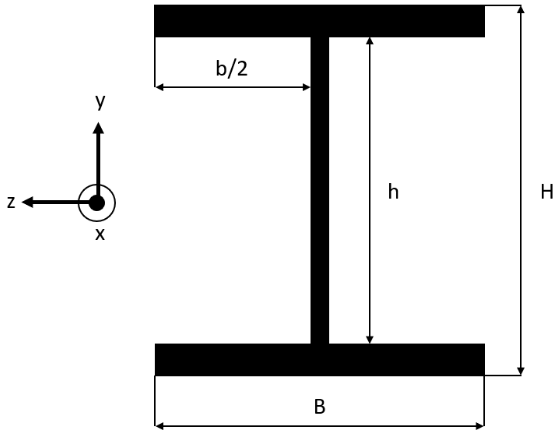


Figure 7.1: Double-T section with reference system

### Trailer

Analyzing the results obtained for the first vehicle, reported in **Figure 7.2**, it is possible to notice the goodness of the same, as it is noted in fact the difference between numerical and analytical results to be in its maximum value (in the first axis) around 15% while in some traits as in the final part after the second axis the numerical and analytical values have the same trend.

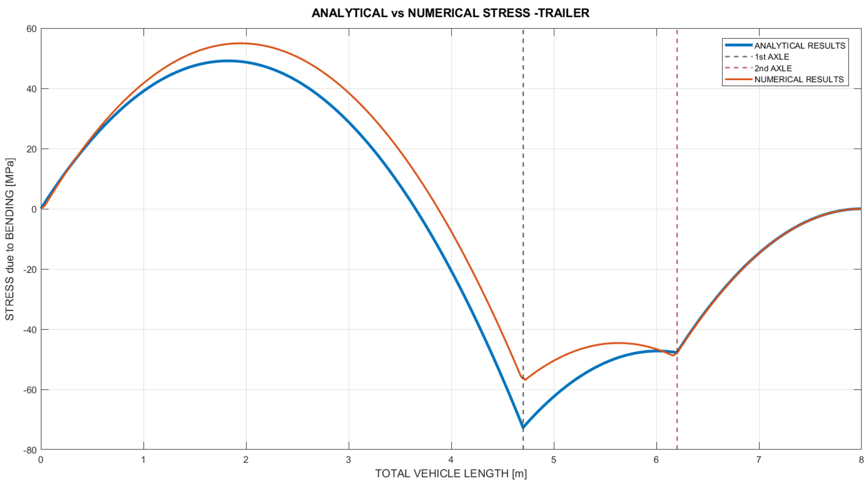


Figure 7.2: Analytical vs Numerical stress trailer

### Semitrailer

Passing now to the analysis of the second vehicle, the semi-trailer. As can be seen from **Figure 7.3**, the numerical and analytical results in this one are also close to each other.

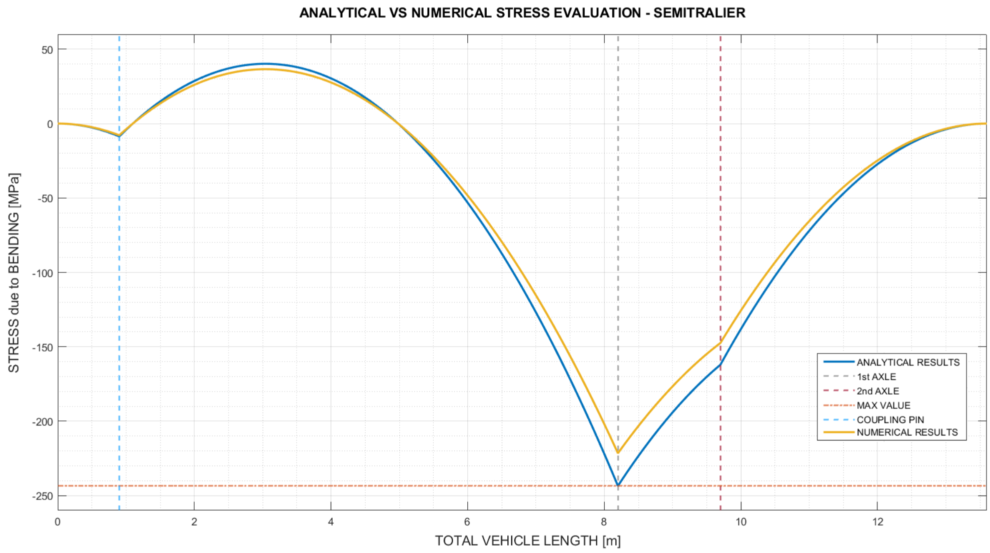


Figure 7.3: Analytical vs Numerical stress semitrailer

The stress trend in both cases is the same and the difference between the two at its highest point is around 8%, even in this case there are points where the values are quite similar, so the results obtained in this case are reliable.

### Biga-trailer

As a final section, the values obtained for the biga vehicle are considered.

The results obtained present the same trend with maximum point in the second axis unlike the other two previous cases. The difference between the two is around 10%.

In conclusion of this chapter, it can be said that the results obtained with both methods, analytical and numerical, led to good results. Therefore, the analytical model implemented is reliable and applicable during design.

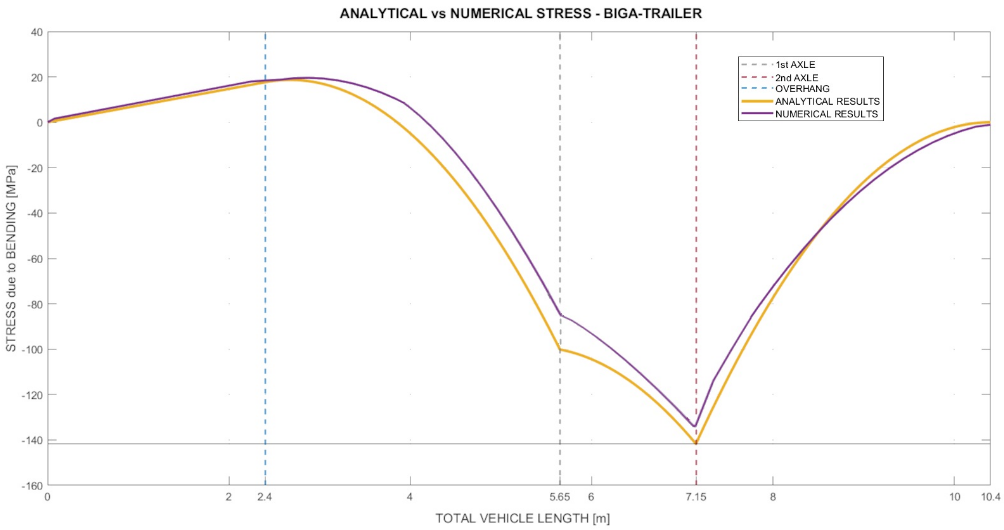


Figure 7.4: Analytical vs Numerical stress biga

# Chapter 8

# Modularity and standardization

The purpose of this chapter is to define the elements underlying the concept of standardization and modularity. It will be defined the concept of product architecture, standard and variable components in order to clarify certain choices that will be made in the following chapters.

The product architecture is now described in detail based on the modular and integral concept.

## 8.1 Product architecture

### 8.1.1 Integral architecture

Integral architecture consists of a complex connection between functions and components. Instead of a one-to-one relationship between functions and components, i.e. a function associated to only one component or subassembly, here it will have a more intricate relationship in which maybe a function is linked to more components or a component performs more functions.

The result of this configuration is that the interfaces are coupled; that is, changing a component involves changing the component to which it is connected. Interactions between subassemblies are not well defined.

### 8.1.2 Modular architecture

Architecture is defined as modular when the function-component relationship is one to one, that is, when a component performs only one function.

The component or subassembly in this case takes the name of module. Interactions between subassemblies are well defined; interfaces are standard and decoupled.

Since they are decoupled, changing the module does not involve changing the component or components connected to it. Modular architecture can be divided into three categories (Ulrich and Eppinger, 1995):

- Slots. The interfaces of the product are all different. The product is modular but modules that perform different functions to each other cannot be interchanged;
- Bus. There is one element to which all other components connect via common interface. So all interfaces are the same and connect components to a single element. Modules can be exchanged in their positions on the common element;
- Sectional. All interfaces are common and components do not connect to a common element. All components can swap with each other.

### 8.1.3 Advantages and drawbacks of the integral and modular architecture

Integral and modular architecture have advantages and disadvantages. These can and should be best exploited depending on the product being referred to. The advantages of integral architecture are:

- Better performance in terms of size, shape and weight
- Greater ease in design; resulting in lower design costs and time.

  The benefits of modular architecture have been organized into three subgroups related to the various stages of product development.

So it will result in:

1. Usage Benefits:
   - Increase in variety;
   - Upgradeable products;
   - Quality improvement;
   - Ease of maintenance;

2. Manufacturing Benefits:
   - Economy of scale;
   - Flexibility, thanks to the presence of common modules and components it will be easier to manage an ATO, assembly to order, system;
3. Design:
   - Less expensive and faster innovation;
   - Easier coordination of work; ability to parallel internal or external project groups that will work on their assigned module independently of each other.

     It can be said that the advantages of one are the disadvantages of the other.

     For this reason, it can be said that there is no best architecture regardless, but it is strictly related to the context, i.e. the product to which it is to be applied.

     If it is taken the automotive sector as an example it can be found examples of application of both concepts. For cars with high production volumes there is a greater use of modular architecture. High volumes allow higher initial design costs.

     Cars that are produced in small numbers and require high performance will justify the extensive use of integral architecture. Of course, the architecture of a complex product is unlikely to be only integral or only modular.

     Usually there is a mixture of the two types; therefore some parts will be modular while others will be integral.

### 8.1.4 Standard components

Standard components are components that are shared by multiple products. It is possible to standardize a component if its function(s) are common to multiple products and if the component's interface is the same for different products.

Making a connection with the previous concepts of modular and integral, it can be argued that a modular component will be more easily standardized since it performs only one function and its interface is decoupled. Decoupled interfaces facilitate the creation of standard interfaces.

This is different for integral components; given the presence of multiple functions in a single component, it is much more difficult to standardize them. In fact, it would only be possible to do so on components that have the same combination of functions.

The main advantage of standardization lies in the possibility to produce the component in high volumes pursuing the economy of scale and reducing the resources and the time related to their design and development.

All this translates into a reduction in costs. A standard component has generally higher performance and quality than a non-standard component since the producer can concentrate his energies on a single configuration instead of many variants of the same.

The disadvantages are a reduced drive for innovation and the use of standard components for applications that may require lower performance than those for which the component was designed, leading to increased costs.

### 8.1.5 Variable components

Variable components are those that vary from one product to another.

They are those that cannot be standardized and therefore go to differentiate products from each other. Their standardization would result in the loss of external product variety.

## 8.2 Product platform

The definition of standard and variable components allows to take a step further and present the concept of a product platform.

The platform consists of a shared architecture among several models and versions of the product, which are usually called derivatives, and which can be launched in the market after the introduction of the new product (Ulrich and Eppinger, 1995).

Using the words of another author, it can be defined as a common technological base from which a product family is derived through platform modifications to target certain market niches (Qian Ma et al., 2011).

Reducing the concept of platform to only physical elements it will consist of all those standardized elements shared across multiple product models and versions.

As reported by Ulrich and Eppinger (1995) with the platform it is seeked the balance between differentiation and sharing. In fact, the platform is a response to a growing customer demand for variety (Cameron and Edward, 2014).

The complexity that this variety brings can be curbed with internal product simplification. For example, automakers face this problem on a daily basis. A car model can have as many as over five million combinations considering all the options that are offered (Cameron, 2011).

With the platform, companies are able to standardize as much as possible, reducing internal variability but preserving external variability.

Developing a platform requires a significant investment of resources and knowledge since it represents the meeting point of different products. If not carefully planned, it can lead to excessive similarity of its derivatives.

### 8.2.1 Drawbacks of product platform

The main disadvantages of the platform are (Suh, 2005):

1. standardize product performance;
2. cannibalize products;
3. inhibit new product development.

Thus, using the same platform on different products can lead to similar performance, or even loss of performance, and limit innovation due to the fact that some of it will always be tied to the past.

Cannibalization refers to the risk that different products from the same company, sharing the same platform, will eat each other's market share (Sanderson and Uzumeri, 1995).

As reported by Cameron and Edward (2014) this phenomenon is all the more evident the more similarity there is between them. That is, products belonging to the same market segment have a greater ease of common platform introduction but with them there is also a greater risk of cannibalization. In the eyes of consumers, they would be too similar and there would be a natural tendency to choose the one with the lowest cost.

An example of this occurred in the 1990s at the Volkswagen Group. Consumers noticed that Skoda cars shared 60% of the parts with Volkswagen cars, had the same quality standards and had a lower price (Suh, 2005).

### 8.2.2 Flexibility on platform

The concept of platform can be tied to that of flexibility.

Flexibility refers to the ability a system has to cope with changing conditions or instability caused by the environment, i.e. to be future-proof (Diffner, 2011).

Flexible elements are elements that are able to incorporate this adaptive capacity and transfer it to the system to which they are bound. They are thus able to meet different requirements, producing 12 different products/processes.

They are modifiable with less investment than fixed components that would perform the same task (Suh, 2005).

A particular example of a flexible platform is the scalable platform; this manifests its flexibility in its ability to cover products in a family that differ from each other in scalable variables.

By scalable variables is intended variables that can contract or expand the products of a family so that they can offer different performances (Simpson, 2001).

A product family is a group of assets that share specifications, components, and subsystems (Simpson, 2001). They also share processes, customer segments, distribution channels, pricing methods, promotional campaigns, and other marketing methods.

## 8.3 Scope of the study and company purpose

At the end of this introduction on the concept of modularity and standardization it is now briefly described the purpose of the study for the company.

The idea from which it is born the plan is based on the desire from the company to realize adaptable standard components for the majority of the vehicles produced in order to speed up the production and to reduce the plurality of the parts.

The objective of the reduction of the components brings like first advantage a better management of the warehouse and improves the production since it allows the realization of a smaller number of components and this can influence besides in the improvement of the quality of the products.

As it is described therefore the advantages of this choice can carry to have one smaller complexity in some parts of the productive chain while to increase the complexity of others like in the case of the installation of the several components.

# Chapter 9

# Clustering of frames

## 9.1 Chassis splitting

In this section is taken as a case study the biga frame and then go to expand the speech to other vehicles products.

As a first analysis on the possible grouping among the various projects realized the chassis of the vehicle is divided in 3 components, front, central and rear.

Front section will enclose the part related to the drawbar for the biga vehicle or the trailer and the front part of the semi-trailer where there will be the towing hook of the vehicle.

Central section will enclose the axles and suspension.

Rear section will contain the rear part of the vehicle, from the end of the diapress onwards.

It has been chosen to divide the chassis in these three components because in the past a project for the biga-trailer has already been realized where the vehicle was designed in three parts and because the will of the company is to work considering this subdivision.

The study in the particular case of this project will mainly consider the module concerning the central section.

In the **Figure 9.1** it is possible to see a first consideration on the subdivision between standard and variable components.

It is then visible a first draft of the possible realizable platform in which is reported the division into three parts of the vehicle studied, the central body will be the fundamental part of the study.

From the **Figure 9.1** above is evident the subdivision between single and twinned wheels, this partition is at the same time intuitive and clear.

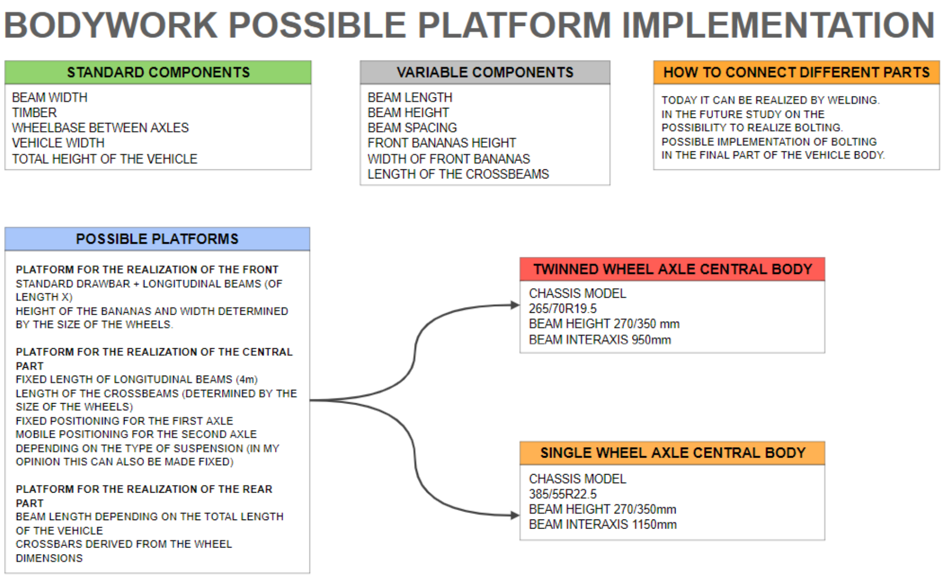


Figure 9.1: Bodywork possible platform implementation

## 9.2 Central module

The module that will be studied in this project foresees a standard configuration of some components and subassemblies in order to make them applicable in most cases and more particularly to collect within them the major volumes of the company.

### 9.2.1 Upper frame and suspension department

The idea at the base of the module foresees the subdivision into two fundamental parts of the module itself.

The first one foresees the upper part of the frame where the longitudinal beams and the reinforcing crossbeams will be included.

They will support the loads linked to the axles and will reinforce the structure in order to obtain bending and torsion deformation values acceptable for the studied vehicle and for the applications that will follow.

The lower part foresees instead a configuration that goes to adapt to the various models of axles present on the market and requested by the customer in order to always guarantee the optimal choice for the customer's request.

### 9.2.2 Adopted components and constructive choices

The realization of the module provides some constructive choices that go to consider the technologies present in the company.

An introduction of the bolting technique within the realization of the frame has been discussed at length; given the company's lack of knowledge of this technique, it has been decided to maintain the welding method for the joining of the components in the most stressed points and in most cases.

It will be seen later a study on the less stressed parts of the bolting technique in order to introduce knowledge within the project and start to have data on vehicles produced.

### 9.2.3 Various chassis configurations and grouping

The study of the realized company projects brings to light a first possible grouping:

- Distinction between twinned and single wheels, in the case of the realization of the chassis, the choice of adopting an axle with single wheels or with twin wheels goes to influence the distance between the longitudinal beams, a greater distance leads to have a greater stability of the vehicle and a less marked effect of the torsion.

  The measures collected for the distance between the longitudinal beams are:

  - 1200 mm
  - 950 mm
  - 900 mm
  - 1000mm

- Height of the longitudinal beam, as seen above, varies according to the size of the wheels and axles mounted and can assume various heights.

  In this case it is chosen to produce two different types of beam that will replace the variety of sizes present until now. The measures chosen will be:

  - 270 mm
  - 325 mm

- Distance between the axles, in this case are kept two different distances within the project (1310 and 1500 mm) measures adopted for 95% of the trailers and semi-trailers produced.

- The chassis realized will be applicable to both vehicles with one axle and vehicles with two axles, for the moment the realization also of a third axle is not considered.

The dimensions presented are the basis for the realization of the upper or main part of the frame, as will be presented in the following the different configurations first supported by the various heights of the beam will be corrected by introducing components in the suspension department made.

## 9.3 Choice of the part to work on

It is now time to introduce the sections of interest of the various vehicles in which it will be possible to adopt the central module.

The purpose for which it is chosen to work on a maximum length of 4 meters comes from the technological limit of the company's laser machine, it has a maximum length of the sheet metal workable equal to 4 meters. It is therefore considered to work on this length to avoid wasting material and at the same time maintain production within the company.

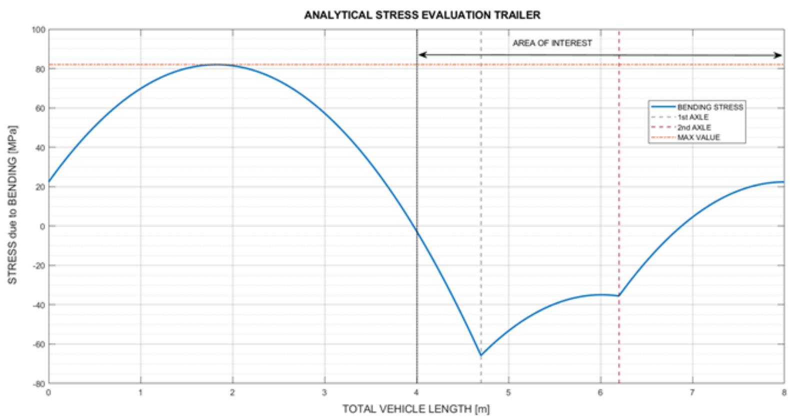


Figure 9.2: Trailer area of interest

The choice of the area of interest of the trailer (**Figure 9.2**) foresees the rear part of the vehicle so in the case studied from 4 to 8 meters of the vehicle. The case of the semi-trailer vehicle (**Figure 9.3**) will be studied between 7 and 11 meters of the vehicle this in order to optimize the 4 meters available of the company laser machine. Regarding the choice of the part on which it will be realized the module of the biga-trailer is found the part shown in the **Figure 9.4** or about one meter from the first axle and then continue with 4 meters that will contain both axles with relative diapress.

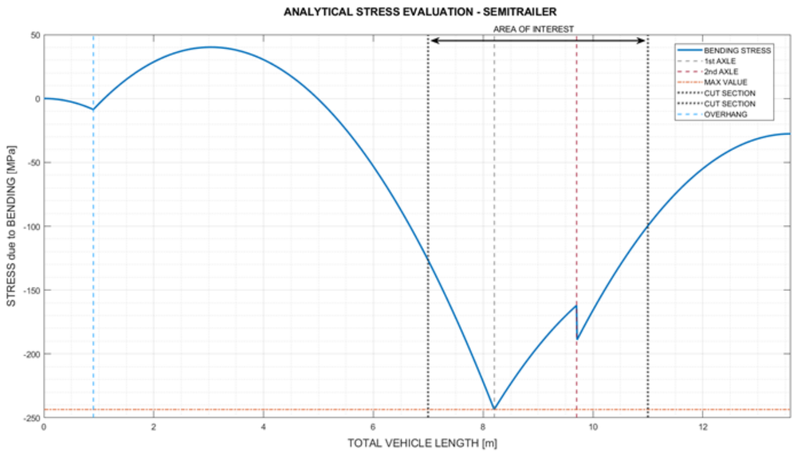


Figure 9.3: Semitrailer area of interest

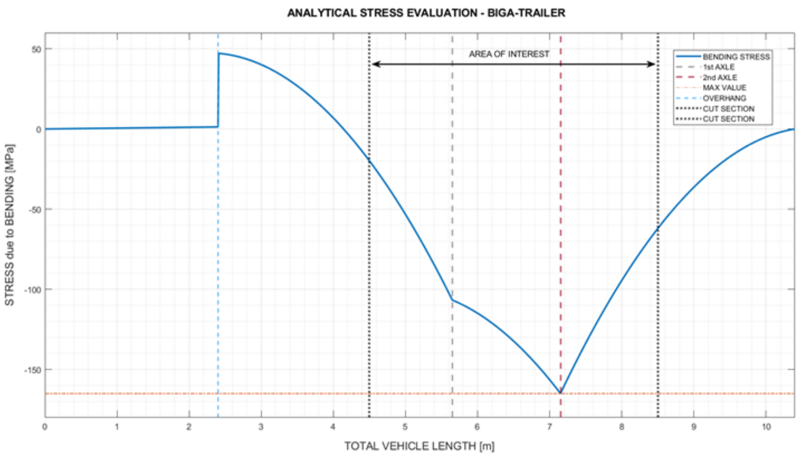


Figure 9.4: Biga-trailer area of interest

## 9.4 Longitudinal beam section

The section of the longitudinal beam chosen represents a compromise between the measurements adopted today for the biga-trailer vehicle and those used for the trailer or semitrailer.

Table 9.1: Longitudinal beam section dimensions in different vehicles

| | SEMITRAILER | TRAILER | BIGA-TRAILER |
|---|---|---|---|
| t [mm] | 5 | 5 | 5 |
| s [mm] | 10 | 10 | 8 |
| H[mm] | 350 | 290 | 270 |
| W[mm] | 150 | 150 | 120 |
| $W_t[mm^3]$ | $5.81 * 10^5$ | $4.62 * 10^5$ | $2.94 * 10^5$ |

The study carried out on the sections of the vehicles produced is now reported, for brevity's sake the sections most adopted in the three categories of vehicles produced are reported.

As can be seen from the data shown in the table, different dimensions are adopted for the beam section.

The characteristic measure reported in the index line $W_t$ represents the bending resistance module of the studied section along the axis on which the bending moment acts.

It has been chosen to report for simplicity only this section characteristic since it represents the characteristic of interest for the calculation of stresses as already seen above.

In the **Figure 9.5** is represented the chosen section of interest with length 4 meters of the longitudinal beam.

In the **Figure 9.6** are shown the characteristic stresses of the three vehicles analyzed. It can be seen that the most stressed vehicle is the semitrailer while the biga-trailer and the trailer are less stressed.

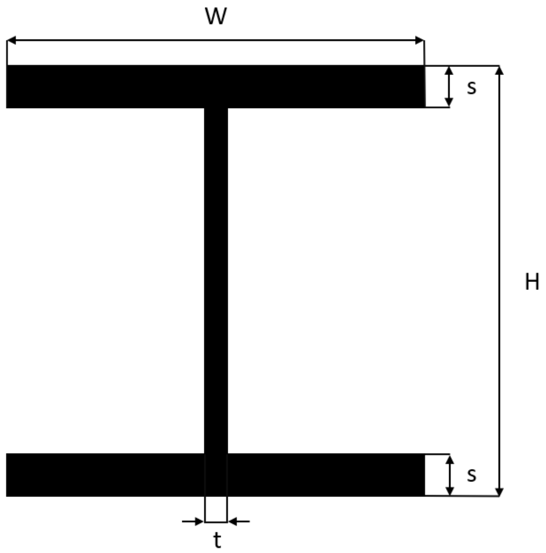


Figure 9.5: Double-T section with parameters


Figure 9.6: Stresses in the section of interest for the different vehicles

## 9.5 Clustering

Inside the company is used a laser machine for cutting metal sheets, this tool allows to cut sheets up to a maximum length of 4 meters, from this limit comes the idea to create a module that will have as longitudinal length 4 meters.

From the data obtained in the analysis of the company volumes and of the realized projects we pass now to subdivide the project in different frames for the possible configurations.

### 9.5.1 First frame concept

The first possible grouping involves a chassis with a longitudinal beam spacing of 1200 mm, adoptable for vehicles with single-wheel axles and a beam height of 270 mm.

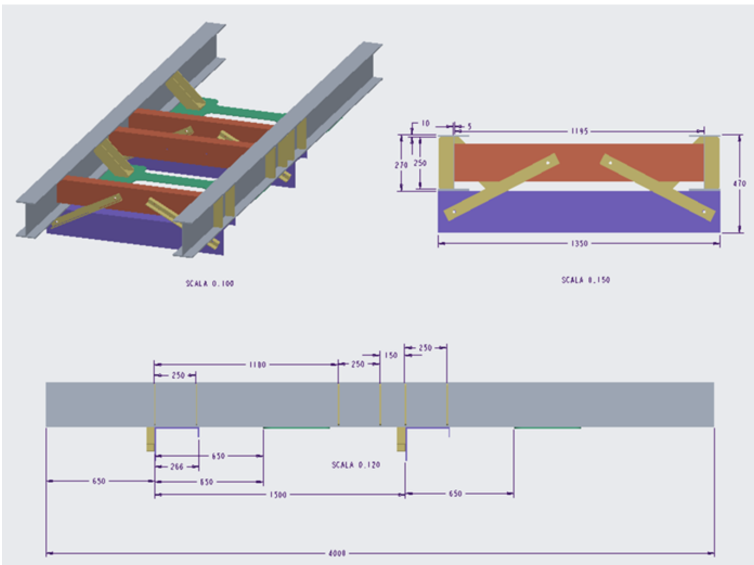

Figure 9.7: First frame concept

The realization of this frame allows to collect 19% of the volumes collected by this analysis, as already specified the project involves the realization of vehicles with fixed axle and/or liftable single axle or two axles close together.

As shown in the table you can see that within this category have been included even the vehicles to date produced with a core of 290 and 295 mm, the solution to reduce the production of beams of different height is the realization of a suspension support that act to increase the modulus of resistance of the entire structure and allows the realization of a single frame applicable in different configurations.

The idea of realization of this model will be the basis for the realization of the next frames with different sizes.

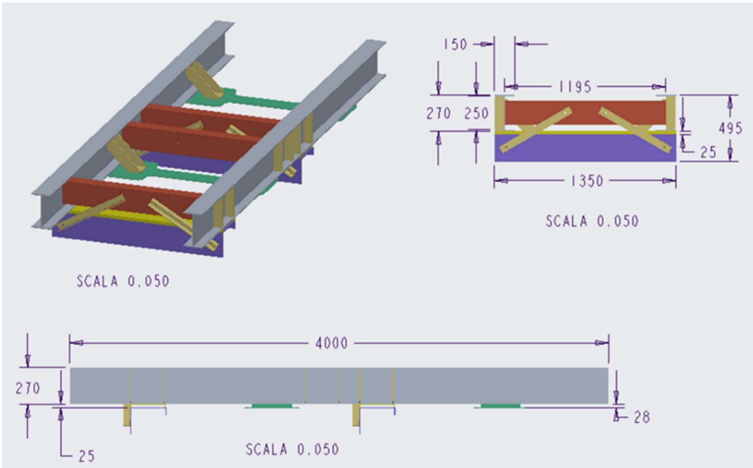


Figure 9.8: First frame concept with height variation

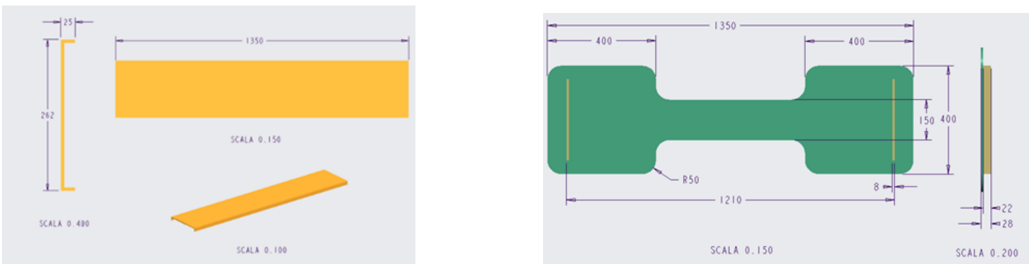


Figure 9.9: Components for the height variation

The **Figure 9.9** represents the additional components that have been inserted to allow the adaptability of the 1200/270 chassis to chassis with a height of 295 mm.

The modifications adopted allow to raise the vehicle of 25 mm useful for the assembly of wheels of different sizes.

The additional elements are simple and easy to realize but at the same time they increase the cross section and therefore the bending moment resistance of the vehicle.

Moreover, the adoption of an element that connects the two wheels of the same axle increases the torsion resistance of the vehicle.

Table 9.2: Volumes for the first frame concept

| Tire | Volumes | Rim | Coupling | Wheelbase [mm] | Beam height [mm] |
|---|---|---|---|---|---|
| 385/55 | 17.28% | 22.5 | SINGLE | 1200 | 270 |
| 445/45 | 1.66% | 19.5 | SINGLE | 1200 | 295 |

### 9.5.2 Second frame concept

The second possible grouping foresees the realization of a chassis with a distance between longitudinal beams of 1200 mm, adoptable for vehicles with single wheel axles and a beam height of 325 mm.

The realization of this chassis (**Figure 9.10**) allows to collect about 5% of the volumes from this analysis, as already specified the project provides for the realization of vehicles with fixed and or liftable single axle or with two axles close together.

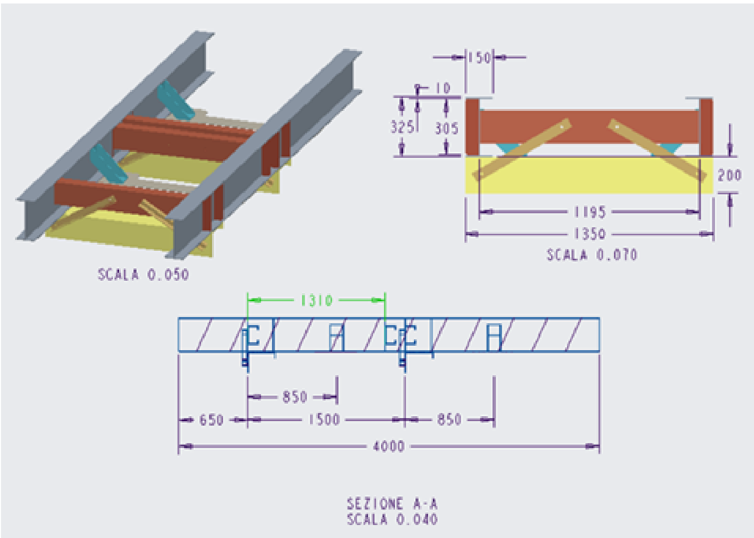


Figure 9.10: Second frame concept

As shown in the **Table 9.3** it is possible to see that within this category have been included even the vehicles to date produced with a core of 325 and 355 mm, the solution to reduce the production of beams of difference in height is the realization of a suspension support that act to increase the modulus of resistance of the entire structure and allows the realization of a single frame applicable in different configurations.

The difference with respect to the configuration of the first frame is due to the change of height of the adopted beam which has passed from 270 mm

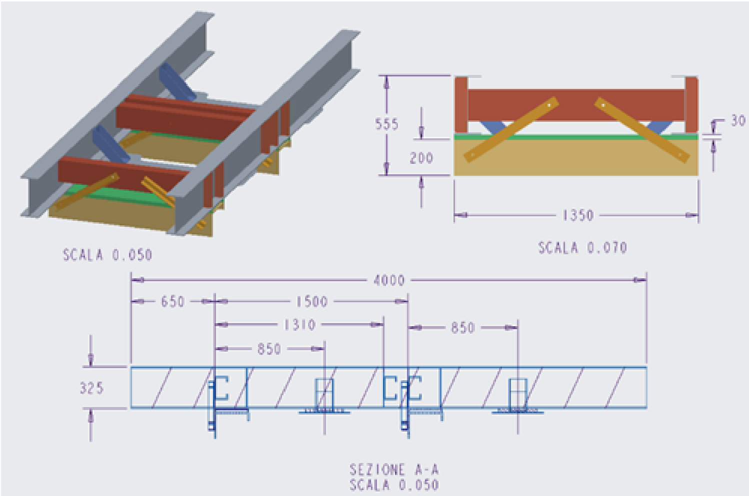


Figure 9.11: Second frame concept with height variation

to 325 mm. Also in this case the possibility to insert the two additional components in the axle and in the diapress allow to adopt the chassis for different configurations. (Figure **9.11**)

This chassis will be much more useful in vehicles such as trailers and semi-trailers compared to the biga trailer because in these first two the weight of the maximum net load is greater than in the biga one.

Table 9.3: Volumes for the second frame concept

| Tire | Volumes | Rim | Coupling | Wheelbase [mm] | Beam height [mm] |
|---|---|---|---|---|---|
| 385/65 | 3.77% | 22.5 | SINGLE | 1200 | 325 |
| 435/50 | 1.11% | 19.5 | SINGLE | 1200 | 355 |

### 9.5.3 Third frame concept

The third possible grouping foresees the realization of a chassis with a distance between longitudinal beams of 900 mm, adoptable for vehicles with twin-wheel axles and a beam height of 325 mm. (reported in **Figure 9.12**)

The realization of this chassis allows to pick up approximately 8% of the volumes from this analysis, as already specified the project foresees the realization of vehicles with fixed axle and or liftable single axle or with two axles close together.

As shown in the **Table 9.4**, it is noted that within this category have been included the vehicles to date produced with a core of 350 mm, the solution

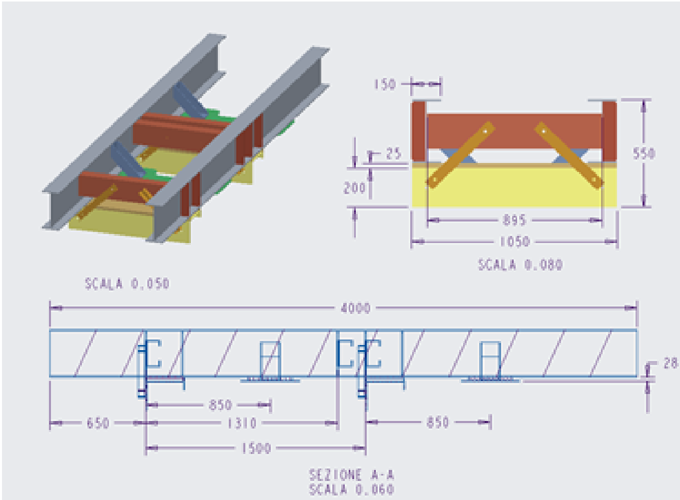


Figure 9.12: Third frame concept

for reducing the production of beams of different height is the realization of a suspension support, that is reported later, acting to increase the resistant module of the entire structure and allows the realization of a single frame applicable in different configurations.

Table 9.4: Volumes for the third frame concept

| Tire | Volumes | Rim | Coupling | Wheelbase [mm] | Beam height [mm] |
|---|---|---|---|---|---|
| 315/70 | 6.20% | 22.5 | TWINNED | 900 | 350 |
| 315/80 | 1.88% | 22.5 | TWINNED | 900 | 350 |

### 9.5.4 Fourth frame concept

The fourth possible grouping foresees the realization of a chassis with a longitudinal beam spacing of 950 mm, adoptable for vehicles with twinned wheels axles and a beam height of 270 mm. (reported in **Figure 9.13**)

The realization of this chassis allows to collect the 38% of the volumes from this analysis, as already specified the project foresees the realization of vehicles with fixed axle and or liftable single axle or with two axles close together.

As shown in the **Table 9.5**, it can be seen that within this category the vehicles produced to date with a 310 mm core have also been included. The **Figure 9.14** shows the standard configuration with a height of 270 mm and the configuration that can be used for a height of 310 mm.

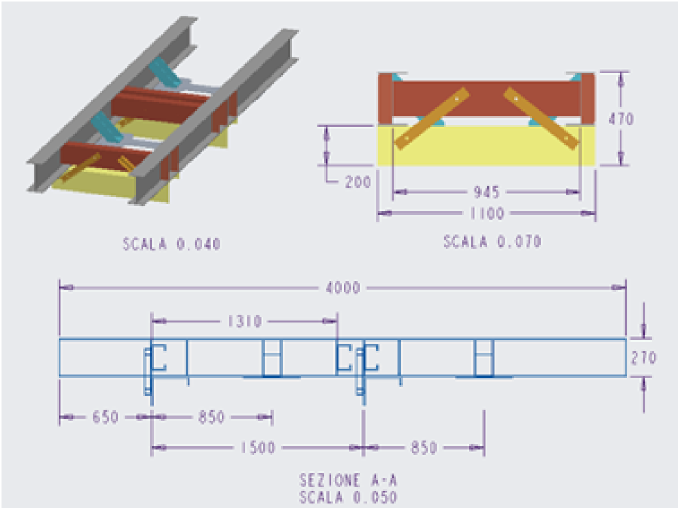


Figure 9.13: Fourth frame concept

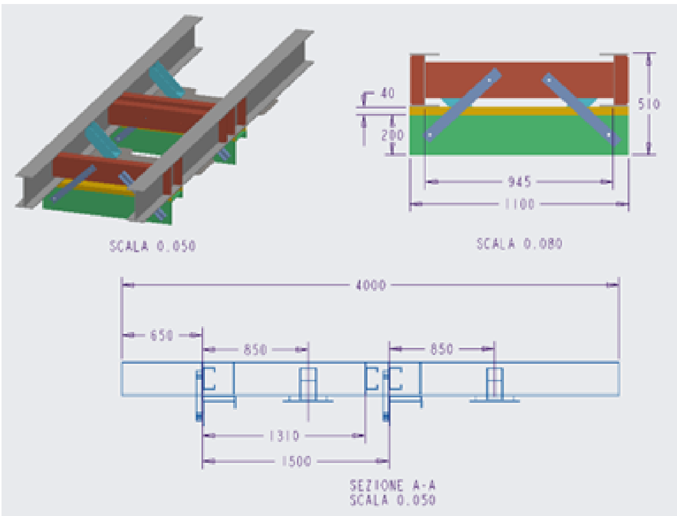


Figure 9.14: Fourth frame concept with height variation

Table 9.5: Volumes for the fourth frame concept

| Tire | Volumes | Rim | Coupling | Wheelbase [mm] | Beam height [mm] |
|---|---|---|---|---|---|
| 245/70 | 12.62% | 17.5 | TWINNED | 980 | 310 |
| 265/70 | 25.03% | 19.5 | TWINNED | 950 | 270 |

### 9.5.5 Fifth frame concept

The last possible grouping foresees the realization of a chassis with spacing between longitudinal beams of 1000 mm, adoptable for vehicles with twinned wheels axles and a beam height of 325 mm. (**Figure 9.15**)

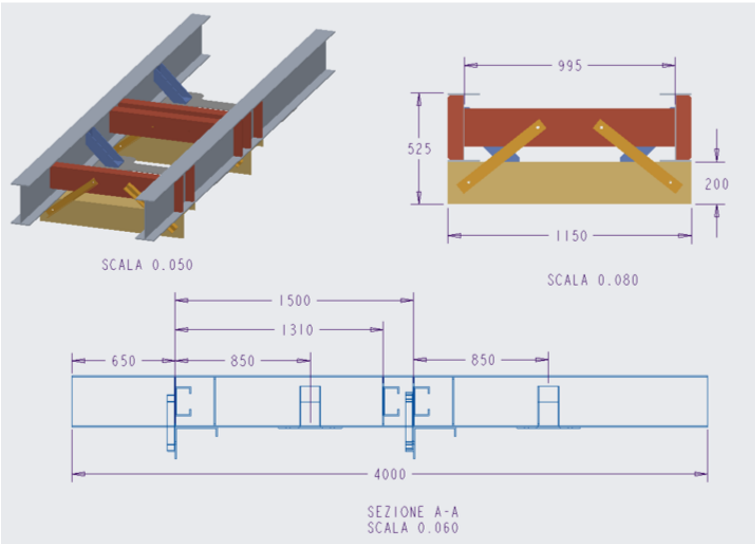


Figure 9.15: Fifth frame concept

The realization of this chassis allows to collect 2.1% (as reported on **Table 9.6**) of the volumes from this analysis, as already specified the project foresees the realization of vehicles with fixed and or liftable single axle or with two axles close together.

Table 9.6: Volumes for the fifth frame concept

| Tire | Volumes | Rim | Coupling | Wheelbase [mm] | Beam height [mm] |
|---|---|---|---|---|---|
| 205/65 | 2.10% | 17.5 | TWINNED | 1000 | 330 |

# Chapter 10

# Basic components for the frame

The purpose of the creation of these five different frames is to simplify the production process allowing to leave in production only a minimum number of components, the basic components for the chassis realization are now described.

As it is possible to notice from the different frames, has been chosen to always consider the same components in the different configurations proposed, what has been varied are the lengths of the components to adopt them in different frames.

## 10.1 Longitudinal beams

The realization of longitudinal beams according to the current method, core with welded lower and upper plates, section that remains double-T.

The decision to use this section derives from the company's many years of knowledge in the realization of this structure and from the advantageous characteristics of this structure, such as the high module of resistance to bending moment with respect to its area, it turns out to be the best compromise between resistant structure and light structure. It is reminded that the weight represents an important characteristic to take into account in the design of industrial vehicles, a lower weight of the structure allows a greater load and at the same time during the motion with unloaded vehicle, a reduced mass allows to save fuel.

The choice made is to maintain the production of two different sizes of beams. The dimensions of the section of the plates are kept unchanged and equal to 10 mm for the thickness and 150 mm as length (W in the **Figure 10.12**).

What does vary is the height of the core, in this case a height of 270 mm

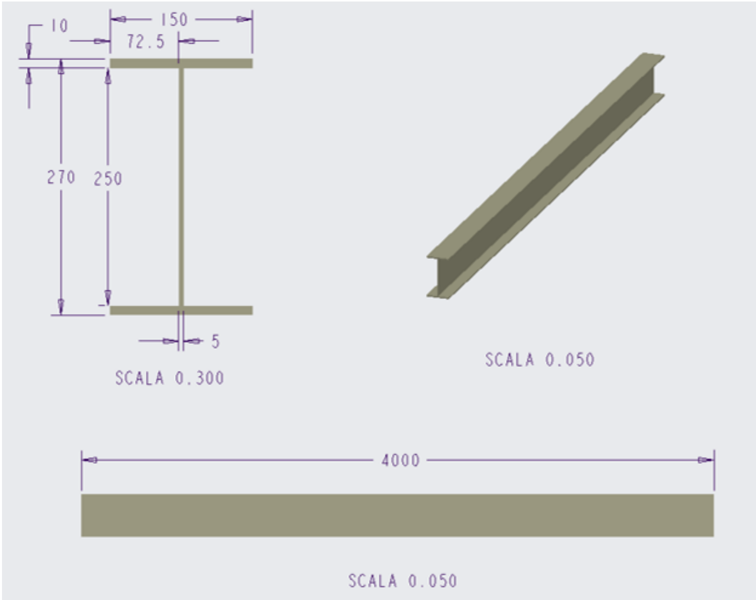


Figure 10.1: Longitudinal beam

and a height of 325 mm have been chosen.

The choice of these two dimensions, as shown above, is inspired by the need to increase resistance to bending moment for applications with heavier loads, such as semi-trailers and trailers, where a height of 325 mm will be adopted, while in cases where greater compactness with good resistance is required, a height of 270 mm will be adopted, as will be the case for the majority of chariots produced.

Only two heights are considered in order to try to keep low the number of components produced within the company, however, the project is not reduced to a single height in order not to distort the vehicle and to maintain high resistance to stress.

## 10.2 Suspension department

The considerations made on the suspension department have been carried out considering the adoption of the current system with the diagonals currently applied and then moving on to the study of different configurations aimed at improving the unloading of efforts on the entire frame structure.

The analysis was carried out using finite element analysis software and, more specifically, Altair Hypermesh was used.

The different configurations presented have been studied by means of 3D model imported on HyperMesh.

It is now possible to analyze the various studies carried out.

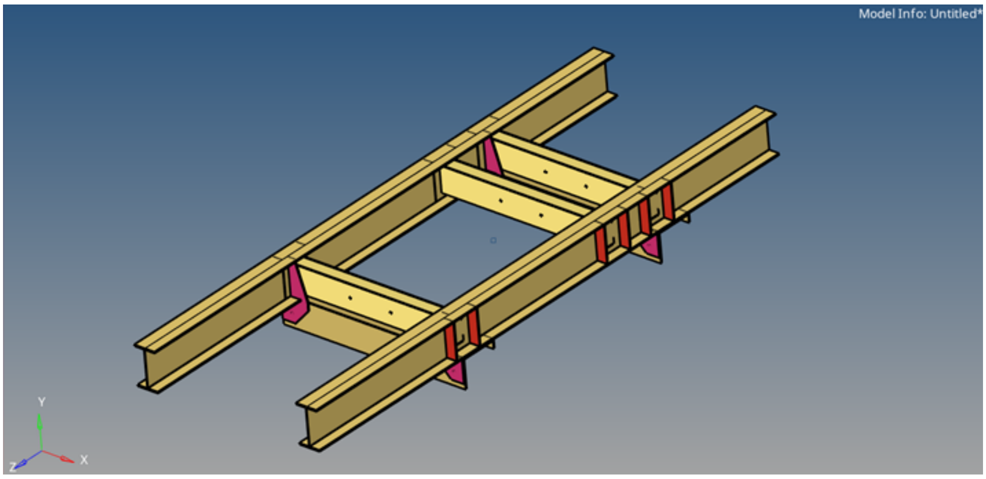


Figure 10.2: Chassis with actual reinforcements

The first configuration (**Figure 10.2**) that will be analyzed concerns an evolution of the chassis currently present in the company, in this case have been adopted of the crossbars of conjunction between the two longitudinal C-beams and the reinforcement of the suspensions has been considered as the one currently in production, it has also included in this case the reinforcements or Gusset plates on the longitudinal beams only in the outer part of the frame at the height of the anchorage point of the axles.

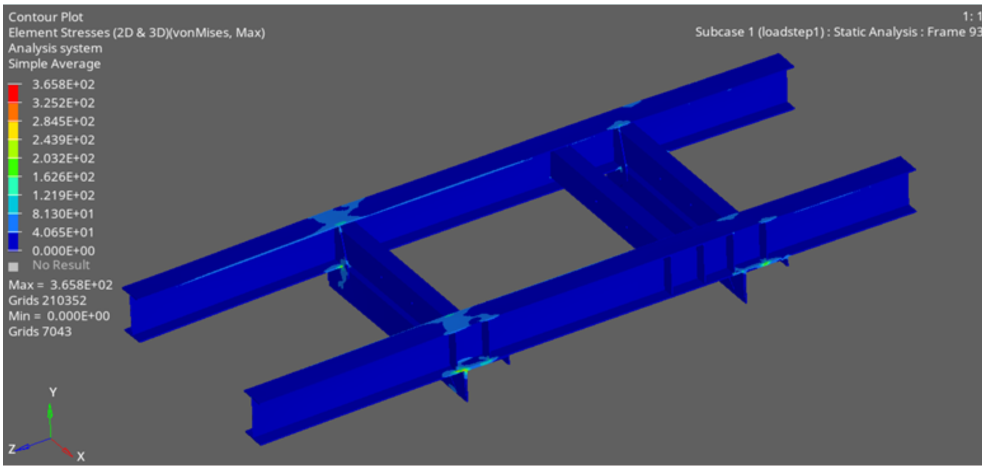


Figure 10.3: Stress results with actual reinforcements

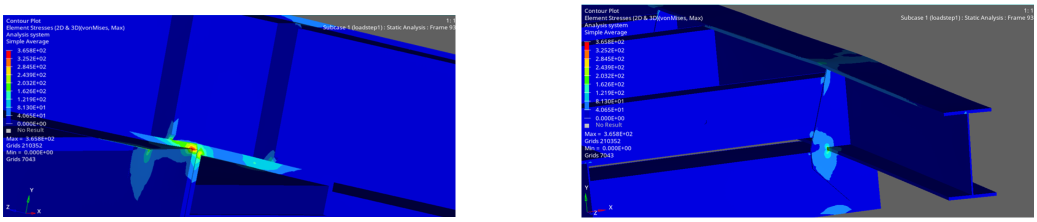

Figure 10.4: Detailed views of Figure 10.3

**Figures 10.3** and **10.4** show the results obtained from the structure presented, with a distributed applied load equal to twice the maximum load of the semi-trailer (as required by the standard).

The obtained results can be considered good for the structure itself, but it is noted that in the points where the axle is anchored there is a concentration that goes beyond the yield strength of the material considered, in this case this solution is not acceptable for the purpose of our analysis.

The constraints have been applied as reported by the analytical case on an axle, 3 degrees of freedom have been constrained while on the first axle the constraints have been applied on 2 degrees of freedom.

The structure is mainly loaded in the part concerning the axles while it is much more unloaded in the remaining parts.

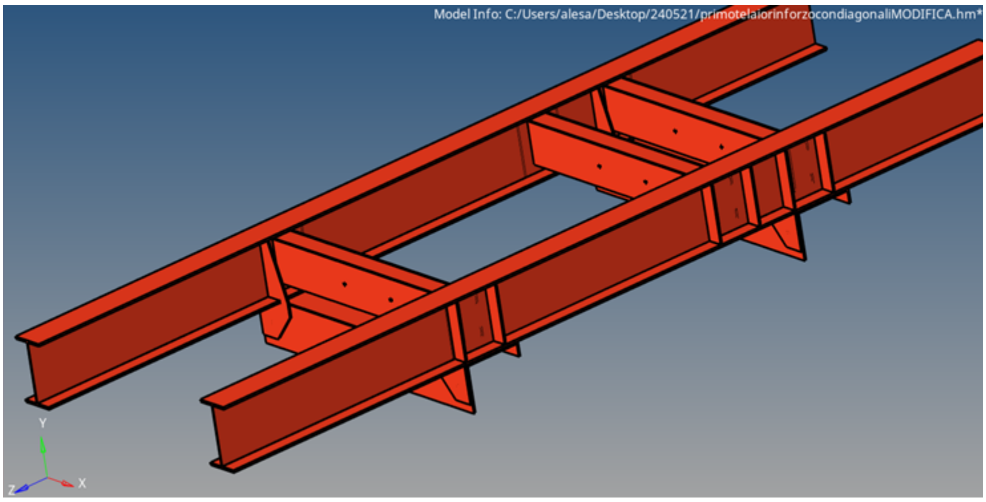


Figure 10.5: Actual chassis with reinforcement modifications

The first modification carried out on the frame was to move the anchorage point of the front part of the axle just in coincidence with the front reinforcement (type of reinforcement visible on (Figure **10.11**)), therefore the area seen above was considered as more stressed.

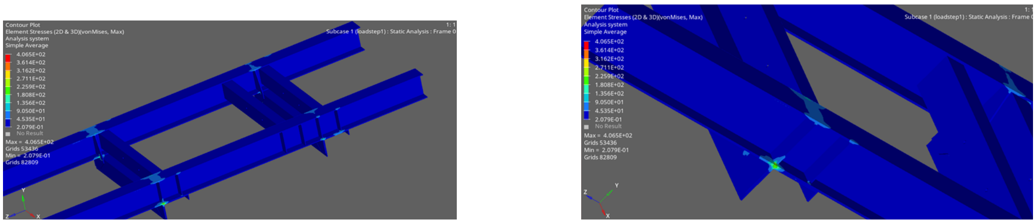

Figure 10.6: Stress results of actual chassis with Gusset plates modifications

As shown in **Figure 10.6**, an improvement in the stressed region is noted with respect to the previous case, however, there remains a singular point where the stress exceeds the yield value of the material chosen and compared to before this value is increased.

It was then passed to a modification of the diagonals that go to help the structure in the distribution of efforts, in this case we have inserted the connecting crossbeams to C with a thickness of 6 mm and dimensions shown in the **Figure 10.7**. The idea is inspired by some solutions already present on the market and some already adopted previously by the same company. It was preferred also in this case to keep the reinforcements on the longitudinal beams.

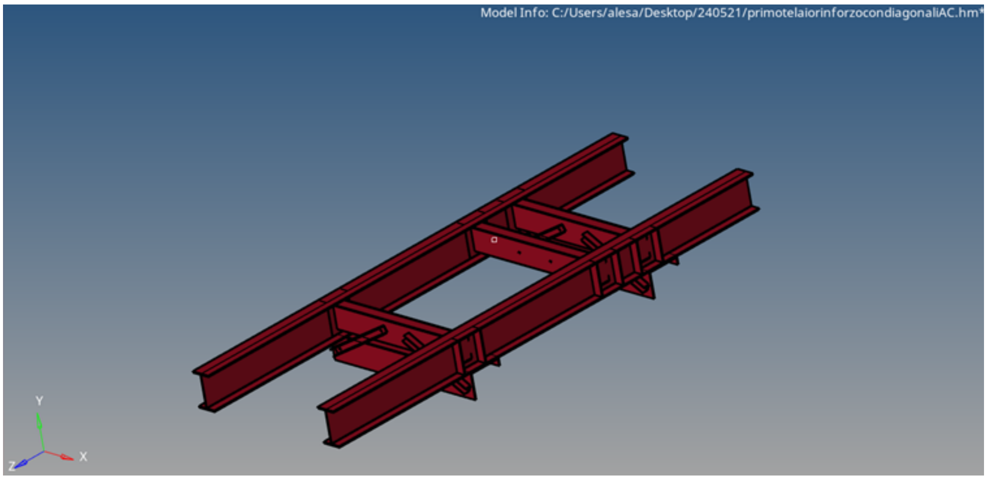


Figure 10.7: New chassis with C-reinforcements

The results of the stress on the structure (Figure **10.8**), show lower values than the previous case, it is also noted that in this case the structure is stressed in a wider region than in the previous case.

It should also be noted that in this case the structure stressed at maximum load shows stress values that are all below the yield strength (**Figure**

**10.9**). It is therefore proposed a new system of attachment for the axles that combines on one hand the need to make the structure rigid and resistant to the stresses that in this region of the frame are the highest of the entire structure and at the same time allows to apply the solution to different heights.

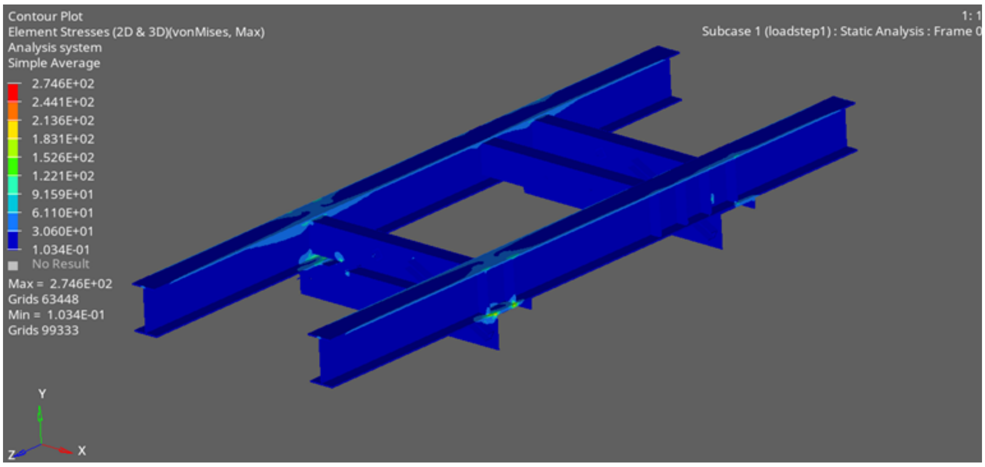


Figure 10.8: Stress results with new configuration

The study carried out also reports the importance of the adoption of Gusset plates in the proximity of the axle assembly.

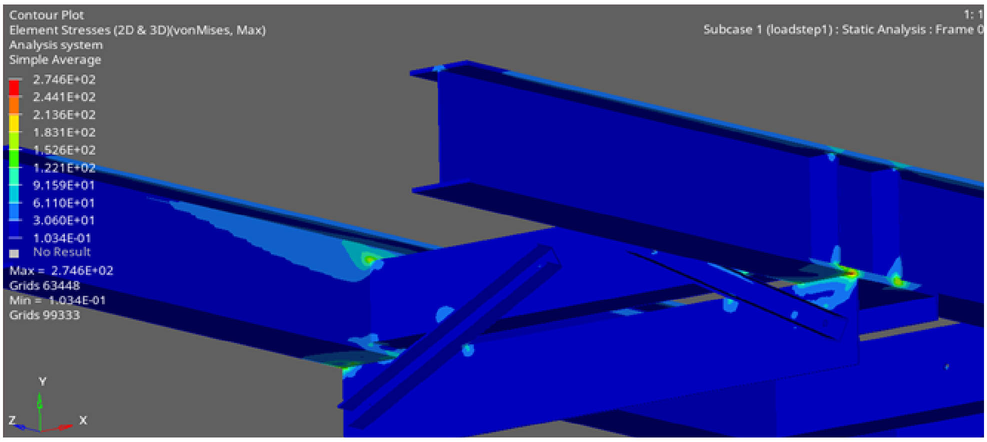


Figure 10.9: Detailed front view of stress results with C-reinforcements

In the beam that will be adopted in this project, Gusset plates (**Figure 10.11**) will be adopted, this choice has been made both for the good results of the distribution of the loads obtained with the Gusset plates and because it is recommended by the sellers of axles.

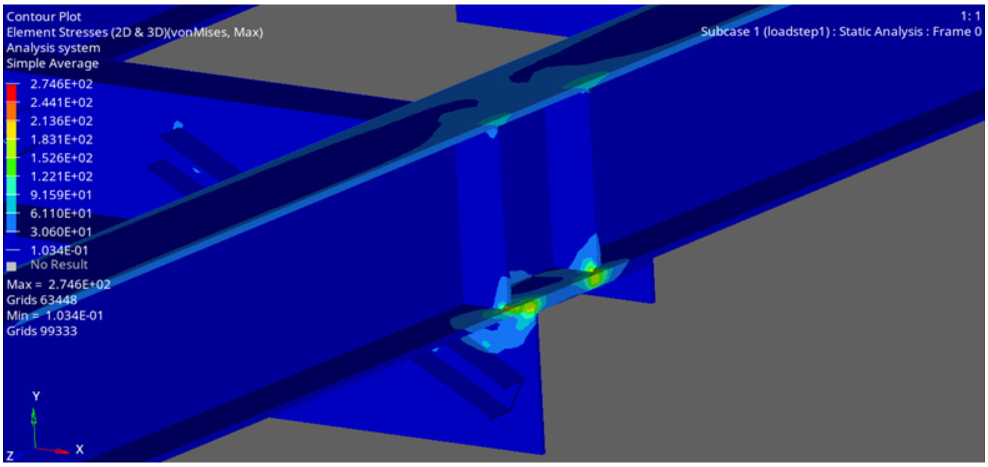


Figure 10.10: Detailed view of stress results with C-reinforcements

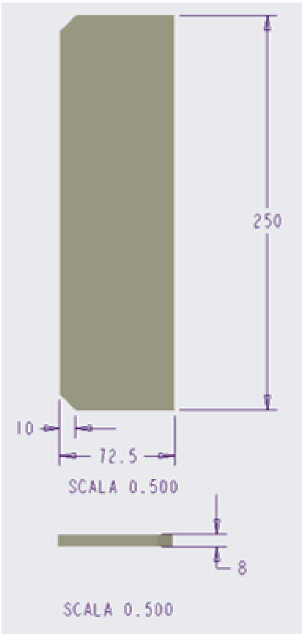


Figure 10.11: Gusset plates for longitudinal beam

## 10.3 Verification of selected beams

Moving on now to the verification of the chosen beams, with the characteristics reported in the (**Figure 10.1**). In both cases the application of the maximum load linked to the application in the semi-trailer vehicle is considered.

Through the Matlab file it was possible to evaluate the value of the bending stress in the most stressed structure, that is in the application of the semi-trailer vehicle.

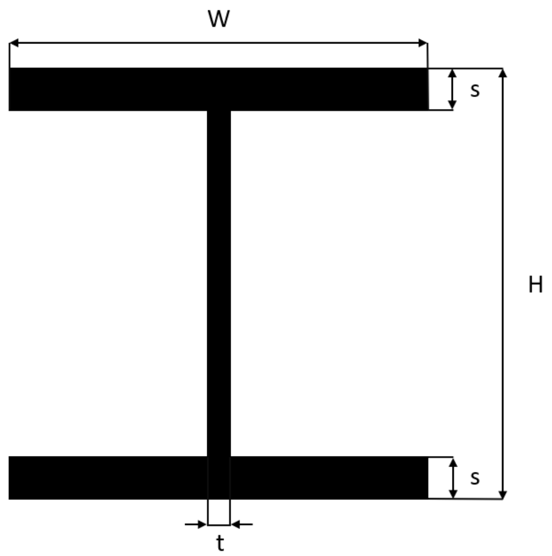


Figure 10.12: Double-T section with parameters

Table 10.1: Dimensions of selected beams

| | MINOR BEAM [mm] | MAJOR BEAM [mm] |
|---|---|---|
| t [mm] | 5 | 5 |
| s [mm] | 10 | 10 |
| W [mm] | 150 | 150 |
| H [mm] | 270 | 325 |
| $W_t[mm^3]$ | $4.24 * 10^5$ | $5.31 * 10^5$ |

The **Figure 10.13** and **Figure 10.14** show the trend of these stresses in the case of the two beams of our interest. As it is possible to see, the stress values are always below the elastic limit (355 MPa for the material considered).

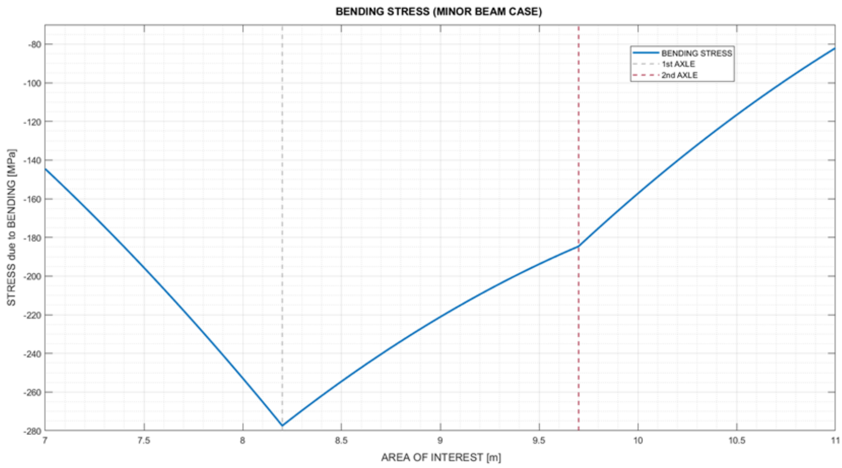


Figure 10.13: Stress trend on the minor section beam

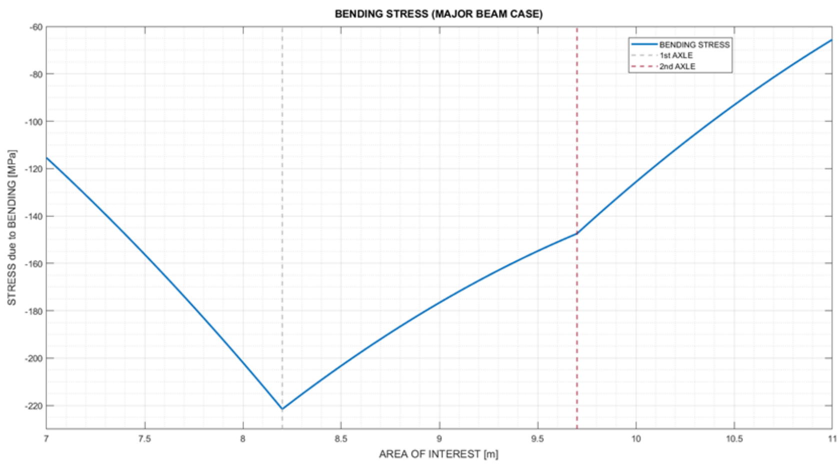


Figure 10.14: Stress trend on the major section beam

## 10.4 Linking crossbars between the two longitudinal beams

The characteristics of the crossbar adopted to connect the two longitudinal beams are now reported.

It was decided to place the crossbeam at the height of the front part of the axle, in this case therefore three crossbeams are inserted at the height of the possible mountable axles.

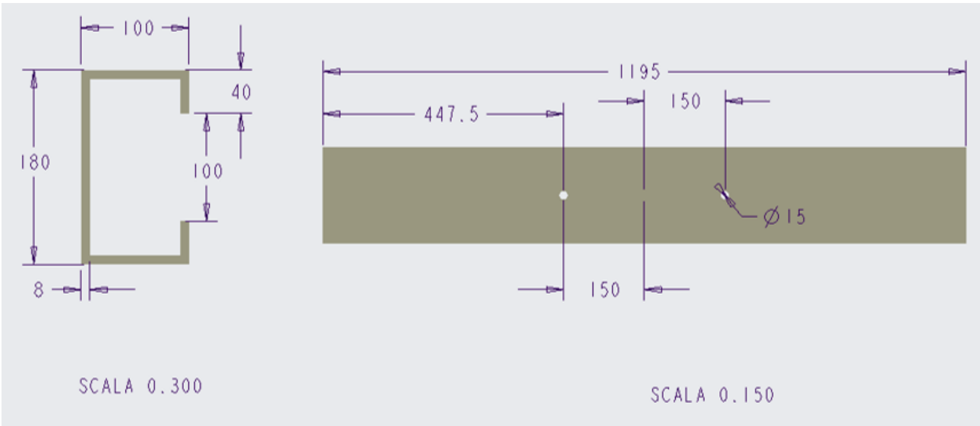


Figure 10.15: Linking crossbars

The section chosen for this structure is a compromise between the open section that allows the processing both for galvanizing and for an eventual assembly with bolts of the crossbars (visible on Figure **10.15**).

At the same time a G section has been adopted in order to increase the torsion resistance of the structure, which is greater than a simple C-section.

The thickness of the sheet metal adopted and the height have been chosen as a compromise between the possibility of realizing the structure inside the company through the folding machine and at the same time not to increase excessively the height as a matter of obstructions.

## 10.5 Junction crossbars for suspensions

The element that are now described regards the part of junction between the axle and the chassis, then goes to connect the part of the suspension to the chassis.

In this case, as seen from the different configurations, it was decided to join the two components through a C-section, this increases the resistance module compared to the diagonals adopted previously and also allows, through the holes visible in the **Figure 10.16**, to adopt a bolted solution. However, there is still the possibility of welding the component.

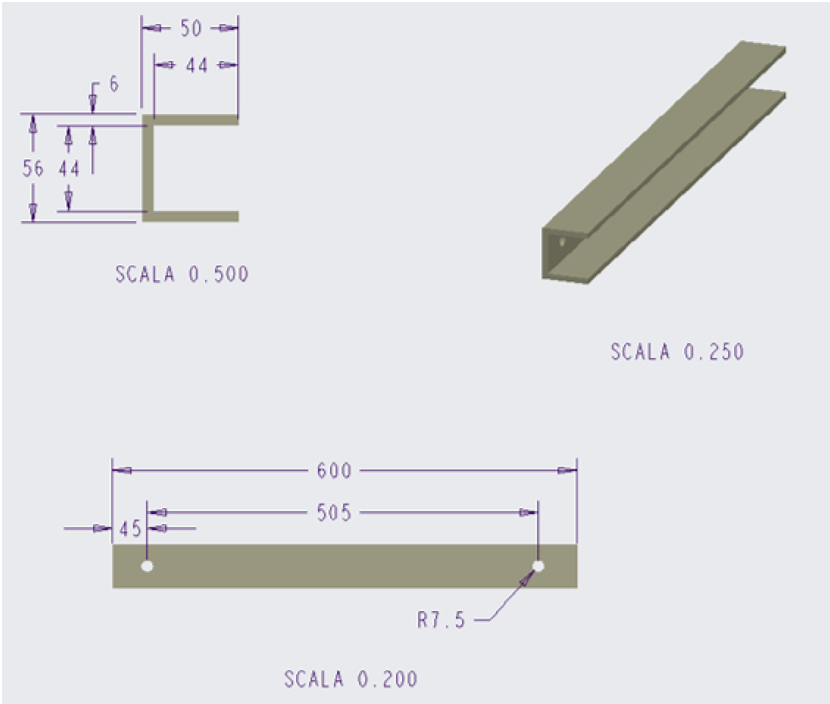


Figure 10.16: Junction crossbars for suspensions

The crossbars between the part where the axles are mounted and the main frame are made from a C-shaped element 6 mm thick, the thickness also being chosen as a compromise between rigidity and workability.

## 10.6 Axles setup

The description of the element on which the axles will be mounted is now presented.

For the axle mounting it has been thought to join the left side to the right side of the axle in order to increase the stiffness of the component and of the frame.

In this case it has been chosen to adopt the visible section shown in the Figure **10.17**, also here the section is a closed one in order to increase the torsion resistance.

This solution allows to distribute the load more evenly, at the same time it was chosen to insert two holes in the front of the structure that permits to bolt the component with the C-junction crossbar presented above.

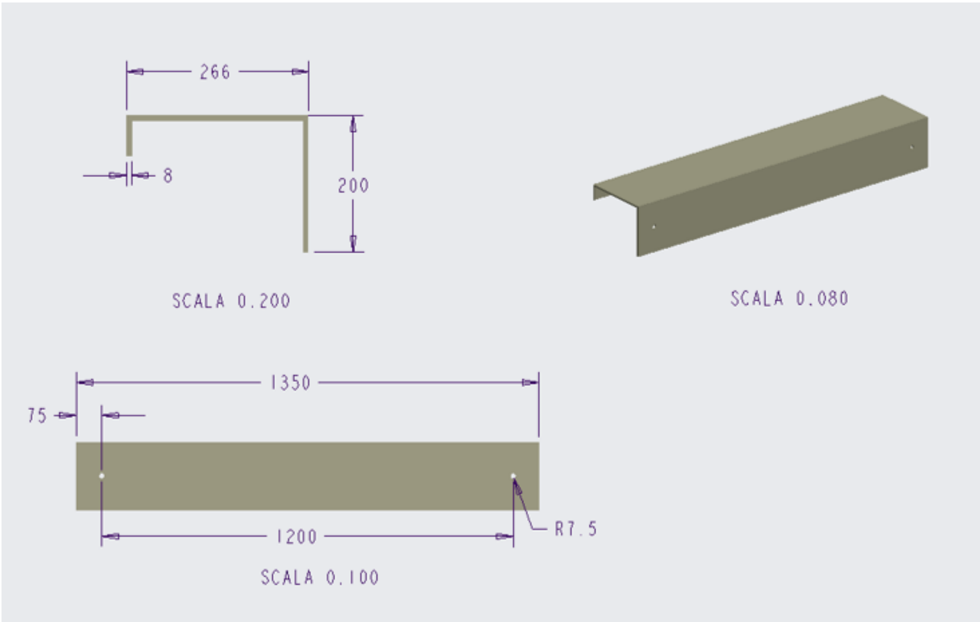


Figure 10.17: Axles setup

The dimensions turn out to be a compromise between the effectiveness of this structure, the workability and the weight of the object adopted.

## 10.7 Diapress holder

The rear part of the axle assembly is now discussed, in this case a particular section is chosen, allowing to adopt the component for the different possible heights of the various chassis, both the height of the element that its inclination have been designed in order not to modify the component in different applications.

The thickness of the sheet metal chosen has been kept to 6 mm, also here is the result of a compromise between workability of the component and its resistance.

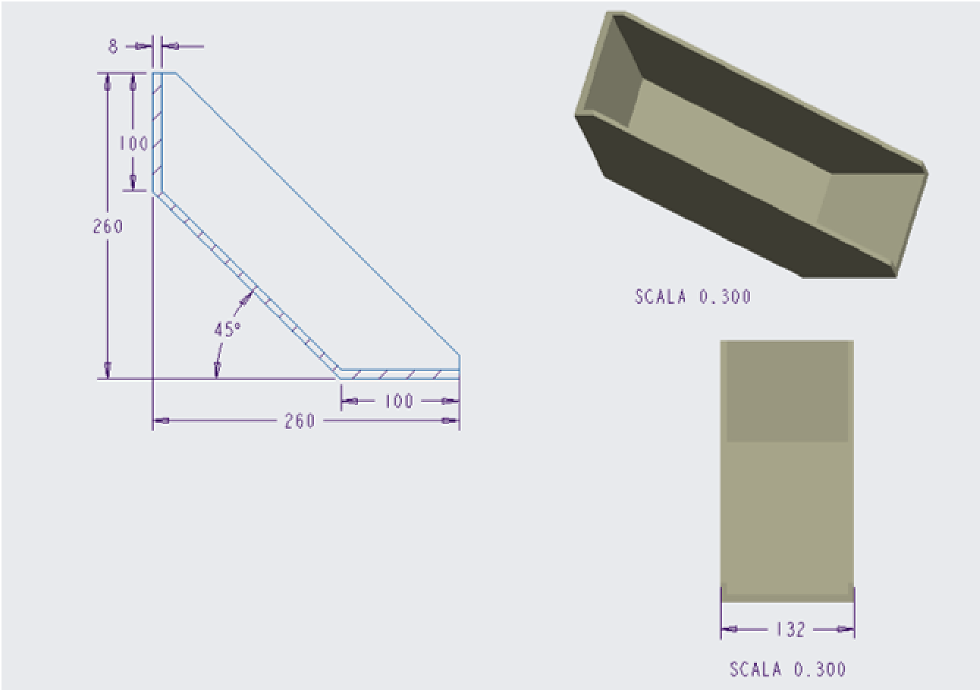


Figure 10.18: Diapress holder

## 10.8 Diapress stand

The component that will now be exposed is the diapress support.

**Figure 10.9** shows that the part is quite large, even in this case the larger area at the endpoints permits to apply the component for different diapress interaxis.

The function of this element is to connect the diapress with the chassis of the vehicle.

The diapress support is connected to the frame through the diagonal diapress presented above, this connection can be done either by bolting or welding.

## 10.9 Wheelbase

Another important dimension for the design of the frame is the distance between the beams.

As shown in the **Tables 9.2, 9.3, 9.4, 9.5, 9.6** the measures considered are 900, 950,1000 1200 mm.

The proposed solutions consider the fact of maintaining high resistance of

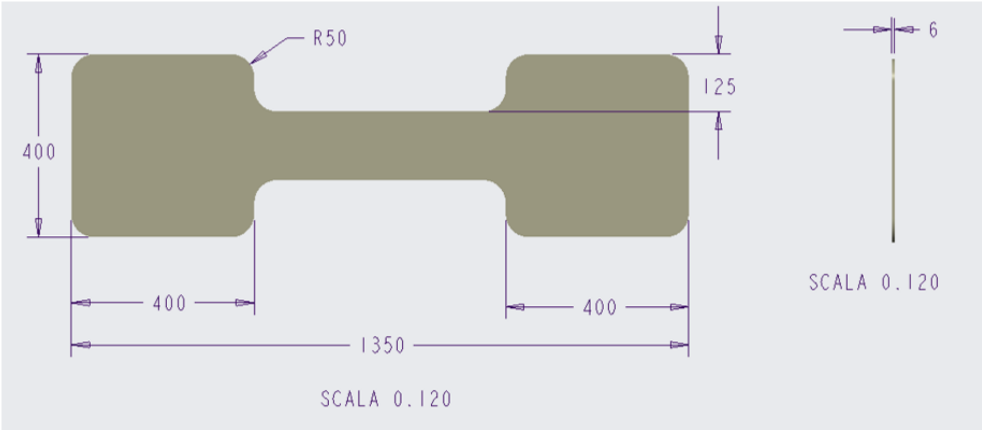


Figure 10.19: Diapress stand

the vehicle to torsion, the greater the distance between the beams the greater this resistance will be and at the same time foresee the application of single wheel axles (1200 mm pitch) and twin wheel axles (1000, 950 and 900 mm).

## 10.10 Components installation

A representation of the new chassis is shown in the **Figure 10.20**, in this case the second axle has been inserted at 1500 mm from the first axle, this configuration is commonly adopted for biga and trailer vehicles.

The designed frame turns out to be a compromise between the company's current knowledge and the part of innovation, also for this reason structures have been chosen that can be both bolted and welded, this choice allows to adopt the configuration of the frame to the current production keeping alive the realization of the welds but at the same time it allows to adopt the frame without particular changes to the case of bolting for a near future or for a part of research and development useful to the company.

The longitudinal beam is made using the welding method, drawing on the company's knowledge and experience. The crossbeams joining the two longitudinal beams are made by bending and then welded to the longitudinal beams.

The adoption of these joining crossbeams, through a simple modification, makes it possible to apply them also to bolting.

The component linked to the assembly of the axles involves welding the axles to the component, which is then welded to the lower part of the two longitudinal beams. The joint element with C-section unloads the stresses on the central part of the joint crossbeams; this element is supposed to be

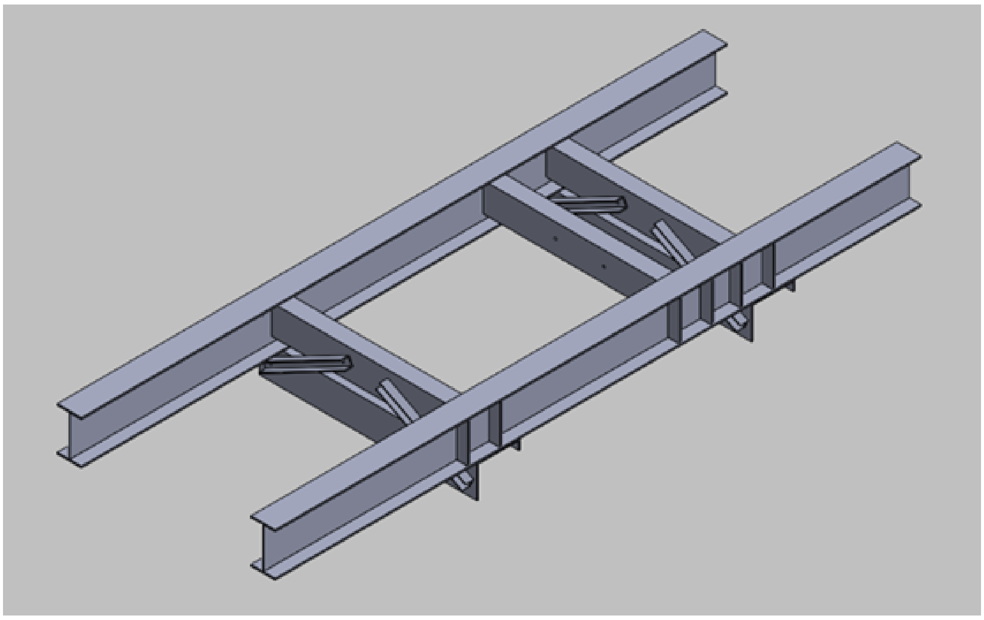

Figure 10.20: New chassis complete module

bolted between the element containing the axles and the joint crossbeam.

It was decided to introduce some elements related to bolting in the design of the frame in order to verify the possibility of realization of some couplings between the parts with the method of bolting. This choice is justified by the company's need to deepen its knowledge in this area in the coming years.

## 10.11 Considerations

The basic concept behind the presentation of these five different chassis is not only to enclose within these frames the largest number of vehicles made, but to note the different possible configurations starting from the elements presented.

The section in each component remains unchanged and varies only the length of the components.

At the same time, the verifications made for parts result to be resistant to the major stress caused by the semi-trailer, therefore the other two vehicles are in safe conditions.

# Chapter 11

# Front and rear couplings

One issue to be addressed once the above modules have been made concerns the junction between the parts.

Remember that the modules on display represent the central part of a vehicle, therefore the need to add front and rear parts to this module arises.

As previously mentioned, the junctions between the parts of the chassis are made by the welding method; in this section it will be tried to join the parts both with the welding method and with the bolting method.

## 11.1 Welded joint

### 11.1.1 Current materials and applications

The knowledge in the field of welding, within the company, is high due to the years of company experience in this field.

Welding inside vehicles is carried out by means of two different types of welding. The first type of welding is submerged arc welding, which is applied when the plates of the longitudinal beam are welded to the core of the beam itself. An image from production is shown in the **Figures 11.1**.

The second type of welding used is MAG (Metal Active Gas) welding, which is more economical than submerged arc welding but at the same time reliable. This type of welding is applied to the remaining welds, such as the various crossbeam junctions and the crossbeams on which the frame will be mounted. The **Figures 11.2** shows an image from the production sector of the material chosen for welding.


Figure 11.1: Material for beam welding


Figure 11.2: Material for common use welding

### 11.1.2 Welding design

The purpose of studying welded joints is to connect two parts of the frame, such as the central part and the rear part or the central part and the front part.[1]

The study that will be presented is based on what is reported in the "Quaderni di progettazione strutturale" (Structural Design Notebooks) of the "Fondazione Promozione Acciaio".

As a first analysis, the forces acting on the welded joint are studied and the case of interest is traced among the various cases.

#### Directional approach

The most common method for strength testing of welds is the directional method, which considers the throat section in its actual position.

The complexity of this method lies in having to evaluate the stress components in the plane of the throat section as shown in the **Figure 11.3**.

The normal stress ($\sigma_{//}$) parallel to the weld bead is neglected.

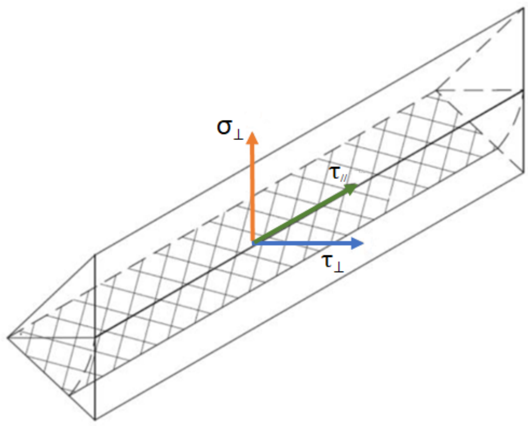


Figure 11.3: Tensional state in the groove section

The verification formulas are as follows:

$$\sqrt{\sigma_{\perp}^2 + 3(\tau_{\perp}^2 + \tau_{\parallel}^2)} \leq f_{tk}/\beta\gamma_{M2}$$

$$\sigma_{\perp} \leq f_{tk}/\gamma_{M2}$$

[1]this section has been realized thanks to [1]

Where:

- $\sigma_\perp$ is the normal tension at the throat section
- $\tau_\perp$ is the tangential tension orthogonal to the throat section
- $\tau_\parallel$ is the tangential tension parallel to the throat section
- $f_{tk}$ is the breaking strength of the weakest of the connected elements
- $\gamma_{M2}$ is the partial safety coefficient for partial penetration and corner welds (NTC2018 - Table 4.2. XIV)
- $\beta$ is a weld efficiency coefficient dependent on the strength class of the steel shown in the **Table 11.1**

Table 11.1: Coefficient values $\beta$

| Grade | efficiency coefficient $\beta$ |
|---|---|
| S235 | 0.80 |
| S275 | 0.85 |
| S355 | 0.90 |
| S420 and S460 | 1.00 |

### 11.1.3 Stress study

In the study of stresses, the maximum load conditions of the vehicle and the towing force imposed by the towing vehicle are also taken into consideration.

The stresses that will be considered derive from the vehicle with the highest loaded mass (i.e. the semi-trailer) and from them also the towing force.

In this study we have chosen to include also the towing force in order to apply the welding model also to the junction between the front and the central part.

As far as the rear part is concerned, it is considered as acting forces and moments those linked to the maximum distributed load of the vehicle and we apply an additional mass linked to the rear part itself and to the various masses of the additional objects mounted on it.

### 11.1.4 Backside study

As a first case, has been studied the rear part of the vehicle. This part is assigned a length of 2 meters, which is the maximum length for vehicles such as biga-trailers and semi-trailers.

The acting force is considered as the maximum load of the semi-trailer (140 kN due to the division between the two beams) distributed over the 13.6 m available. A force per meter of 10295 N/m is therefore obtained.

The force will be applied at a distance of 1 m. A force of 25 kN is considered as a conservative value.

### 11.1.5 Joint component

The component (**Figure 11.4**) that will be mounted between the two parts is now introduced. It is inspired by an assembly already applied on particular semitrailer vehicles.

The components studied are made with C-sections that can be internally produced, the assembly is made in such a way as to increase the stiffness of the frame in this particular area of junction.

Another change that has been made compared to the basic model is an increase of the core that goes from 5 mm to 8 mm. This modification has been made for a longitudinal beam length of 500 mm both in front and rear.

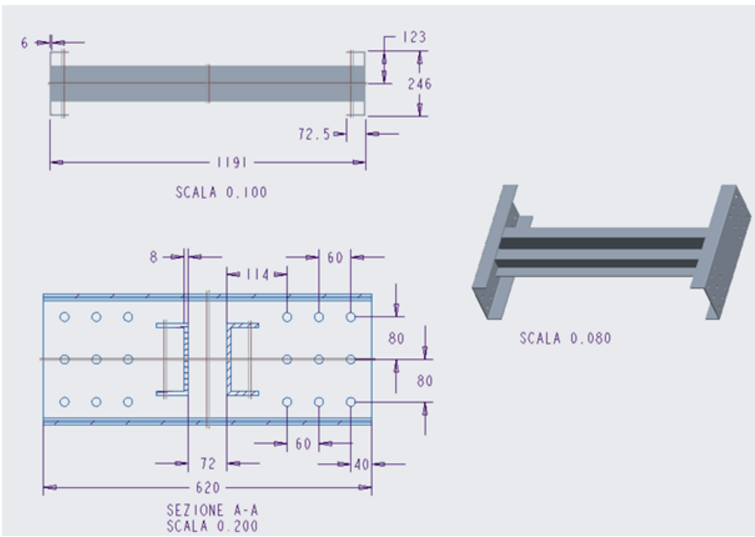


Figure 11.4: Complete joint component

The joint component has been designed for both bolting and welding.

In the case of welding, the joint assembly will be inserted in the inner part of the central frame (between the two longitudinal beams) and then welded on the sides, welding sections are highlighted in the **Figure 11.5**.

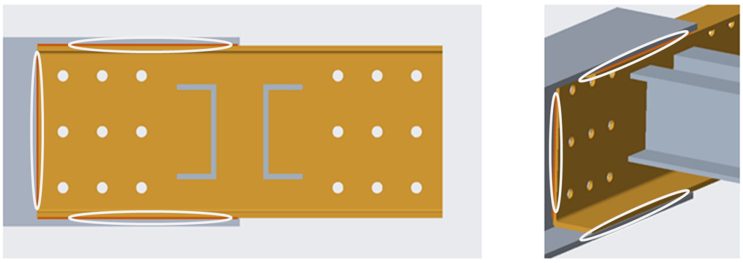

Figure 11.5: Welding spots

The formulas for calculating the strength of welded joints in the case under consideration can be obtained from the text "Quaderni di progettazione strutturale". As a first calculation, consider the structure loaded by a force F acting at a distance and from the center of the weld. The joint described above falls within this model, since for simplicity's sake a concentrated force F applied at a certain distance e was considered.

As can be seen from the formulas, the load creates shear and torsion on the weld seams; the load is distributed in the seams according to the laws shown in **Figure 11.6**.

Table 11.2: Coefficient values

| $f_{tk}$ | $\beta$ | $\gamma$ |
|---|---|---|
| 510 | 0.90 (for FE510) | 1.25 |

Table 11.3: Values for calculating the useful value for the verification formula

| L[mm] | $L_1[mm]$ | $L_2[mm]$ | $a_1[mm]$ | $a_2[mm]$ | h[mm] |
|---|---|---|---|---|---|
| 310 | 220 | 300 | 4.24 | 4.24 | 236 |

### Shear and torsion joints with bead combination

Assumptions of total torque distribution T into two rates $T_1$ and $T_2$ absorbed by the frontal (1) and lateral (2) chords, respectively. Conventionally made in relation to the maximum torques that can be entrusted to the two pairs of chords, $T_{1,max}$ and $T_{2,max}$. The maximum values $T_{1,max}$ and $T_{2,max}$,max can

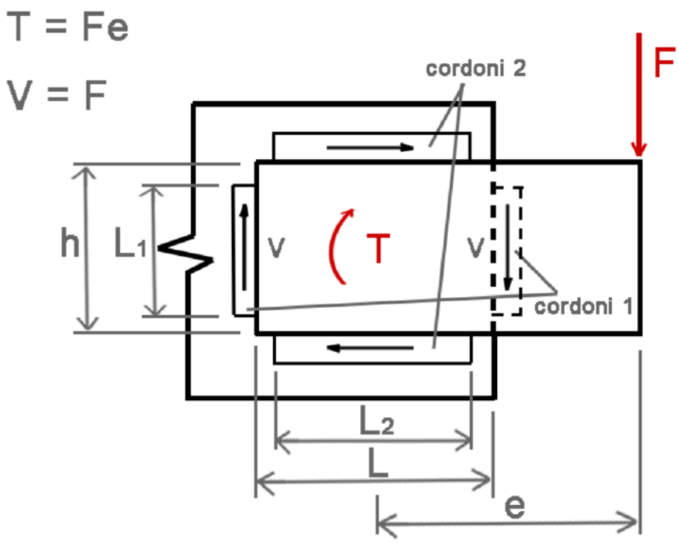


Figure 11.6: Shear and torsion joints with bead combination

be obtained by adopting a maximum voltage $f_s$ considered acceptable and an appropriate safety coefficient.

$$T_{1,max} = a_1 L_1 f_s h$$

$$T_{2,max} = a_2 L_2 f_s h$$

$$T_1 = T\frac{a_1 L_1 L}{a_1 L_1 L + a_2 L_2 h}$$

$$T_2 = T\frac{a_2 L_2 L}{a_1 L_1 L + a_2 L_2 h}$$

Having determined the distribution of the load on the lateral and frontal cords, it is now possible to calculate the stresses.

The formulas shown below make it possible to evaluate the stresses in the two different types of beads (frontal and lateral).

Once the stresses have been evaluated, it is then possible, using the formula of the directional method, to assess whether the weld is in the safe region or not.

### Shear and torsion joints with side chords

Throat section in the actual position:

$$\tau_{\parallel} = \frac{Fe}{haL} = 41.1MPa \quad \sigma_{\perp} = \frac{Fcos(\alpha)}{2aL} = 3.43MPa \quad \tau_{\perp} = \frac{Fsin(\alpha)}{2aL} = 3.43MPa$$

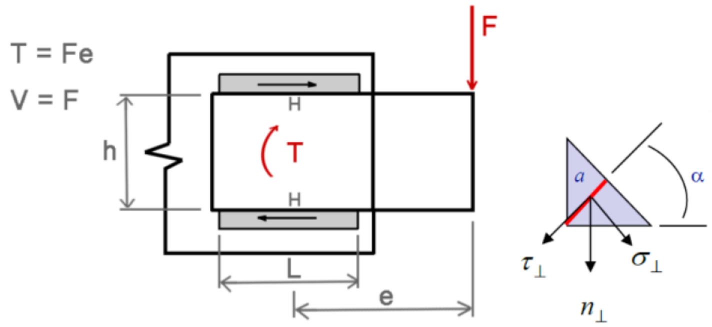


Figure 11.7: Shear and torsion bonding with lateral cords

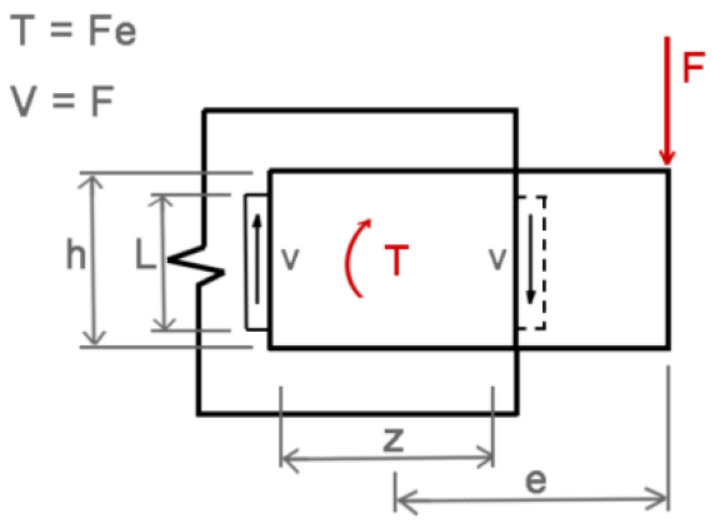


Figure 11.8: Shear and torsion bonding with front beads

### Shear and torsion joints with front beads

Throat section in the actual position:

$$\tau_{\parallel} = \frac{F}{aL}\left(\frac{1}{2} + \frac{e}{z}\right) = 49.0MPa$$

### Tensile joints with combined beads

Another stress that is taken into consideration during the design phase is the towing force due to the towing vehicle. This force can have quite high modulus values as in the case of the semi-trailer where this value can reach up to 100 kN for each longitudinal beam.

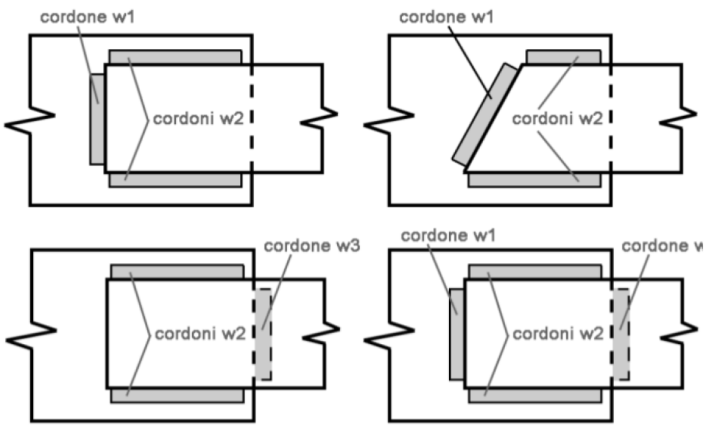


Figure 11.9: Tensile bonding with combined beads

In the use of combined beads it is advisable to entrust the entire load to the lateral or frontal beads because of the different behavior in terms of stiffness and ductility in the response found experimentally. it is also advisable to avoid different groove thicknesses and, in the case of entrusting the load to both types of bead, to make compact joints.

In this case, as reported by the reference text, it is chosen to distribute this load only in the lateral or frontal chords. The verification will be carried out for both frontal and lateral chords.

**Tension joints with side chords** Throat section in the actual position:

$$\tau_{\parallel} = \frac{F}{4aL} = 76.0MPa$$

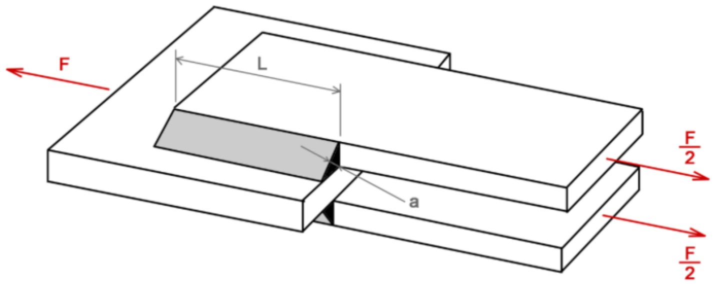


Figure 11.10: Tension joints with side chords

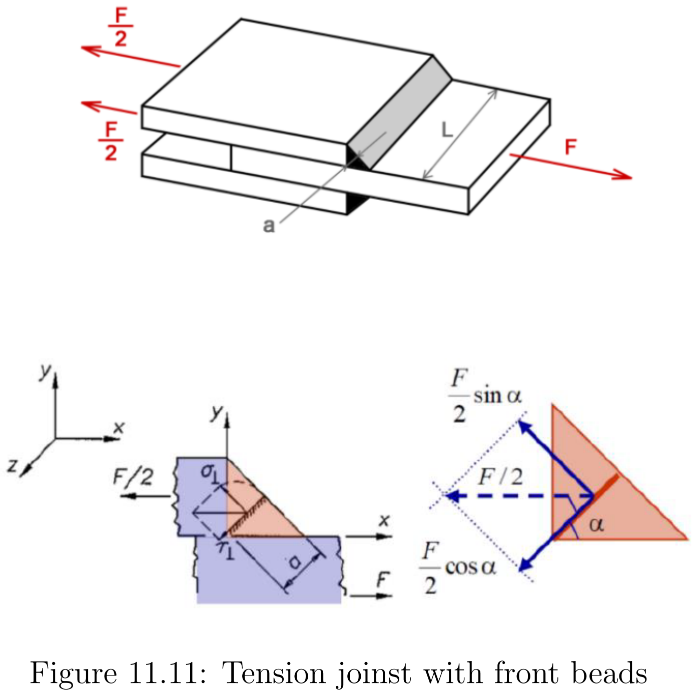


Figure 11.11: Tension joinst with front beads

**Tension joinst with front beads** Throat section in the actual position:

$$\sigma_{\perp} = \frac{Fsin(\alpha)}{2aL} = 37.9MPa$$

$$\tau_{\perp} = \frac{Fcos(\alpha)}{2aL} = 37.9MPa$$

Carrying out the calculations with the above formulas and considering as forces for the bending moment 25 kN applied at 1 m distance from the joint and 100 kN as traction force, the values of the equivalent stresses in the frontal and lateral joints are obtained (114 MPa for the frontal joint and 203 MPa for the lateral joint) according to the formula for the directional method and considering the application of the joint to the frame with S355J0 material, wthe equivalent stresses must be kept below 453 MPa.

In the case just considered, the static design belongs to the safety zone.

### Fatigue verification for welded joints

For the fatigue test discussed in this paragraph, the minimum and maximum forces that will act on the joint are evaluated in order to assess the equivalent stresses useful for fatigue analysis. The four different types of welding

Table 11.4: Alternating forces for stress calculation

| | | |
|---|---|---|
| Minimum case | Traction force [N] | 0 |
| | Loading force [N] | 5000 |
| Maximum case | Traction force [N] | 80000 |
| | Loading force [N] | 25000 |

were reported in the **Table 11.5** along with their respective equivalent and alternating stresses useful for fatigue analysis.

Table 11.5: Alternating stresses for different welding joints

| Welding joint | $\sigma_{min}[MPa]$ | $\sigma_{max}[MPa]$ | $\sigma_m[MPa]$ | $\sigma_a[MPa]$ |
|---|---|---|---|---|
| Shear&torsion side (1) | 0 | 105.4 | 52.7 | 52.7 |
| Shear&torsion front (2) | 75.8 | 152.0 | 113.9 | 38.1 |
| Tension side (3) | 77.0 | 113.8 | 95.4 | 18.4 |
| Tension front (4) | 11.43 | 71.43 | 41.43 | 30 |

Fatigue verification was carried out using the Haigh diagram applied to the four different welds present in the joint. This graph was created using Matlab software, as shown in the **Figure 11.12, 11.13, 11.14, 11.15**. The calculation of the safety coefficients for the fatigue life of the components was carried out considering constant $\sigma_m$ stress and $\sigma_a$ variable. The fatigue strength value of the material was considered as ninety percent of yield strength ($0.9*R_{p_{02}}$) for a considered life of 2 million cycles ($N_c$=$2*10^6 cycles$).

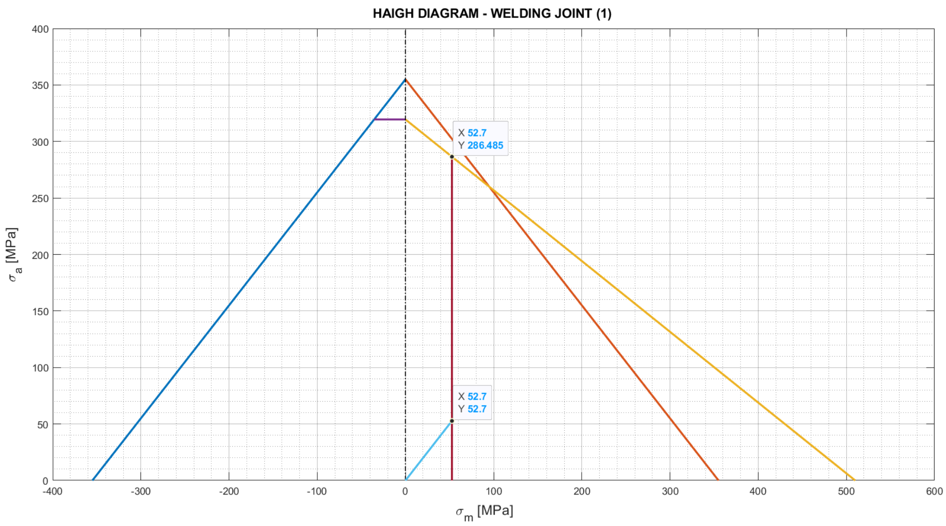


Figure 11.12: Haigh diagram joint 1

Table 11.6: Safety factor relative to fatigue verification

| Welding joint | Safety factor |
|---|---|
| Shear&torsion side (1) | 5.44 |
| Shear&torsion front (2) | 6.33 |
| Tension side (3) | 14.1 |
| Tension front (4) | 9.78 |

**Table 11.6** shows the safety factor results for the cases studied, the safety coefficient can be calculated through the ratio of:

$$SF = \frac{y_B}{y_A}$$

The points A and B are visibile in **Figure 11.15**. The point B is identified by the vertical line passing through the operating point A of coordinates ($\sigma_m$,$\sigma_a$) of **Table 11.5**, this point lies on the first line encountered which can be either the line passing through the points (0,$R_{p_{02}}$) and ($R_{p_{02}}$,0) or the line passing through the points (0,0.9*,$R_{p_{02}}$) and ($R_m$,0).

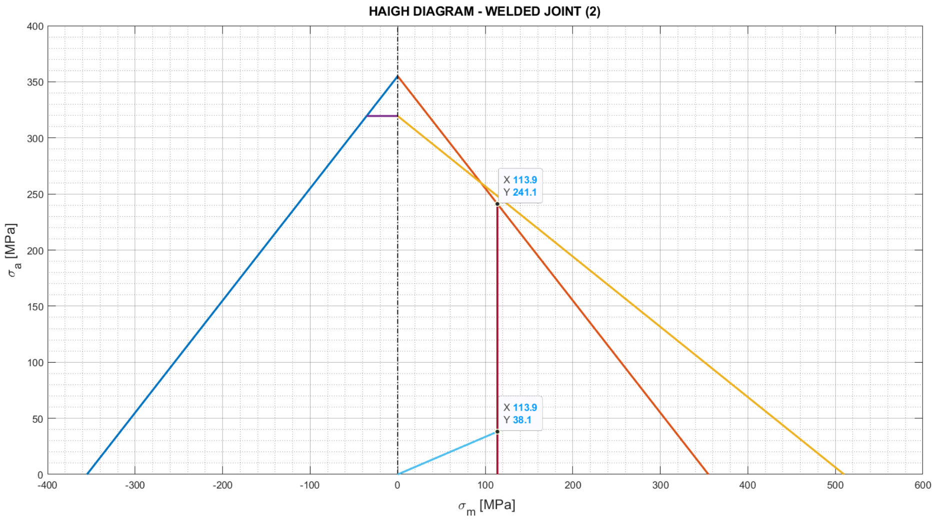


Figure 11.13: Haigh diagram joint 2

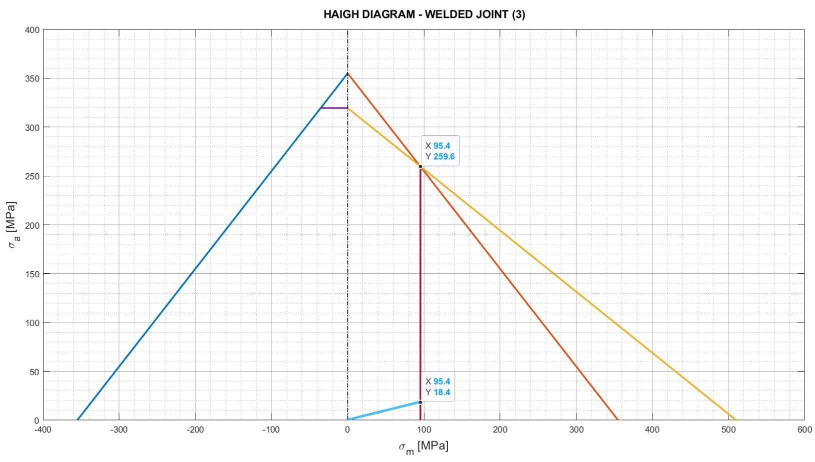


Figure 11.14: Haigh diagram joint 3

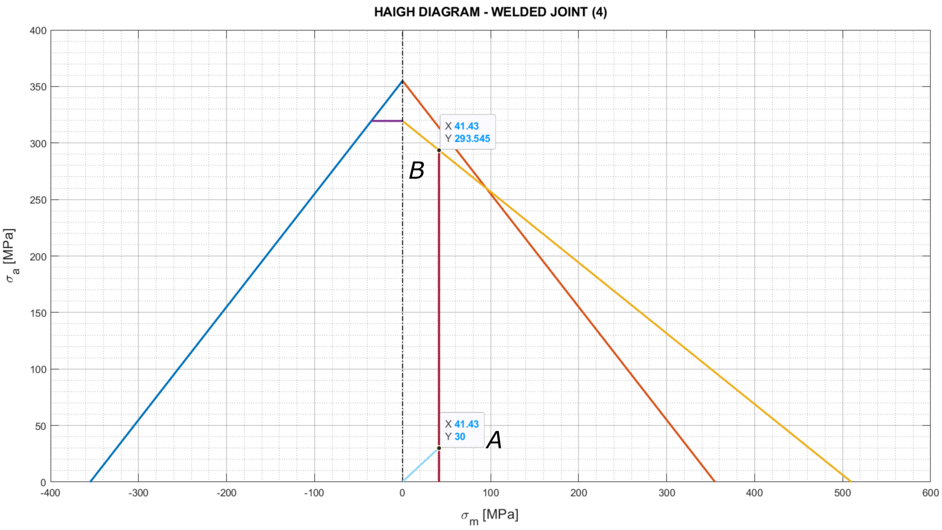


Figure 11.15: Haigh diagram joint 4

## 11.2 Bolted joint

Moving on now to the study of the bolted joint.[2]

In this case, a different approach method is chosen for the rear and the front.

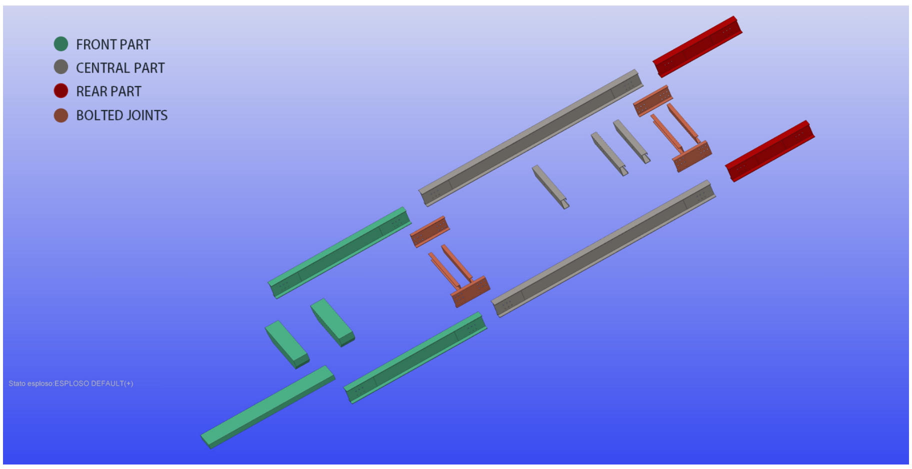


Figure 11.16: Biga-vehicle parts

[2]this section has been realized thanks to [1]

**Figure 11.16** shows the configuration according to the new approach of the biga vehicle, in this case the key elements have been reported in order to correctly understand the vehicle and its assembly. The figure shows the three main parts, front, middle and rear and between them are the two connecting joints.

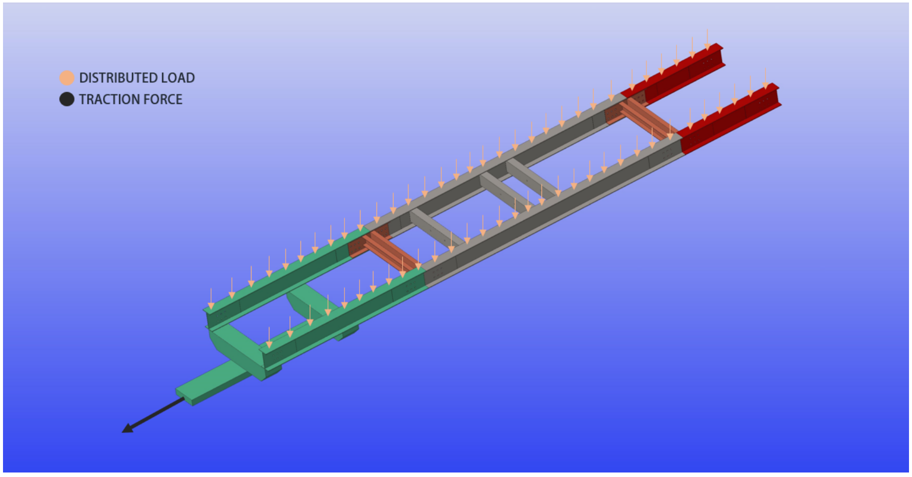


Figure 11.17: Biga vehicle loads for bolt design

The loads considered for the design of the screws for bolting the joint are shown in **Figure 11.17**, the forces considered also in this part of the design are due to the maximum permissible load for the semi-trailer, i.e. the most stressed vehicle among those studied.

The junction of the middle part with the rear part takes into account the distributed load of the rear part of the vehicle as the main load.

The junction of the middle part with the front part also considers the towing force caused by the towing vehicle.

It is applied a different approach with different loads on the two structures (**Figure 11.19**, **Figure 11.23**) in order not to oversize the rear part unnecessarily and at the same time we want to study in detail the front part with its towing force in order not to neglect the forces involved in this part of the structure.

### 11.2.1 Bolts

The bolts chosen also in this case represent a compromise between the various conditions, such as the need to have a limited number of components and therefore also of bolts and joints and at the same time allow the application of this joint and therefore of the frame itself for more stressed structures such as in the case of semi-trailers.

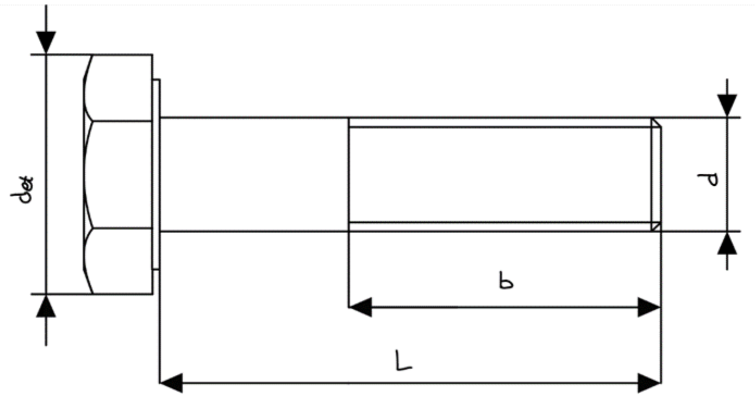


Figure 11.18: Bolts dimensions

### 11.2.2 Rear bolted joint

For the joint in the back it is considered the joint structure already introduced earlier, this allows us to recall the main part of this paper (i.e. component reduction by introducing standard components).

#### Design of bolts for the rear part

I=2.5
$M_{max}$=25 kNm
$L_p$=16 mm
d=420 mm
$R_a$=1.6 $\mu$m
SF=2
$R_m$ = 1000 MPa
$R_{p02}$ = 900 MPa
$n_{bolts}$ = 18
f=0.4

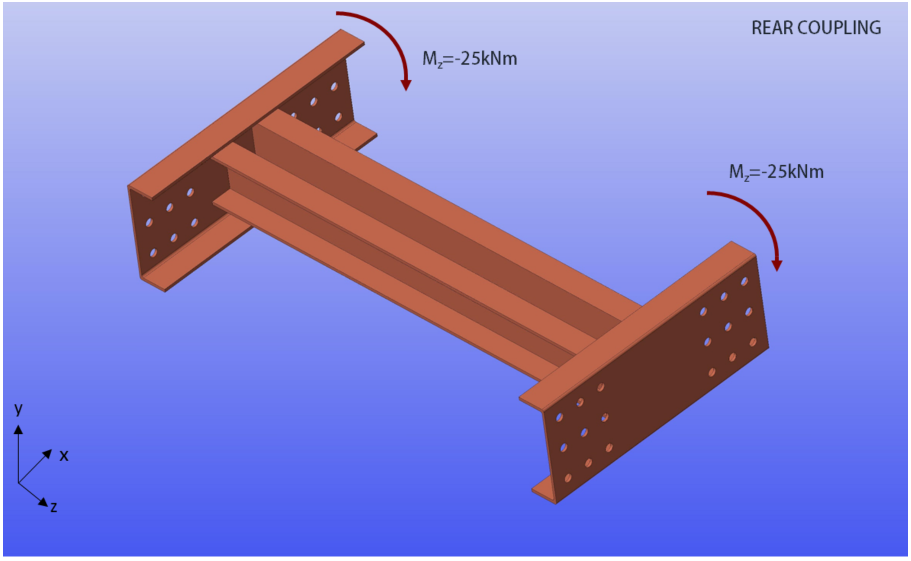


Figure 11.19: Loads on rear bolted joint

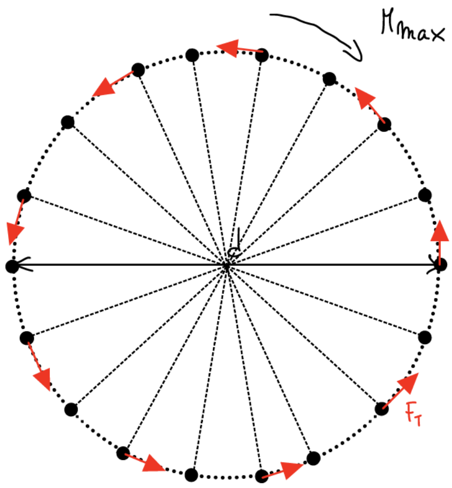


Figure 11.20: Rear bolts configuration with loads

$$F_T = \frac{M_{max}}{18*d/2} = 6,6kN \;\; N = \frac{F_T}{f} = 16.5kN \;\; F_{plim} = SF*N = 33kN$$

$$A_{num} = \frac{4*F_{plim}}{R_{p02}} = 147mm^2$$

it is possible to choose M16 $A_{res}$=157 $mm^2$

Bolt M16x2
L=50mm
b=38mm
L-b=12mm

$$\sigma_{amm} = 0.9*R_{p02} = 810MPa = \sigma_{idlim}$$

$$\sigma_{idlim} = \sigma_{alim}*\sqrt{1+3*k^2}$$

tan($\phi$)=0.12

$\beta$=30°

$$k = \frac{\tau}{\sigma} = \frac{2}{d_n}*(\frac{p}{\pi}+d_m\frac{tan(\phi)}{cos(\beta)}) = 0.36374$$

$$d_n = d - 1.2268*p = 13.5464mm$$

$$d_m = d - 0.6495*p = 14.701mm$$

$$\sigma_{alim} = \frac{\sigma_{idlim}}{\sqrt{1+3k^2}} = 685MPa$$

$$F_{vmax} = F_{vlim} = \sigma_{amm}*A_{res} = 100695N$$

$$F_{vmin} = \frac{F_{vmax}}{I} = 40278N$$

$l_1$=12mm

$l_3$=4mm

$\Delta_i$=16 $\mu$m

$E_p$=210GPa

$$\Delta F_v = \frac{\Delta_i}{\delta_p+\delta_v}$$

$$\delta_p = \frac{L_p}{E_pA_p} = 2.15*10^{-7}\frac{mm}{N}$$

$$A_p = \frac{\pi}{4}(d_{et}+0.5*L_p*tan(30))^2 - d_f^2$$

$d_f$=d+1

$L_p$=16mm

$d_{et}$=24mm

$$\delta_v = \frac{1}{E_v}\left(\frac{l_1+0.4*d}{A_1} + \frac{l_3+0.4*d}{A_3}\right) = 7.275*10^{-7}\frac{mm}{N}$$

$$A_1 = \frac{\pi*d^2}{4}$$

$$A_3 = \frac{\pi*d_m^2}{4}$$

$$\Delta F_v = \frac{\Delta_i}{\delta_p+\delta_v} = 16976N$$

$$R_{P02}A_{res} = 132300N$$

$$F_A = \frac{M_{max}}{n_{bolts}*1m} = 1389N$$

$$\Delta C_v = \frac{F_A\delta_p}{\delta_p+\delta_v} = 317N$$

$$\Delta C_p = \frac{F_A\delta_v}{\delta_p+\delta_v} = 1072N$$

$$F_{vmax} + \Delta C_v = 101012N < 132300N \quad OK$$
$$\frac{F_{vmax}}{I} + \Delta F_v + \Delta C_p = 58326N > 33000N \quad OK$$

**Fatigue verification for rear bolted joint**

The force $C_{min}$ was obtained from the rear mass of the vehicle, this force was evaluated through the 3D model of the chassis.

The $C_{max}$ force was derived from the sum of the maximum allowable load from the vehicle in the rear area added to the mass in the rear area of the vehicle with the various auxiliaries.

The interference diagram in the case where there is an external load oscillating between a $C_{min}$ value and a $C_{max}$ value is shown in **Figure 11.22**. From the formulas derived from machine design notes[3] it is therefore possible to fatigue test the designed bolts.

$$C_{min} = 8000N$$

$$C_{max} = 28590N$$

$$\Delta C_{minv} = \frac{8000}{2} = 4000N$$

$$\Delta C_{maxv} = \frac{28590}{2} = 14295N$$
$$F_{vmax} = F_{vlim} + \Delta C_{maxv} = 114990N$$

$$F_{vmin} = F_{vlim} + \Delta C_{minv} = 104695N$$

$$F_{vm} = \frac{F_{vmax+F_{vmin}}}{2} = 109842.5N$$

$$F_{va} = \frac{F_{vmax}-F_{vmin}}{2} = 5147.5N$$

$$\sigma_a = \frac{F_{va}}{A_{num}} = 35MPa$$

[3]this section has been realized thanks to [14]

$$\sigma_m = \frac{F_{vm}}{A_{num}} = 747MPa$$
$$\frac{\sigma_m}{R_{p02}} = 0.83$$

From the graph of **Figure 11.21** it is possible to retrieve the $\sigma_D$ value:

$$\sigma_D = 85MPa$$
$$\sigma_{a,amm} = 0.9 * \sigma_D = 76.5MPa$$
$$SF = \frac{\sigma_{a,amm}}{\sigma_a} = 2.13$$

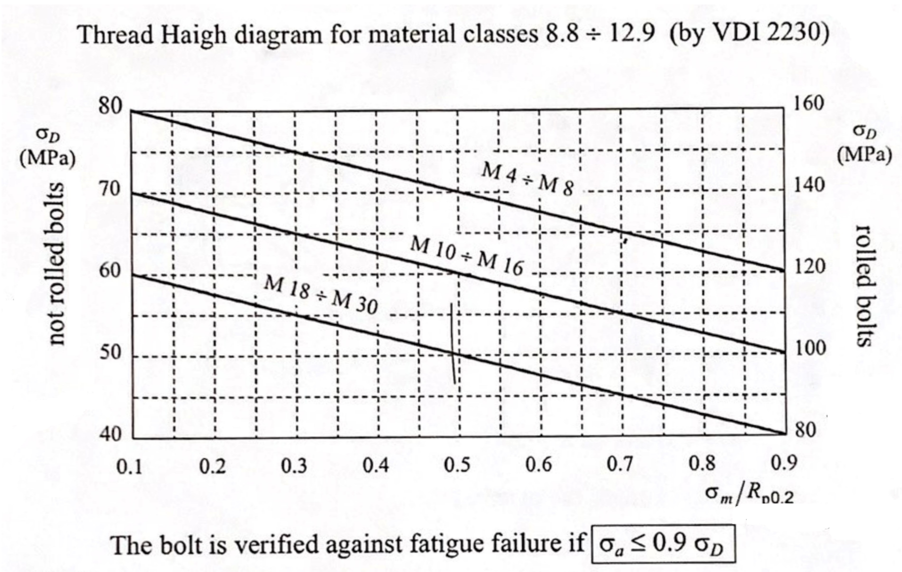


Figure 11.21: Thread Haigh diagram (by VDI 2230)

Fatigue verification shows a safety coefficient greater than two, which is reasonable in the case of application.

### 11.2.3 Front bolted joint

As far as the front joint is concerned, the same procedure already seen in the case of the rear joint is followed, however, in this part the stress linked to the driving force comes into play, which in this case is considered equal to 100 kN.

The insertion of this new stress varies the stress acting on the bolts considered.

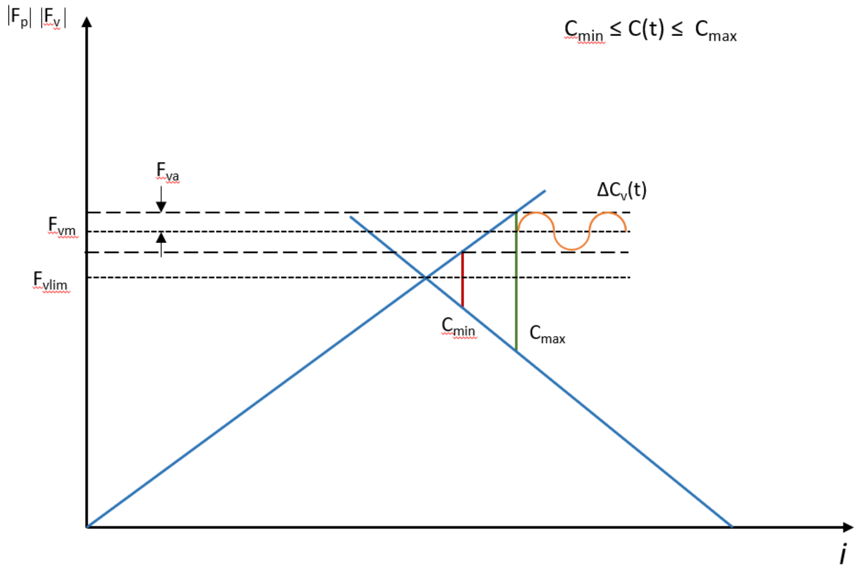


Figure 11.22: Interference diagram of bolts for external loads

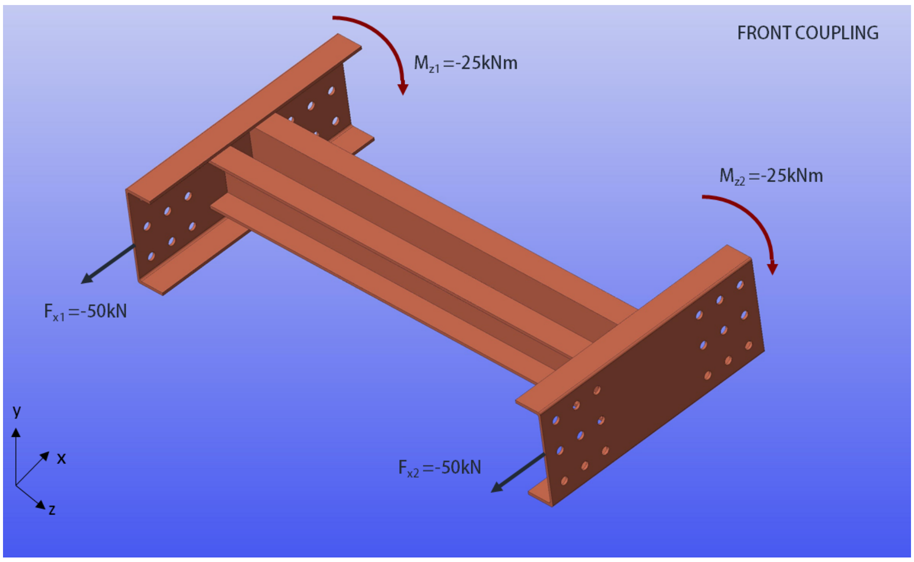


Figure 11.23: Loads on front bolted joint

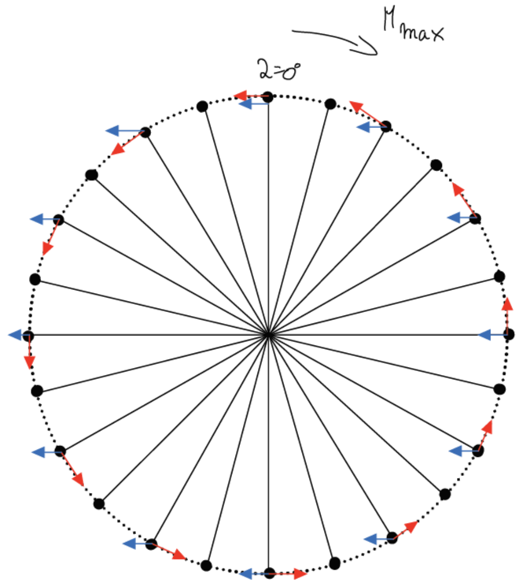


Figure 11.24: Front bolts configuration with loads

**Design of bolts for the front part**

I=2.5
$M_{max}$=25 kNm
$F_{towing}$=100kN $L_p$=16 mm
d=700 mm
$R_a$=1.6 $\mu$m
SF=2
$R_m$ = 1000 MPa
$R_{p02}$ = 900 MPa
$n_{bolts}$ = 24
f=0.4

$$F_T = \frac{M_{max}}{24*d/2} = 2.98kN$$

$$F_{horizontal} = \frac{F_{towing}}{24} = 4170N$$

$$F_{BOLT} = F_{horiziontal} + F_T = 7150N$$

$$N = \frac{F_T}{f} = 17875N \; F_{plim} = SF * N = 35.75kN \; A_{num} = \frac{4*F_{plim}}{R_{p02}} = 159mm^2$$

it is possible to choose M18 $A_{res}$=192 $mm^2$

Bolt M18x2.5
L=55mm
b=42mm
L-b=13mm

$$\sigma_{amm} = 0.9 * R_{p02} = 810MPa = \sigma_{idlim}$$

$$\sigma_{idlim} = \sigma_{alim} * \sqrt{1 + 3 * k^2}$$

$\tan(\phi)$=0.12

$\beta$=30°

$$k = \frac{\tau}{\sigma} = \frac{2}{d_n} * (\frac{p}{\pi} + d_m \frac{tan(\phi)}{cos(\beta)}) = 0.41049$$

$$d_n = d - 1.2268 * p = 14.933mm$$

$$d_m = d - 0.6495 * p = 16.376mm$$

$$\sigma_{alim} = \frac{\sigma_{idlim}}{\sqrt{1+3k^2}} = 660.15MPa$$

$$F_{vmax} = F_{vlim} = \sigma_{amm} * A_{res} = 126749N$$

$$F_{vmin} = \frac{F_{vmax}}{I} = 50700N$$

$l_1$=13mm

$l_3$=3mm

$\Delta_i$=16 $\mu$m

$E_p$=210GPa

$$\Delta F_v = \frac{\Delta_i}{\delta_p + \delta_v}$$

$$\delta_p = \frac{L_p}{E_p A_p} = 1.796 * 10^{-7} \frac{mm}{N}$$

$$A_p = \frac{\pi}{4}(d_{et} + 0.5 * L_p * tan(30))^2 - d_f^2$$

$d_f$=d+1

$L_p$=18mm

$d_{et}$=27mm

$$\delta_v = \frac{1}{E_v}(\frac{l_1 + 0.4 * d}{A_1} + \frac{l_3 + 0.4 * d}{A_3}) = 4.739 * 10^{-7} \frac{mm}{N}$$

$$A_1 = \frac{\pi * d^2}{4}$$

$$A_3 = \frac{\pi * d_m^2}{4}$$

$$\Delta F_v = \frac{\Delta_i}{\delta_p + \delta_v} = 24484N$$

$$R_{P_{02}} A_{res} = 172800N$$

$$F_A = \frac{M_{max}}{n_{bolts}*1m} = 1042N$$

$$\Delta C_v = \frac{F_A \delta_p}{\delta_p + \delta_v} = 286.4N$$

$$\Delta C_p = \frac{F_A \delta_v}{\delta_p + \delta_v} = 756N$$

$$F_{vmax} + \Delta C_v = 127036N < 172800N \quad OK$$

$$\frac{F_{vmax}}{I} + \Delta F_v + \Delta C_p = 75940N > 35750N \quad OK$$

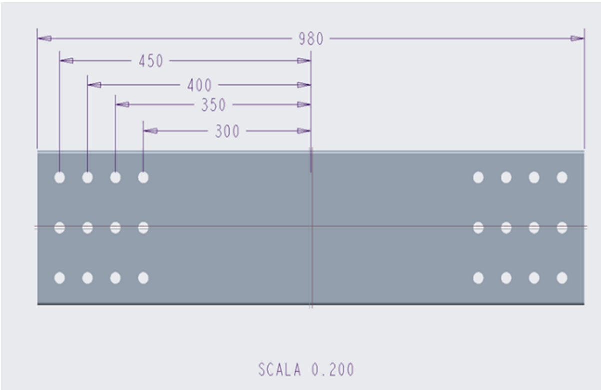


Figure 11.25: Joint configuration for front part application

### Fatigue verification front bolted joint

The force $C_{min}$ was obtained from the front mass of the vehicle, this force was evaluated through the 3D model of the chassis and considering also the maximum towing force of the vehicle during braking condition.

The $C_{max}$ force was derived from the sum of the maximum allowable load from the vehicle in the front area added to the mass in the front area of the vehicle with the various auxiliaries, also in this is added the maximum towing force of the vehicle during acceleration.

The interference diagram in the case where there is an external load oscillating between a $C_{min}$ value and a $C_{max}$ value is shown in **Figure 11.22**. From the formulas derived from machine design notes it is therefore possible to fatigue test the designed bolts.

$$C_{min} = 10000N$$

$$C_{max} = 37000N$$

$$\Delta C_{minv} = \frac{10000}{2} = 5000N$$

$$\Delta C_{maxv} = \frac{37000}{2} = 18500N$$

$$F_{vmax} = F_{vlim} + \Delta C_{maxv} = 119195N$$
$$F_{vmin} = F_{vlim} + \Delta C_{minv} = 105695N$$
$$F_{vm} = \frac{F_{vmax+F_{vmin}}}{2} = 112445N$$
$$F_{va} = \frac{F_{vmax} - F_{vmin}}{2} = 6750N$$
$$\sigma_a = \frac{F_{va}}{A_{num}} = 35MPa$$
$$\sigma_m = \frac{F_{vm}}{A_{num}} = 585.7MPa$$
$$\frac{\sigma_m}{R_{p02}} = 0.651$$

From the graph of **Figure 11.21** it is possible to retrieve the $\sigma_D$ value:

$$\sigma_D = 95MPa$$
$$\sigma_{a,amm} = 0.9 * \sigma_D = 85.5MPa$$
$$SF = \frac{\sigma_{a,amm}}{\sigma_a} = 2.44$$

Fatigue verification shows a safety coefficient greater than two, which is reasonable in the case of application.

# Chapter 12

# FEM static verification of new chassis

After the design of the new chassis with standard components and the description of the possible ways to join the various parts of the chassis in order to realize the complete vehicle chassis, the numerical verification is now done in order to prove the goodness of the project realized.

As already described in the previous chapter the joining between parts of the frame is done in two different ways: welding and bolting.

In this last section the simulation software for finite element analysis is different from the previous analysis, no longer use of Altair Hypermesh but instead ANSYS MECHANICAL is chosen.

## 12.1 Central module verification

As a first case of interest, is consider the core module frame described in previous chapters.

The central module is shown in the **Figure 12.1**.

### 12.1.1 Material

The material applied to the geometry is structural steel according to the already reported characteristics of S355J0 used in the company.

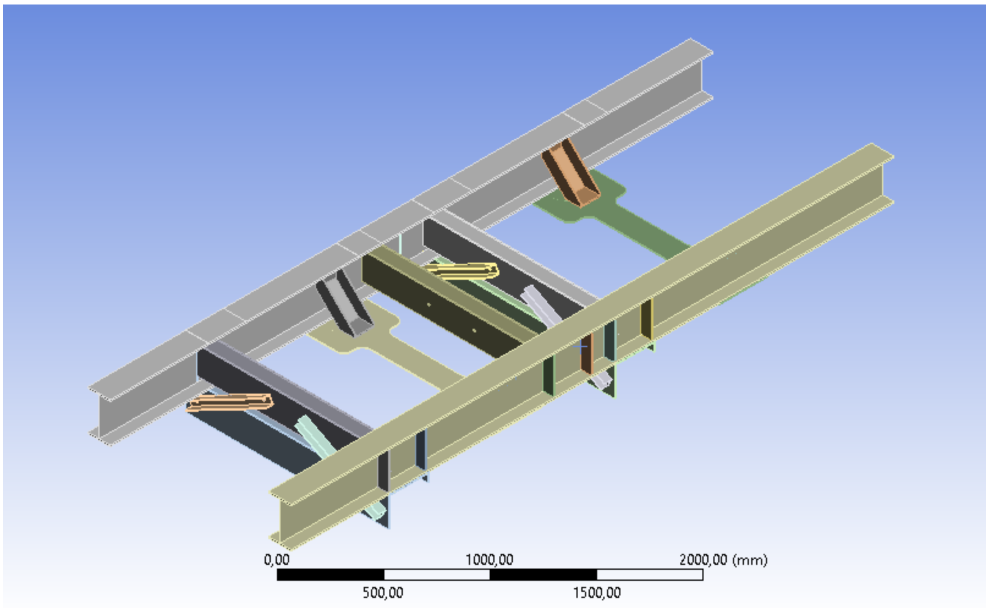


Figure 12.1: Central module geometry

### 12.1.2 Connections

The ANSYS software allows simple management of contact between the various frame components; in the case studied, all welded components are considered as shown in the **Figure 12.2**.

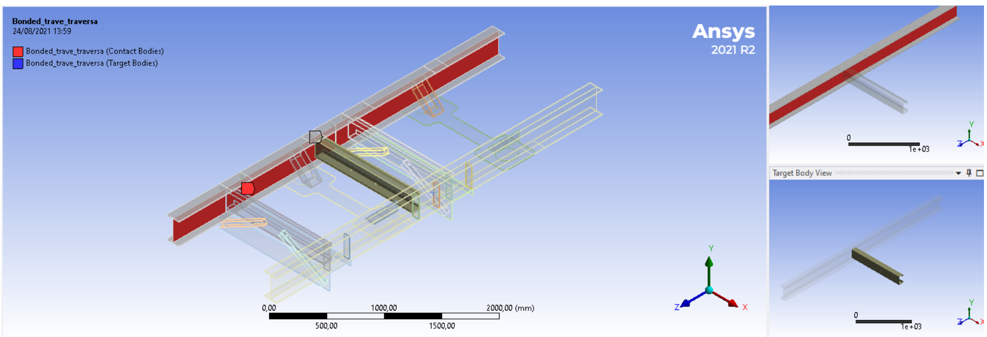


Figure 12.2: Contact property on ANSYS

This characteristic results to be a constraint for the ANSYS software, that is it binds the two components in such a way that in the contact section the two bodies have the same deformations and the same tension field.

### 12.1.3 Mesh implementation

The mesh realization through ANSYS software turns out to be very good due to the power of the software.

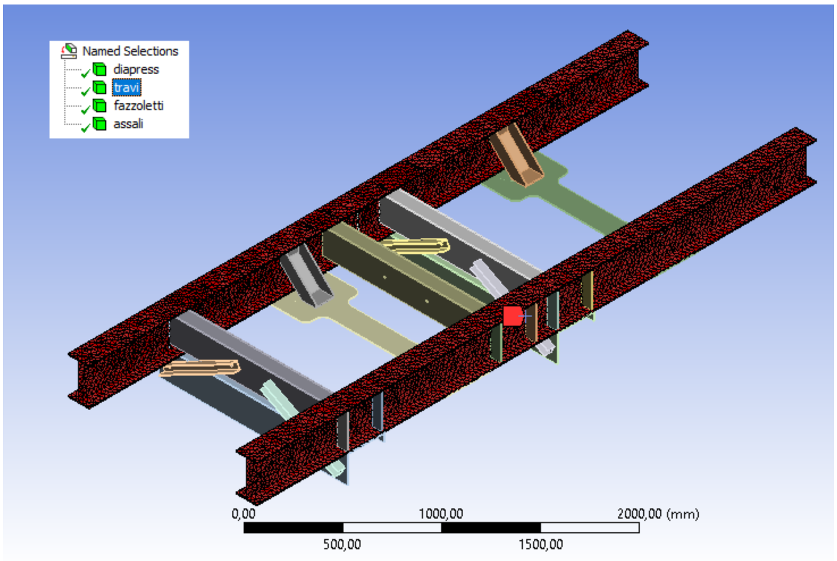


Figure 12.3: Mesh of beams on ANSYS

In this case, the various components were grouped using the "Named Selection" command. Each "Named Selection" was associated with a mesh method and a size in order to optimize the mesh and concentrate the greatest number of elements in the points of interest.

### 12.1.4 Loads and constraints

As already seen in the finite element analysis (**Chapter 6**) of the part frame, the same loads and constraints are considered in order to obtain results comparable to the original model.

The loads are visible from **Figure 12.5** and the constraints are reported on **Figure 12.6**. The frame of the central module is considered loaded with a distributed load given by the maximum loadable mass of the semi-trailer vehicle (this is the heaviest case among the three analyzed).

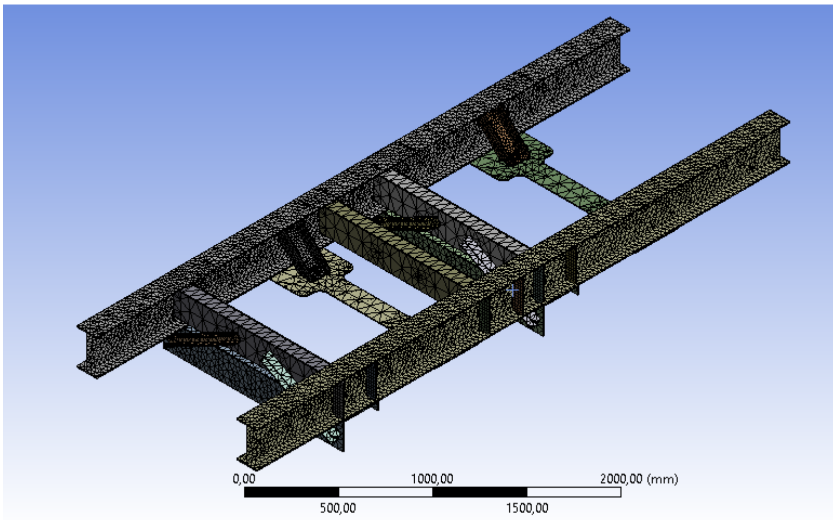


Figure 12.4: Complete mesh on ANSYS

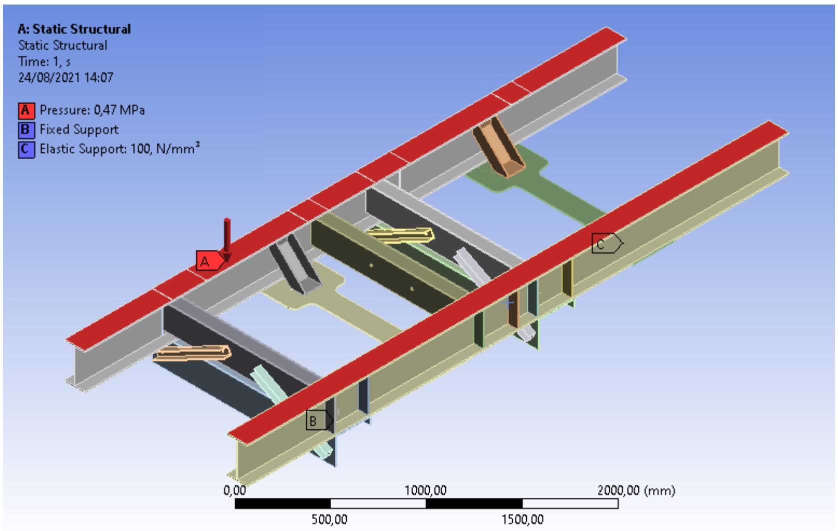


Figure 12.5: Loads applied to the module

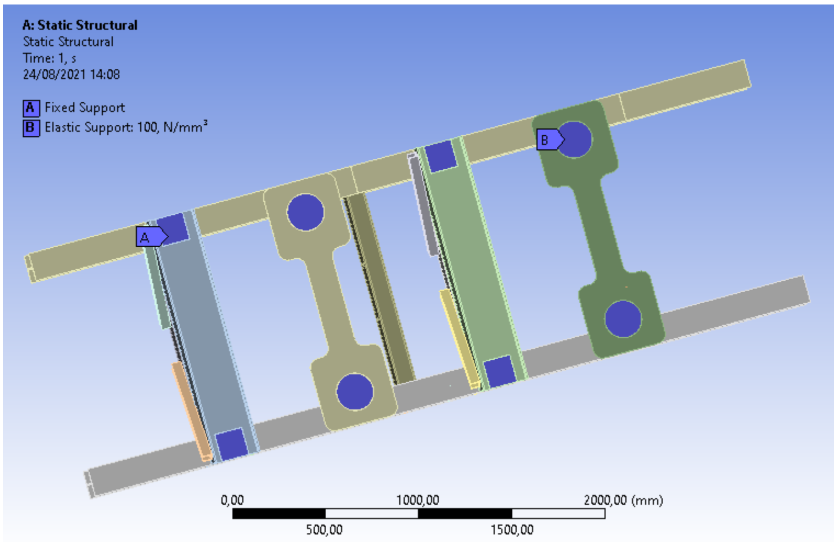


Figure 12.6: Constraints applied to the module

### 12.1.5 Results of simulation

Simulation results are now reported. Again, both deformations and equivalent stresses are taken into account. The results shown in the **Figures 12.7,12.8,12.9** report much lower strain and stress values than the complete vehicle produced today and seen in **Chapter 6**. It is now desired to create a model that is comparable to the model currently in production and studied in Chapter 6 of this document.

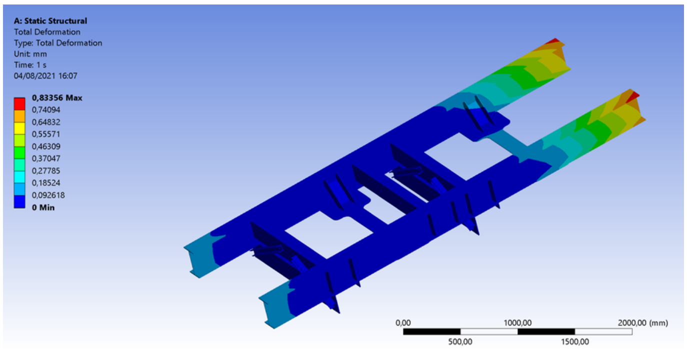


Figure 12.7: Deformation results of the module

It will now go to create the chassis for the three vehicles seen (trailer, semi-trailer, biga) in order to analyze and compare them with the results obtained previously.

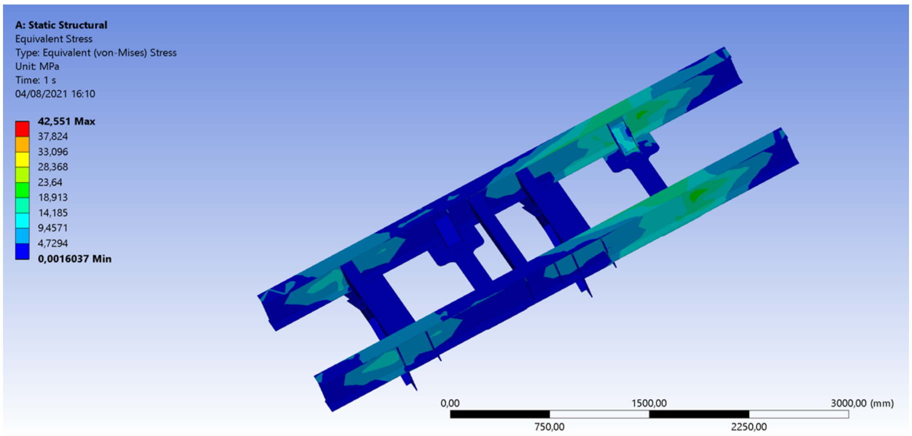


Figure 12.8: Stress results of the biga module

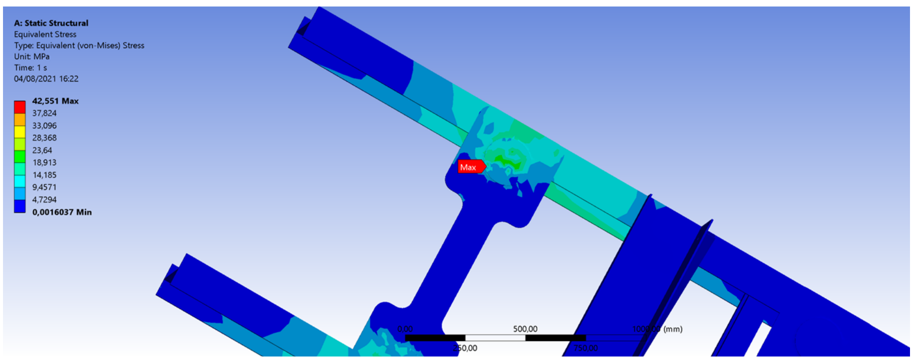


Figure 12.9: Bottom detailed view of Figure 12.8

## 12.2 Biga verification

The first vehicle studied is the biga or close-axle trailer, in this case the length of the vehicle frame is 8 meters. This measure has been chosen because this length includes 95% of the vehicles realized.

The front and rear modules have been built starting from the components realized for the creation of the central module and have been shortened to the need in order to create a complete chassis similar to the actual case but with the new components designed.

Regarding the rudder and the joints to which it is attached to the frame have been schematized in a simplistic way because the purpose of this analysis is to focus on the central module and the verification of the goodness of the frame.

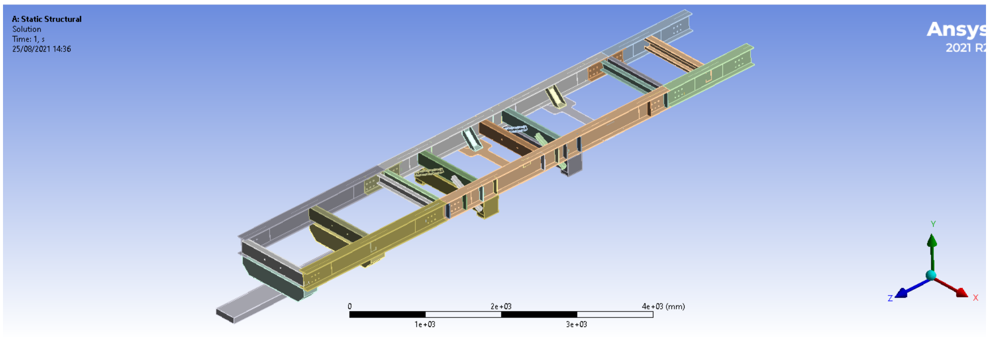


Figure 12.10: Biga with new module chassis

The **Figures 12.11 12.12** show the constraints and loads applied to the studied vehicle. It was chosen to apply as maximum load the maximum loadable weight of the biga, the towing force was calculated through the formulas reported in **??**.

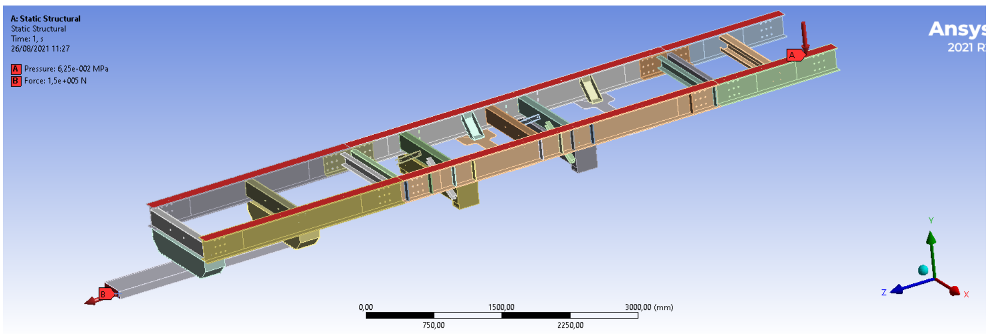


Figure 12.11: Loads on biga new chassis

Regarding the constraints it has been chosen in this case to simulate the axes as fixed supports in the program ANSYS while in the points where the diapress are installed it has been inserted an elastic constraint with module of elasticity equal to 100 $N/mm^2$ in order to simulate the elastic and not rigid behavior of the diapress.

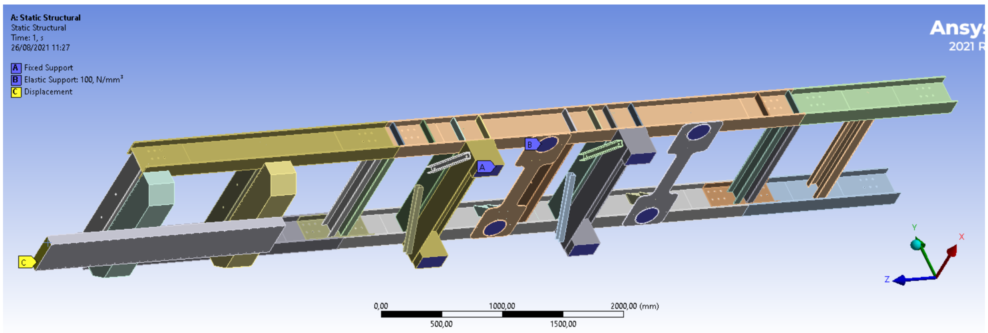


Figure 12.12: Constraints on biga new chassis

In the front part a displacement constraint has been inserted as if it were a trolley and therefore the translational degree of freedom has been constrained along the y axis.

### 12.2.1 Biga simulation results

As a first result, the deformation of the studied vehicle is analyzed.

The **Figure 12.13**, shows that the maximum deformation is in the rear part of the vehicle and is in the order of 6 mm, the result if compared with the case of the original chassis shows a decrease of the deformation, and more in detail of the maximum deformation.

This can be associated to the increase of the stiffness of the new frame and of the various connections that have been created between the two longitudinal beams.

The stresses derived from the simulation are now shown in the **Figures 12.14,12.15**.

As it is possible to observe from the first image it is noticed that the point of maximum stress goes to place itself in the relative part to the rudder, therefore in the anterior part that for now is not of interest for the carried out study.

As far as the central part is concerned, the good distribution of stress on the longitudinal beams can be appreciated.

It can also be pointed out that the regions concerning the axles and the area of the diapress do not present critical points in which there is a high value

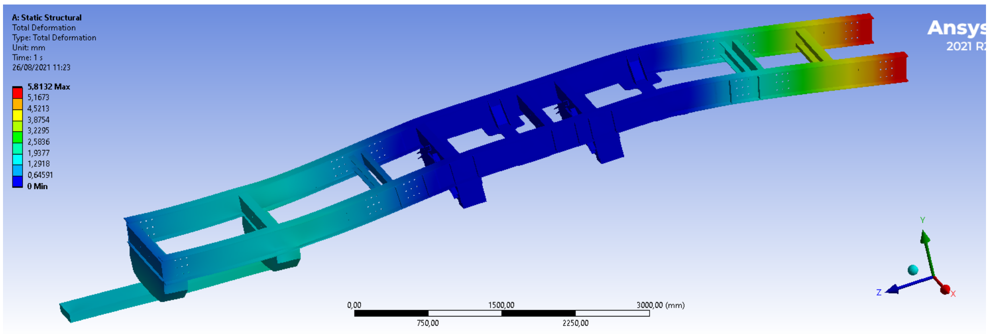


Figure 12.13: Deformation biga new chassis

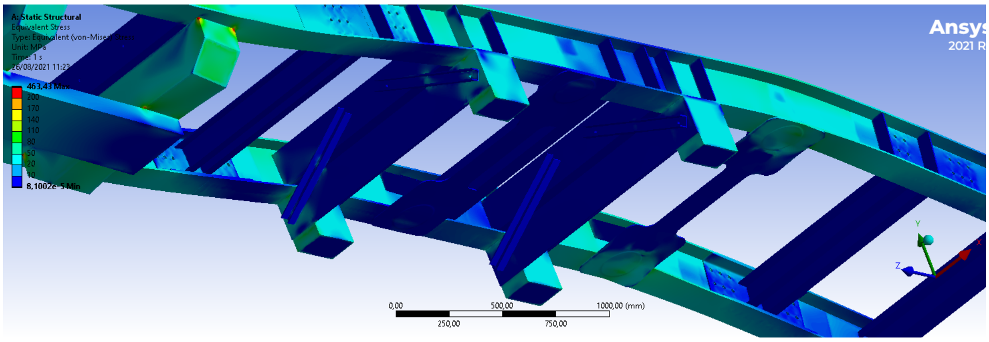


Figure 12.14: Bottom view equivalent stress biga new chassis

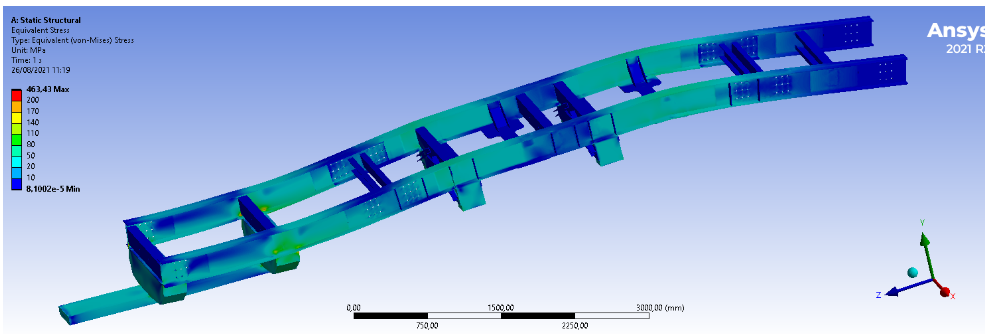


Figure 12.15: Equivalent stress biga new chassis

of stress; on the contrary, as reported, the distribution of stress includes a greater region than in the case of the product currently in production, therefore the structure realized distributes the load on a greater region, allowing to decrease stress in critical areas.

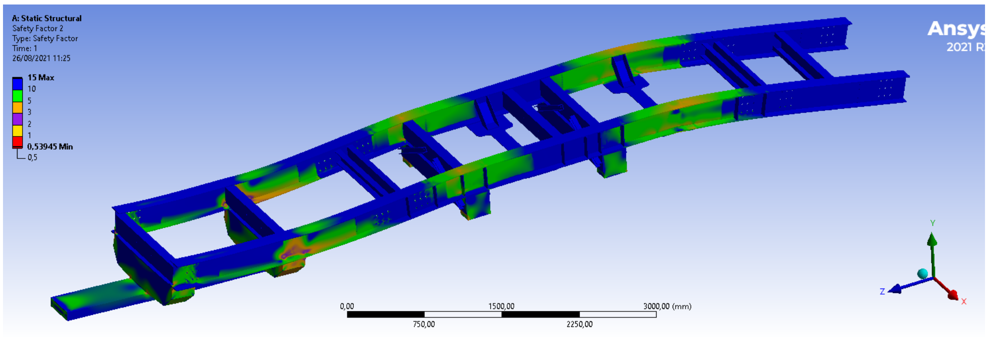


Figure 12.16: Safety factor biga

The safety factor of the chassis is represented in the **Figure 12.16**, as can be seen from the figure in this case the minimum value of safety factor is 0.5, therefore it is in unsafe conditions, however the point where this safety factor has a value of 0.5 is linked to the front part of the vehicle and more specifically to the rudder.

Analysing the central part of the chassis, it can be seen that on these elements the safety factor never goes below the value of 3, even in the most stressed regions such as the axles.

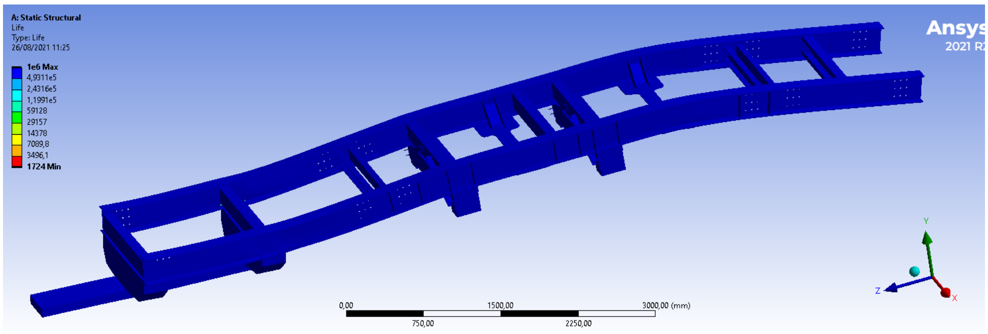


Figure 12.17: Fatigue-life biga

The **Figure 12.17** shows the simulation results for the fatigue life analysis considered as vehicle loading and unloading cycles. This analysis was performed through the fatigue tool present within the ANSYS simulation software. As it can be seen from the image, in general the life of the vehicle presents the maximum value, the points that result to be more subject to fatigue are the junction parts of the chassis where are installed the components for the diapress and for the axles, the minimum value of fatigue life in this case is represented by the supports for the installation of the rudder.

As seen in the static case therefore the front part and in particular the part of the rudder is the most stressed.

In the case of our interest therefore the central module presents an acceptable life for the case in examination since it has a maximum value.

## 12.3 Trailer verification

Now let's move on to the verification of the chassis related to the trailer vehicle. The length of the vehicle in this case is 8 meters, it includes 95% of the vehicles made.

The module studied in this thesis, in case of trailer application is installed as the central part of the vehicle. The vehicle will be composed therefore as in the case of the biga by a front part, a central part and a rear part; the joints used also in this case are those already presented.

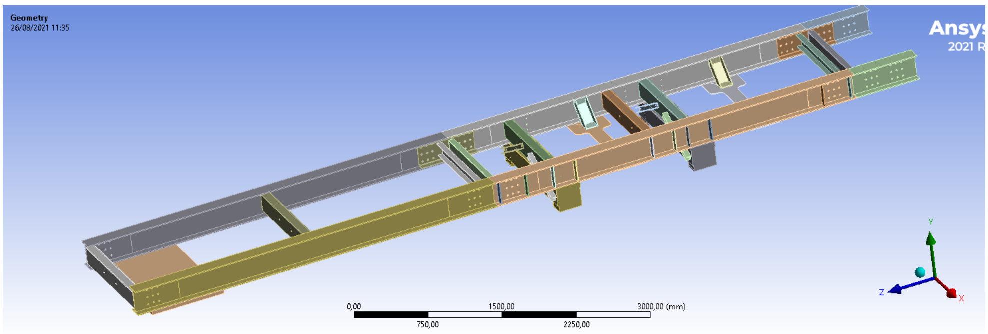


Figure 12.18: Trailer with new module chassis

In the case of the trailer it has been inserted in the front part a component that simulates the fifth wheel coupling, that is the part where the towed vehicle is coupled with the towing vehicle.

As for the meshing of the structure, it followed the same procedure as in the case of the central module study and the biga case.

The results are reported in the **Figure 12.19**. The constraints of the structure have been inserted in the same way as in the case of the biga, the only exception being the front constraint where there is no longer the front rudder constrained but the fifth wheel castle, the constraint always remains a translational constraint on the y axis.

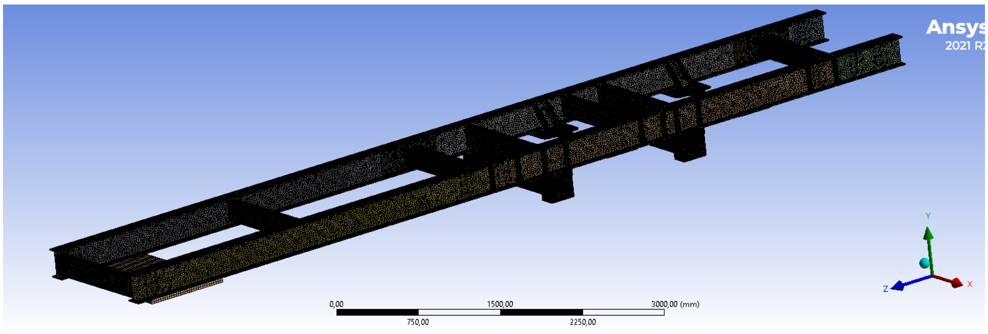


Figure 12.19: Trailer mesh new module chassis

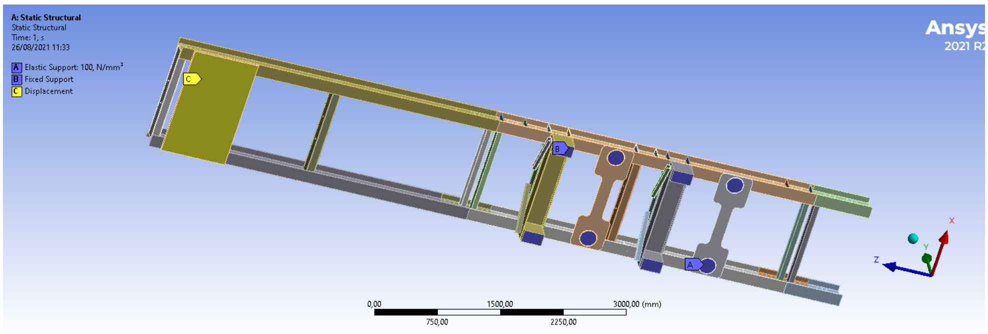


Figure 12.20: Constraints on trailer new chassis

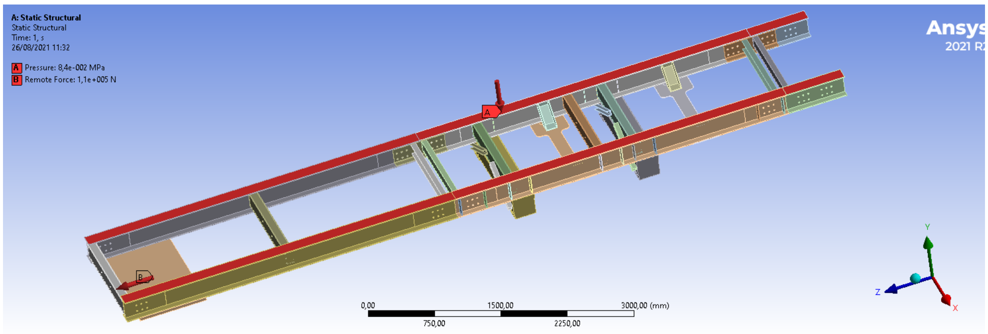


Figure 12.21: Loads on trailer new chassis

The loads applied to the structure are the maximum distributed load for the trailer case and the towing force always calculated using the formulas in **Chapter 5**.

The towing force in this case has been applied through the use of the ANSYS remote point function, this point has been placed in the center of the fifth wheel castle structure.

### 12.3.1 Trailer simulation results

The first result reported here is the frame deformation. The maximum value is located at the rear of the vehicle and has a value around 2 mm.

Also in this case comparing the results with the vehicle currently produced we obtain lower deformation values in the new model than in the old one.

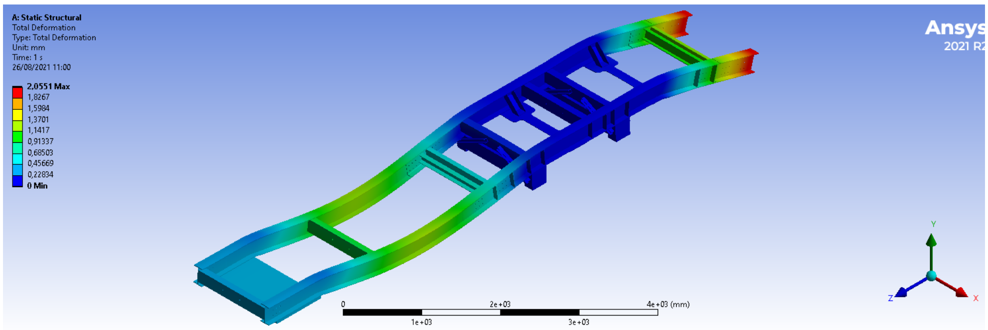


Figure 12.22: Deformation trailer new chassis

Another important deformation area to be taken into consideration is the part between the first axle and the fifth wheel axle of the vehicle.

the study of stresses on the vehicle is now carried out.

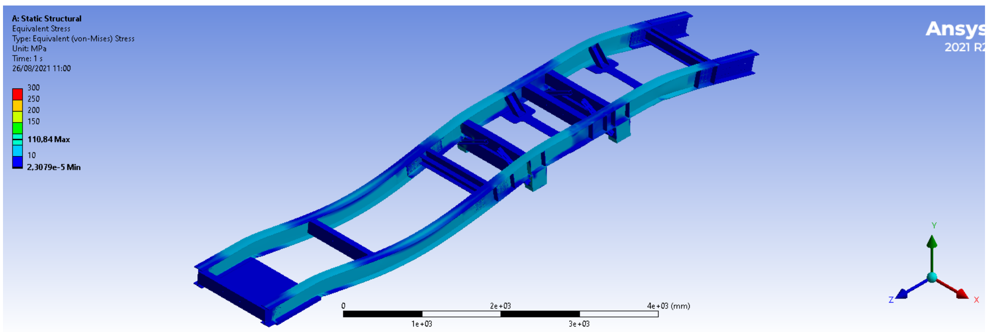


Figure 12.23: Stress results of the trailer module

As can be seen from the **Figures 12.23 12.24**, the vehicle is stressed with maximum stress values around 110 MPa.

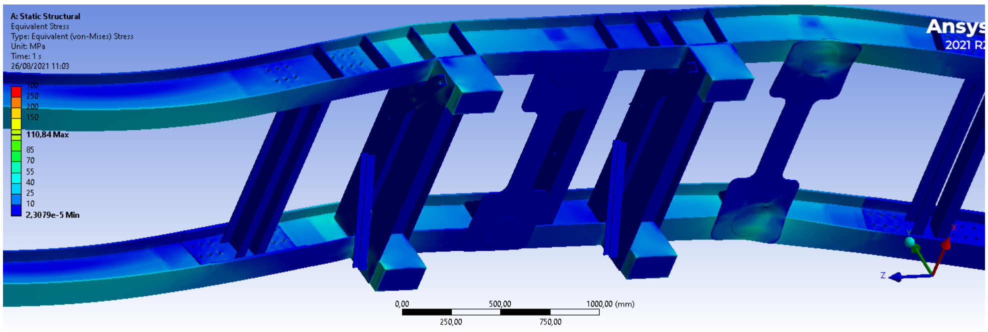


Figure 12.24: Bottom view of Figure 12.23

The stress distribution is continuous and without concentrated points with high stress. The **Figure 12.24** shows a focus on the suspensions and axles of the vehicle, the stress distribution is also very good and uniform in these regions.

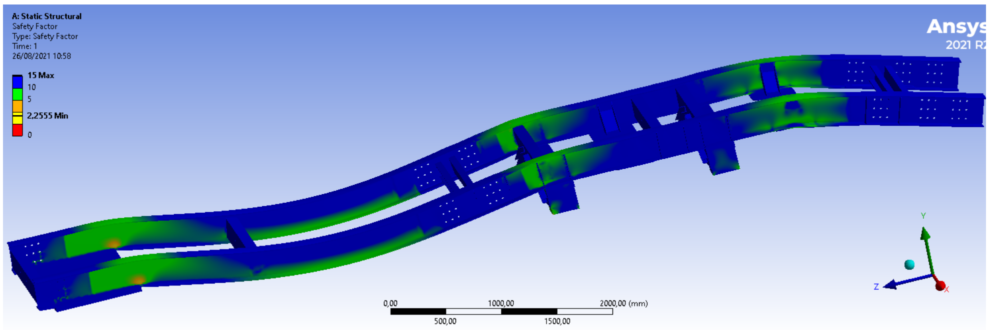


Figure 12.25: Safety factor of trailer module

The safety factor obtained through the results tool on ANSYS reports a minimum value of 2.25, the points with this safety factor are located around the region of the castle ralle and therefore outside the current discussion.

As far as the central module is concerned, studied in the whole geometry, the safety factor is very good (minimum value 5)(**Figure 12.25**).

The regions with a lower safety factor than the central module are precisely the regions related to the first axle and the position of the diapress of the second axle.

Also in this case through the fatigue analysis tool present on ANSYS the fatigue of the vehicle subjected to cycles of loading and unloading of the vehicle has been studied.

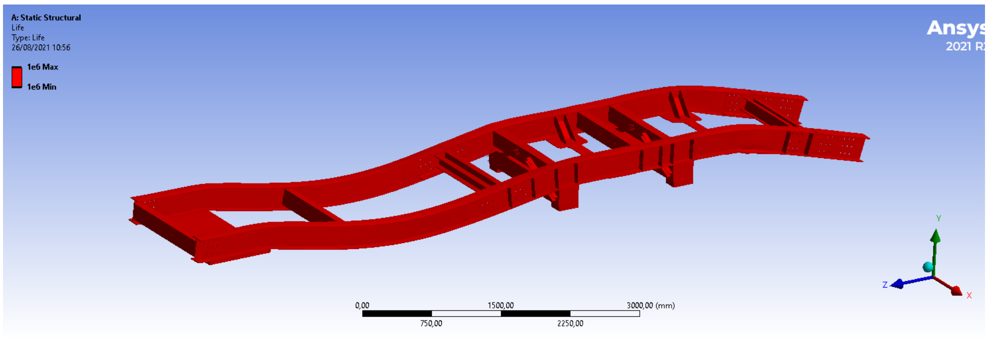


Figure 12.26: Fatigue-life of trailer module

The results are shown in the **Figure 12.26** and as can be seen the distribution is uniform with an excellent fatigue life value.

## 12.4 Semitrailer verification

As a final analysis, the study of the semi-trailer vehicle is retrieved (**Figure 12.27**). Again, the chassis is composed of 3 different parts and the module of interest is the center module.

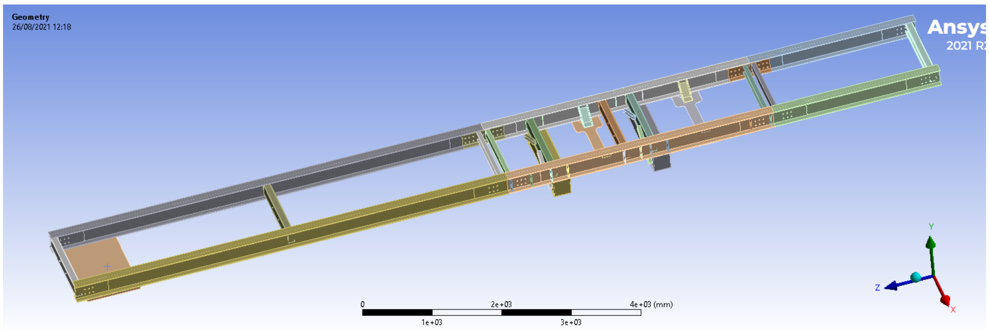


Figure 12.27: Semitrialer new module

In this case the total length of the vehicle is 13.5 meters, the maximum length that can be achieved today for such a vehicle.

The front part was made 6.5 meters in length, the central part 4 meters and the rear part 3 meters.

As seen in the previous sections the meshing was done for each component with the method congruent to it and the dimensions of the elements useful for the application. The constraints inserted are the same as those applied for the trailer vehicle. The loads applied are the load distributed with the

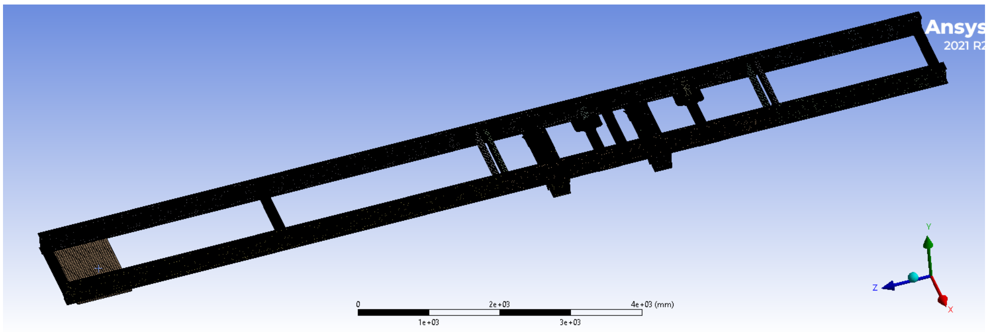


Figure 12.28: Mesh of semitrailer new module

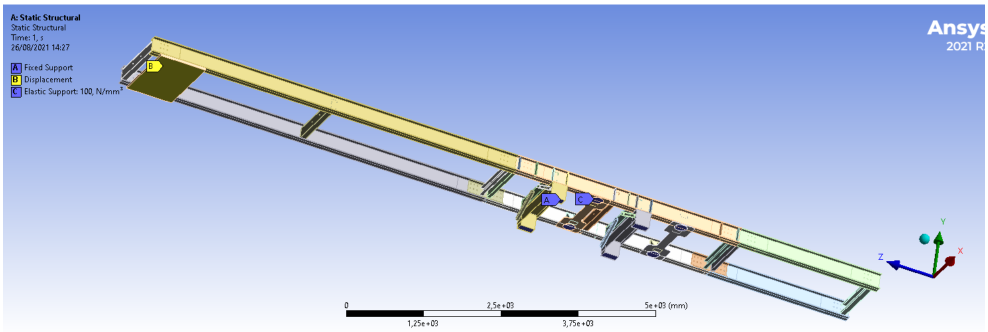


Figure 12.29: Constraints on semitrailer new module

maximum weight loadable by the semi-trailer vehicle and the towing force always calculated as seen in **Chapter 5**.

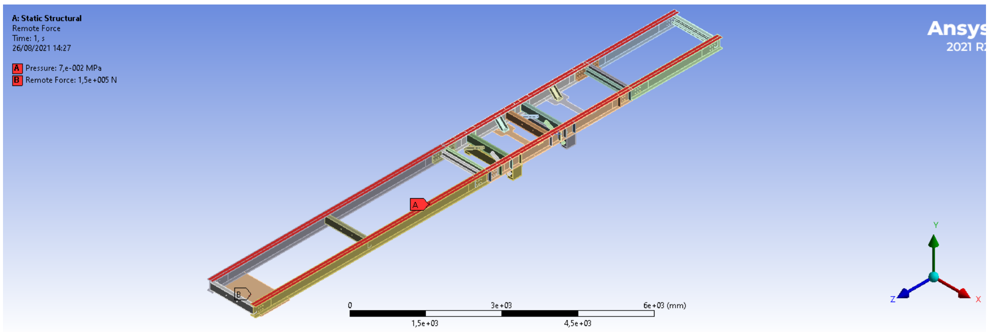


Figure 12.30: Loads on semitrailer new module

## 12.4.1 Semitrailer simulation results

It is now passed to the description of the results obtained through the simulation carried out.

The **Figure 12.31** reports the deformation of the vehicle, also in this case as in the previous ones the greater displacement is in the posterior part of the vehicle; such value is of approximately 22 mm, considering the original chassis also in this application with the new chassis a smaller deformation of it has been obtained. The study of the stresses (**Figure 12.32**) on the

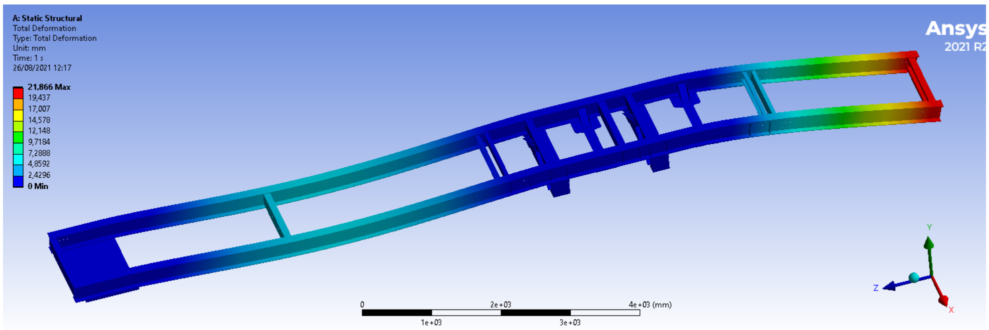


Figure 12.31: Deformation semitrailer new module

vehicle brings to light that the most stressed regions are between the second axle and the diapress of the second axle (values around 120 MPa).

From (**Figure 12.33**) it can be seen that around the diapress of the second axle there is a region where there is an average stress value.

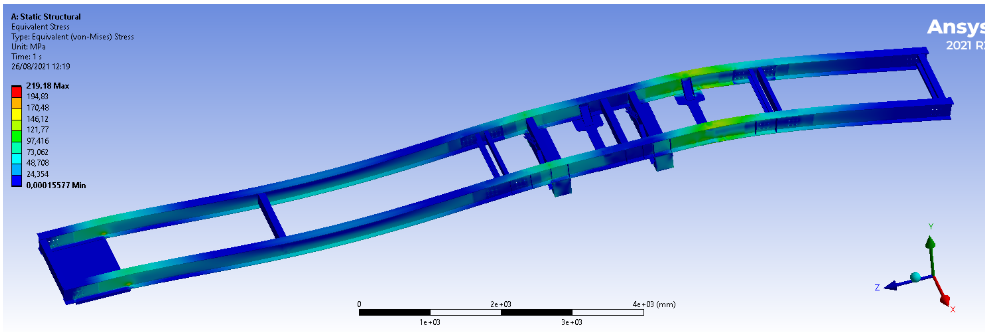


Figure 12.32: Equivalent stress semitrailer new module

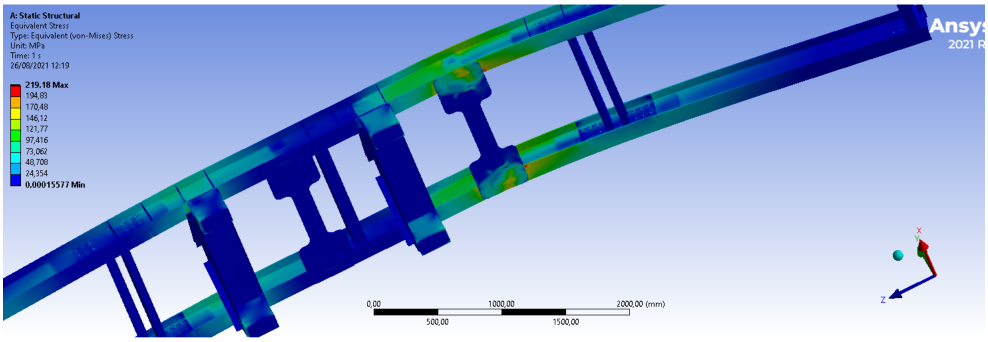


Figure 12.33: Detailed view of Figure 12.32

The analysis of the safety factor shows that the minimum value is around 1.14, but this value does not appear to be in the area of interest (i.e. in the central module).

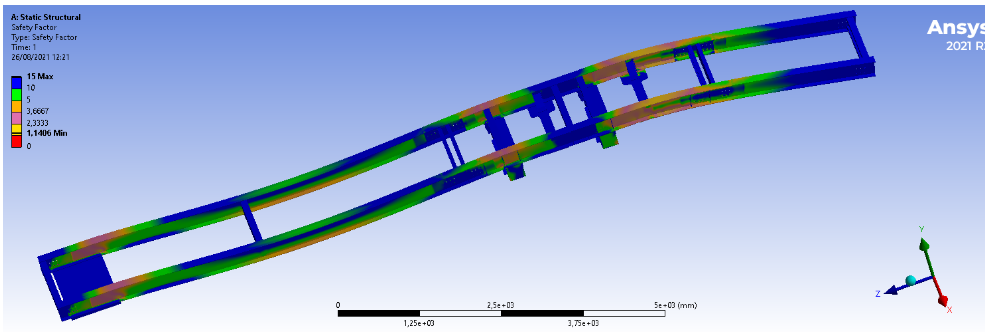


Figure 12.34: Safety factor semitrailer new module

The central module (visible on **Figure 12.35**) shows values higher than 2.3 of safety factor, these values are acceptable for the studied application.

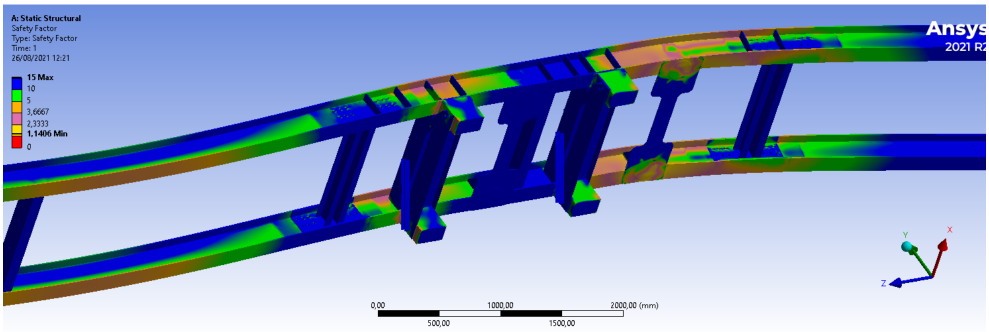


Figure 12.35: Safety factor semitrailer new module (2)

As a final result, the case of fatigue analysis of vehicle loading and unloading is also reported here. As can be seen from the **Figures 12.36 12.37** in this case an important stress point is identified located in the area of the diapress of the second axis.

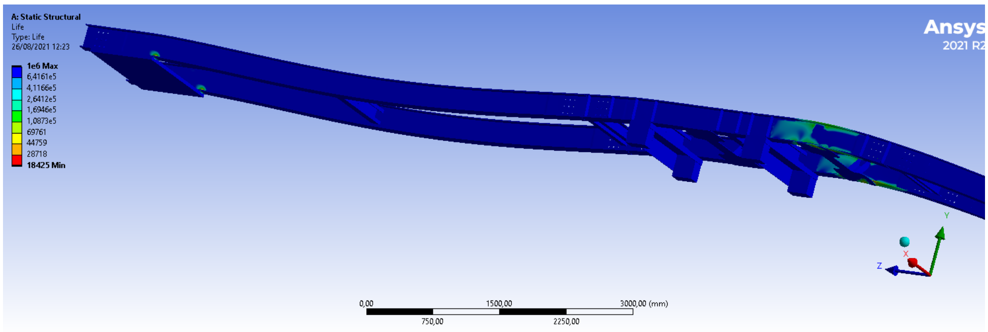


Figure 12.36: Fatigue-life semitrailer new module

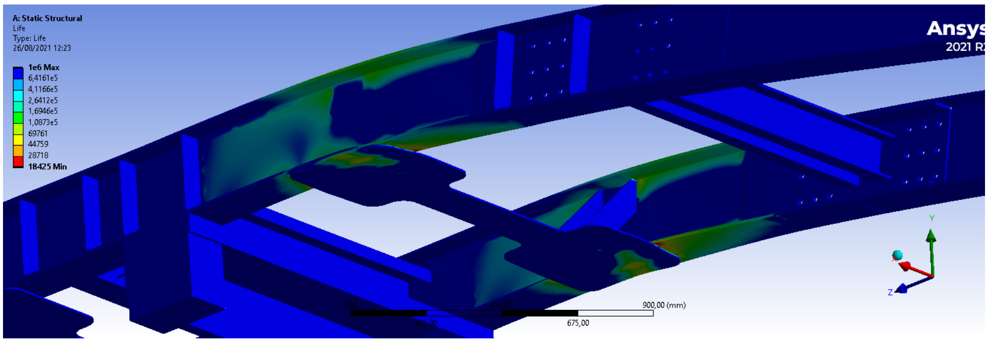


Figure 12.37: Detailed view of Figure 12.36

# Chapter 13

# Final conclusions

The thesis just exposed goes to insert in a more wide plan of renewal and business innovation action to transform the company from handicraft to industry.

The model of standardization and modularity wants here to be the base for the construction of a new method of planning in order to try to improve the efficiency of the technical office and the production, at the same time is wanted therefore to reduce the time of planning and production of the vehicles and therefore also the time passed between the order of the customer and the exit of the vehicle from the company.

The chassis presented are indeed still at the beginning of their development process, they can be improved through a process of lightening and refinement that will continue in the coming months within the company's research and development department.

At the same time, this treatise discussed the central part of the vehicle, as presented in the three vehicles examined, there will then be work to be done on modeling the new modules of the front and rear in order to move forward with the design of the new chassis.

As for the state of the current model it will then be studied and adapted to the production with 2D drawings specific to the manufacturer, at the same time it will be studied both through the finite element method in the case of random vibrations in order to optimize its fatigue life.

Once completed the model for the production it will be realized and then proceed with a more or less long period of road tests that will verify the goodness of the project realized.

This document wants therefore to be a cue for the new method of design that you want to give to the company, reduction in the number of components and therefore simplification both at the production level, design but at the same time also at the level of purchases of components involved in the realization of vehicles.

The new ideology will then tend to be applied to the various elements made by the company.

# Appendix A

# Highway code for heavy duty vehicles

The purpose of this appendix is to introduce some basic rules foreseen by the Highway Code, in this case Italian, but also valid at European level, in order to clarify some concepts of loading capacity, limit weight and limit gauge of vehicles and in particular of heavy vehicles, which is the field studied in this document.

Below is a description of the vehicle contour, i.e. the area projected on the asphalt that the vehicle can occupy while driving.

According to article 61 of the Highway Code, the ”limiting shape” of the vehicle is:

- Maximum width not exceeding 2.55 m; in the calculation of this width are not included the protrusions due to the rear-view mirrors, provided that they are mobile;

- Maximum height does not exceed 4 m; for buses and trolleybuses intended for scheduled urban and suburban public services circulating on predetermined routes and 'allowed that this height is 4.30 m;

- Total length, including towing devices, not exceeding 12 m, excluding semi-trailers, for single vehicles. In the calculation of this length are not considered the rear-view mirrors provided that 'mobile.

- 18-wheeler and articulated vehicles must not exceed a total length, including the towing components, of 16.50 m, provided that the other limits established in the regulation are respected; 18-wheeler and articulated vehicles used for scheduled passenger transport intended to travel along pre-established routes may reach a maximum length of 18 m; road trains must not exceed a maximum length of 18.75 m in compliance with the technical prescriptions established by the Ministry of Infrastructure and Transport.

- The maximum width of vehicles for the transport of perishable goods under controlled temperature conditions (ATP) can reach the value of 2.60 m, excluding protrusions due to rear-view mirrors, provided that they are mobile.

Another very important aspect related to heavy vehicles is the weight and the maximum capacity of the vehicle, also in this case the Highway Code clarifies which aspects have to be respected:

- 12 tons, if they are two-axle vehicles;
- 25 tons, in the case of vehicles with three or more axles;
- 26 tons, if they are three-axle vehicles with the driving axle equipped with coupled tires and air suspension;
- 32 tons, in the case of four-axle vehicles with the driving axle fitted with coupled tires and air suspension;
- 19 tons, in the case of two-axle buses and trolleybuses intended for regular public transport service.

The maximum gross laden mass of trailers equipped with tires (excluding semi-trailers) may not exceed:

- 6 tons, if it is a single-axle trailer;
- 22 tons, if it is a two-axle trailer;
- 26 tons in the case of a three or more axle trailer.

The maximum gross laden mass of trucks, articulated vehicles and articulated vehicles may not exceed:

- 30 tons, if it is a three-axle truck;
- 40 tons, in the case of a four-axle truck;
- 44 tons, if it is a truck with five or more axles.

# Bibliography


[1] Unioni saldate (parte 1 e 2), *Quaderni di progettazione strutturale*, Promozione Acciaio, Milano

[2] Unioni bullonate, *Quaderni di progettazione strutturale*, Promozione Acciaio, Milano

[3] Luca Goglio, (2011) *Fondamenti di meccanica strutturale*, Dispense per il corso, Torino

[4] Gianluca Pagano, (2019) *Modularità di prodotto nel settore delle macchine riempitrici*, Tesi di di laurea magistrale, Padova

[5] Prof. Daniele Zaccaria, (2007) *Meccanica della trave inflessa*, Dispense del corso di scienza delle costruzioni, Trieste

[6] Strenx performance steel, *Guida alla progettazione del rimorchio*, Strenx: il percorso più rapido per un trasporto efficiente

[7] Decreto Legislativo, n. 285 (1.1.1993) *Il codice della Strada*

[8] Decker, M., and G. Savaidis. (2002) *Measurement and Analysis of Wheel Loads for Design and Fatigue Evaluation of Vehicle Chassis Components.* Fatigue & Fracture of Engineering Materials & Structures

[9] Bellec, E., M.L Facchinetti, C. Doudard, S. Calloch, S. Moyne, and M.P Silvestri. (2021) *Modelling and Identification of Fatigue Load Spectra: Application in the Automotive Industry.* International Journal of Fatigue 149 (2021): 106222. Web.

[10] Wang, Wenlin, Bao Huang, Jianming Du, and Siyuan Cheng. (2019) *Structural Optimization for Stiffness and Stochastic Fatigue Life Improvement of a Sport Utility Vehicle Chassis.* IOP Conference Series. Materials Science and Engineering 692.1 (2019): 12030. Web.

[11] Ren, Huanmei, and Lihui Chen. (2016) *Fatigue Analysis of Automobile Control Arm Based on Ncode.*
MATEC Web of Conferences 81 (2016): 8005. Web.

[12] http://www.omarrimorchi.it/

[13] https://www.ferlatacciai.com/it/prodotto/s355j0-fe510-c/

[14] Notes of Machine Design course (2019) *Threaded fasteners notes*
Course of Machine Design, Politecnico di Torino, Automotive Engineering Bachelor Degree, Prof. Belingardi